Comfort oriented nonlinear model predictive control

For autonomous vehicles

Quirinus Wilhelmus Adrianus van der Slot

Master of Science Thesis

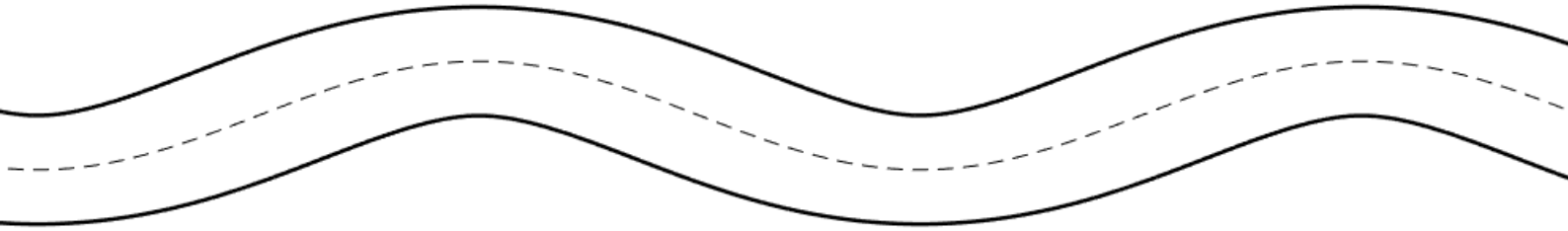

TU Delft Delft University of Technology

Department of Cognitive Robotics

Comfort oriented nonlinear model predictive control

For autonomous vehicles

Master of Science Thesis

Quirinus Wilhelmus Adrianus van der Slot

4240928

April 16, 2020

Faculty of Mechanical, Maritime and Materials Engineering (3mE) · Delft University of Technology

Delft University of Technology
Department of Cognitive Robotics

The undersigned hereby certify that they have read and recommend to the Faculty of Mechanical, Maritime and Materials Engineering (3mE) for acceptance a thesis entitled

Comfort oriented nonlinear model predictive control

by

Quirinus Wilhelmus Adrianus van der Slot

in partial fulfillment of the requirements for the degree of

Master of Science Mechanical Engineering.

Dated: April 16, 2020

Supervisors:

Dr. L. Ferranti

Dr. ir. R. Happee

Readers:

Dr. B. Shyrokau

Ir. Y. Zheng

Abstract

To promote automation in vehicles, autonomous driving should feel comfortable. To achieve low discomfort, a comfort oriented nonlinear model predictive controller is created.

We know humans are sensitive for discomfort in certain frequencies in acceleration. By penalizing the frequencies for discomfort a higher comfort performance can be achieved. Two band pass filters are created to penalise the frequencies. A band pass filter (0.03-0.2 Hz) for the frequency of motion sickness and a band pass filter (1-2 Hz) for general discomfort. Due to the MPC framework the filters can be implemented on the predicted accelerations. The filtered accelerations are penalised within the MPC.

The MPC is made for path following control. To test the MPC a reference generator is built. The reference generator creates reference signals about the path ahead for the controller. To test the performance of the filters, tests are done with different controllers. In the different controllers the filters are penalised individually and together and compared against other controllers. The controllers are tested on multiple scenarios (e.g. double lane change and a sinusoidal trajectory). On the scenarios multiple disturbances are tested (e.g. wind disturbance and sensor noise).

We conclude that the MPC design that relies on the motion sickness filter has a significant decrease of motion sickness in scenarios where a lot of motion sickness is present, with improvements up to 30.7% compared to the basic controller. The MPC design that relies on the general discomfort filter helps bring the general discomfort down. On the double lane change maneuver with a changing velocity the general discomfort filter has improvements up to 10.7% compared to the basic controller.

Table of Contents

Preface **xiii**

1 Introduction **1**
1-1 Comfort . . . 1
1-2 Comfort research . . . 2
1-3 Objectives . . . 3

2 Overview project **5**
2-1 Controller . . . 5
2-1-1 Model predictive control (MPC) . . . 6
2-2 Reference generator . . . 7
2-2-1 Reference path . . . 7
2-3 Vehicle simulator . . . 8

3 Controller **11**
3-1 Model . . . 11
3-1-1 Tire model . . . 11
3-1-2 Vehicle model . . . 13
3-2 Cost function . . . 14
3-2-1 Tracking . . . 15
3-2-2 Comfort . . . 15
3-3 Constraints . . . 17

4 Evaluation **19**
4-1 Evaluation . . . 19
4-1-1 Tracking and solving time . . . 19
4-1-2 Comfort evaluation . . . 20

4-2 Test scenarios . . . 20
4-2-1 Disturbances . . . 20
4-2-2 Trajectory . . . 22
4-3 Tuning . . . 25
4-4 System . . . 25

5 Filter evaluation and implementation 27
5-1 Initializing filter . . . 27
5-1-1 Discussion . . . 28
5-2 Sample time . . . 28
5-3 Time horizon . . . 29
5-4 Filtered signal behaviour . . . 30
5-5 Summary . . . 31

6 Lateral influences on the combined controller 33
6-1 Adding penalties . . . 33
6-2 Double lane change . . . 37
6-3 Motion sickness . . . 39
6-3-1 Double lane change with different time horizons . . . 39
6-3-2 Sine wave . . . 40
6-4 Longitudinal influence due to lateral acceleration penalty . . . 43
6-4-1 Velocity increase . . . 43
6-4-2 Influence lateral acceleration . . . 45
6-4-3 Discussion . . . 45
6-5 Disturbance . . . 49
6-5-1 Lower friction . . . 49
6-5-2 Wind disturbance . . . 50
6-5-3 Sensor noise . . . 51
6-6 Influences of the time horizon . . . 54
6-7 Solving time . . . 55
6-8 Summary . . . 56

7 Longitudinal influences on the combined controller 59
7-1 Adding penalties . . . 59
7-2 Velocity profile . . . 62
7-3 Disturbance . . . 64
7-3-1 Friction change . . . 64
7-3-2 Sensor noise . . . 65
7-4 Influences time horizon . . . 68
7-5 Solving time . . . 69
7-6 Summary . . . 70

8 Results combined lateral and longitudinal control **71**
8-1 Double lane change with velocity shift . . . 71
8-2 Motion sickness . . . 74
8-2-1 Longitudinal control . . . 75
8-3 General discomfort . . . 77
8-4 Disturbances . . . 80
8-4-1 Friction change . . . 80
8-4-2 Wind disturbance . . . 81
8-4-3 Sensor noise . . . 81
8-5 Combinations acceleration terms filtered and unfiltered . . . 83
8-6 Solving time . . . 85
8-7 Summary . . . 85

9 Conclusion and future work **87**
9-1 Conclusion . . . 87
9-2 Future work . . . 88
9-2-1 Tuning . . . 88
9-2-2 Safety controller . . . 88
9-2-3 Disturbance observer . . . 89
9-2-4 Soft/hard boundary constraints . . . 89
9-2-5 Velocity problem . . . 89
9-2-6 Real world test . . . 89

A Vehicle model **91**
A-1 Dynamic bicycle model . . . 91

B Results **95**
B-1 Result influence lateral control . . . 95
B-1-1 Double lane change 80 km/hour . . . 95
B-1-2 Increase time horizon motion sickness . . . 97
B-1-3 Sine wave motion sickness . . . 97
B-1-4 Friction change . . . 101
B-1-5 Wind disturbance . . . 102
B-1-6 Sensor noise . . . 103
B-1-7 Influences of the time horizon . . . 104
B-2 Results influence longitudinal control . . . 105
B-2-1 Velocity profile . . . 105
B-2-2 Friction change . . . 106
B-2-3 Sensor noise . . . 108
B-2-4 Influences of the time horizon . . . 109

B-3 Results combined control 110
B-3-1 Double lane change with velocity change 110
B-3-2 Motion sickness 111
B-3-3 General discomfort 113
B-3-4 Friction change 114
B-3-5 Wind disturbance 115
B-3-6 Sensor noise 116
B-3-7 Combination acceleration terms filtered and unfiltered 117

Bibliography **119**

List of Figures

1-1 Weighting curves 2

2-1 Schematic model of the automated vehicle 5
2-2 Reference signal example 8
2-3 Reference controller 9
2-4 Simplified version of test setup 10

3-1 Schematic model of the automated vehicle, controller 11
3-2 Lateral tire force [1] 13
3-3 Bicycle model [2] 13
3-4 Filters from the controller compared to the weights of motion sickness and general discomfort 16

4-1 Example of the RMS and MTVV performance indicators 21
4-2 Implementation of wind disturbance 21
4-3 White noise implementation in Simulink [3] 22
4-4 Double lane change with boundary conditions 23
4-5 Velocity profile on straight path 23
4-6 Path based on a sine wave 24
4-7 Selecting new weights 25

5-1 Initialize with states of the previous time step 28
5-2 Initialize with zero 29
5-3 Initialize filter with previous time step 30
5-4 Influence sample time on filter 30
5-5 Influence time horizon on filter 31

5-6 Filtered signal behaviour 32

6-1 Effect of changing weight $\triangle\delta$ 34
6-2 Effect of changing weight ay 35
6-3 Effect of changing weight ay, ms 35
6-4 Effect of changing weight ay, gd 35
6-5 Growing discomfort due to increasing the weight on increment delta 36
6-6 Lateral error controller J_3, without soft or hard constraints 39
6-7 Comfort on the sine wave while increasing the weights on the acceleration terms (filtered and unfiltered), higher weight is higher lateral error 41
6-8 Minimizing cost due to increasing velocity and therefore travelled path, positive influences on increment δ and ψ angle cost 44
6-9 No penalties on the velocity weights leads to an increase in driven velocity 44
6-10 Longitudinal influences by penalising lateral acceleration with different weights on the double lane change of 80 km/hour 46
6-11 Longitudinal influences by penalising lateral motion sickness acceleration with different weights on the double lane change of 80 km/hour 47
6-12 Longitudinal influences by penalising lateral general discomfort acceleration with different weights on the double lane change of 80 km/hour 48
6-13 Filter response to a step input, filters from Section 3-2-2 51
6-14 Influences noise on motion sickness and general discomfort using the weights from Section 1-1 53

7-1 Effect of changing weight $\triangle a$ 60
7-2 Effect of changing weight ax 61
7-3 Effect of changing weight ax, ms 61
7-4 Effect of changing weight ax, gd 61
7-5 Comparison controllers J_2 - J_4 on wet road conditions while losing traction, compared to dry road condition with controller J_1 66
7-6 Comparison controllers J_2 on dry and wet road conditions, old constraint is longitudinal control maximum 6.5, new constraint maximum 3.0 67

8-1 Double lane change with velocity shift 72
8-2 Accelerations from double lane change with velocity shift, J_1 has high motion sickness discomfort, J_1 and J_3 high general discomfort 73
8-3 Sine wave for lateral and longitudinal control 74
8-4 Effect of changing weight ax 77
8-5 Effect of changing weight ax, gd 78
8-6 Overall acceleration on low friction scenario 80

List of Tables

1-1 Velocity profile 3
1-2 The SAE levels of automation [4]. 4

2-1 Future position prediction 7

3-1 Linear tire model symbols 12
3-2 Compact model symbols 14

4-1 Conversion factors for sensor noise 22

5-1 Test setup for Figure 5-4 29
5-2 Test setup for Figure 5-5 31

6-1 Weights applied on the controllers, w_{var} is a variable weight 34
6-2 Weights applied on the controllers 37
6-3 Double lane change 80 km/hour 37
6-4 Double lane change 80 km/hour, different time horizons 40
6-5 One period of the sine wave at 80 km/hour 41
6-6 Sine wave at 60 km/hour 42
6-7 Velocity profile 43
6-8 Weights applied on the controllers, w_{var} is a variable weight 45
6-9 Double lane change 80 km/hour with $\mu = 0.5$ 49
6-10 Double lane change 80 km/hour with wind disturbance 50
6-11 Double lane change 80 km/hour with sensor noise 52
6-12 Double lane change 80 km/hour with different time horizons 54

6-13 Solving times on the double lane change 55

7-1 Weights applied on the controllers, w_{var} is a variable weight 60
7-2 Weights applied on the controllers 62
7-3 Velocity profile 62
7-4 Velocity profile with $\mu = 0.5$, Longitudinal control value constraint by maximum of 6.5 65
7-5 Velocity profile with $\mu = 0.5$, Longitudinal control value constraint by maximum of 3.0 66
7-6 Velocity profile with sensor noise 67
7-7 Double lane change 80 km/hour with different time horizons 68
7-8 Solving times on the double lane change 69

8-1 Weights applied on the controllers 72
8-2 Double lane change with velocity change 73
8-3 Sine wave for lateral and longitudinal control 75
8-4 Weights applied on the controllers 76
8-5 Sine wave with different longitudinal terms 76
8-6 Double lane change with velocity shift 78
8-7 Weights applied on the controllers 79
8-8 Double lane change with velocity change, friction change to $\mu = 0.5$ 81
8-9 Double lane change with velocity change under wind disturbance 82
8-10 Double lane change with velocity change with sensor noise 82
8-11 Weights applied on the controllers 83
8-12 Double lane change, different controllers 84
8-13 Solving times on the double lane change with velocity change 85
8-14 Weights applied on the controllers 85

B-1 Double lane change 80 km/hour 96
B-2 Double lane change 80 km/hour 97
B-3 One period of the sine wave at 80 km/hour 98
B-4 Double lane change with same tuning and different velocities 99
B-5 Sine wave at 60 km/hour 100
B-6 Double lane change 80 km/hour with $\mu = 0.5$ 101
B-7 Double lane change 80 km/hour with wind disturbance 102
B-8 Double lane change 80 km/hour with sensor noise 103
B-9 Double lane change 80 km/hour with different time horizons 104
B-10 Velocity profile 105

B-11 Velocity profile with $\mu = 0.5$ 106
B-12 Velocity profile with $\mu = 0.5$, Longitudinal control value constraint by maximum of 3.0 107
B-13 Velocity profile with sensor noise 108
B-14 Double lane change 80 km/hour with different time horizons 109
B-15 Double lane change with velocity change 110
B-16 Sine wave for lateral and longitudinal control 111
B-17 Sine wave with different longitudinal terms 112
B-18 Double lane change with velocity shift 113
B-19 Double lane change with velocity change, friction change to $\mu = 0.5$ 114
B-20 Double lane change with velocity change under wind disturbance 115
B-21 Double lane change with velocity change with sensor noise 116
B-22 Double lane change, different controllers 117

Preface

From beginning the master with little knowledge of automation within vehicles, to creating a controller for automatic driving. The journey has been a learning curve, with at the end the thesis for the graduation of master of science in mechanical engineering. When looking for a subject for the thesis, I got to talk with dr. Laura Ferranti. She introduced me to the subject which became my thesis. The thesis is written with the intention to become beneficial in the future for countering discomfort in autonomous vehicles.

I would like to thank my daily supervisor dr. Laura Ferranti for always willing to help. Her quick responses and feedback has helped me to increase the quality of the research. I would like to thank dr. ir. Riender Happee for asking questions and giving feedback which made me think further and more scientific. I would like to thank the members of the examination committee for their time. Finally, I would like to thank my family for supporting me through this journey.

Q.W.A. van der Slot

Noordwijkerhout

April 16, 2020

Chapter 1

Introduction

The advent of new technologies (such as lane keeping assist [5] and even some autopilot functions [6]) are raising the level of automation in the vehicle. SAE (Society of Automotive Engineers) created standard for automation in vehicles where the level of automation can be distinguished, see Table 1-2. The market is now at SAE level 2 [7]. In level three the driver can start doing side activities. In the higher levels the driver can become the passenger in the vehicle. The change from being a driver to becoming a passenger can lead to an increase in car sickness [8, 9]. The increase in car sickness can have a negative effect in user acceptance for automated vehicles [8]. To promote automation in vehicles, the level of comfort should be high.

An example for why comfort is important: A survey was done on 3256 coach travellers, 28.4% of the passengers reported that they were feeling ill [10]. Even though coach travel is different than a normal passenger vehicle, a lot of people experienced motion sickness. Therefore, researching a controller which maximizes comfort can help a lot of people. In order to maximize comfort an understanding must be made of what leads to discomfort.

1-1 Comfort

In vehicles the discomfort can come from accelerations, yaw, roll and pitch. Assuming in the future the roll and pitch can be countered with active suspension these terms are not taken into consideration. The influence that yaw rate has on comfort is small compared to the accelerations [11]. The vertical motion is not taken into consideration, to improve comfort the focus is only on the horizontal accelerations.

The ISO (International Organization for Standardization) created a standardized norm for comfort. Comfort consists of two parts: motion sickness and general discomfort. The frequencies for comfort are 0.1-0.5 Hertz for motion sickness (ISO 2631, [12]) and for general discomfort 0.5-80 Hertz (ISO 2631, [12]). The ISO norm for motion sickness

is made for vertical acceleration, the vertical acceleration is not taken into consideration [13]. Therefore, the ISO norm can not be implemented for motion sickness. For general discomfort the ISO filter can be applied for the horizontal accelerations [13].

To create an indicator for motion sickness another weighting method is selected. The new weighting curve for motion sickness is described in paper [14]. For longitudinal acceleration is chosen to have the same weighting curve as for lateral acceleration for motion sickness. In Figure 1-1 the weighting curves are given, for general discomfort the ISO norm and for motion sickness the weighting method described in the paper [14].

Since both general discomfort and motion sickness can come from longitudinal and lateral acceleration, the overall acceleration is used:

$$a_{\mathrm{w}} = \sqrt{a_{\mathrm{y,filtered}}^2 + a_{\mathrm{x,filtered}}^2} \tag{1-1}$$

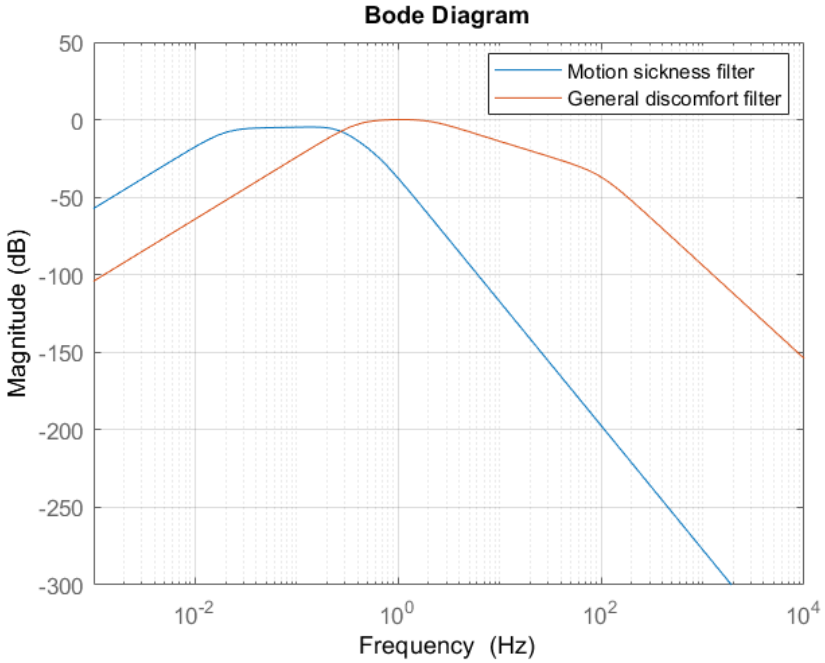

Figure 1-1: Weighting curves

1-2 Comfort research

Comfort can be considered in the path planner and in the controller. To achieve higher comfort in the path planner the lateral and longitudinal accelerations can be constrained. The lateral acceleration in a curvature is depended on the velocity, see Equation 1-2 [15, 16, 17], with the meaning of the symbols given in Table 1-1.

$$a_{\mathrm{l}} = \frac{d\theta}{dt} v = \kappa \cdot v^2 = \frac{1}{\rho} v^2 \tag{1-2}$$

Table 1-1: Velocity profile

Symbols	Meaning
a_l	Lateral acceleration
θ	Vehicle orientation
ρ	Curvature radius
v	Longitudinal velocity
κ	Curvature

To stay within the constrained lateral acceleration the vehicle's velocity can be adjusted [18, 15]. The overall acceleration, which influences comfort, depends on both lateral and longitudinal accelerations. To keep the overall acceleration low the vehicle should brake before the corner.

Instead of adjusting the velocity to the path, both velocity and path can be planned within one optimization algorithm. In paper [19] a MPC path planner plans both lateral and longitudinal control. The MPC path planner reduces the velocity before entering a corner to not exceed 0.5 g. On the steering angle a soft constraint is implemented based on the maximum allowed lateral acceleration. More methods for path planning are available, there are planners which penalises the jerk and acceleration to increase comfort [20].

Instead of in the path planner comfort can be addressed in the controller. By implementing comfort in the controller, the controller can achieve high comfort even when the vehicle behaves differently than expected, for example due to disturbances. Similar to path planning the controller can constrain the accelerations and jerk [21]. Instead of constraining the accelerations and jerk a penalty could be given to achieve more comfort [22]. By giving a penalty to the accelerations and jerk they are minimized at all values, high and low, creating more comfort. In order to maximize comfort the frequencies for discomfort should be minimized. Therefore, the proposed method filters the accelerations for the frequencies of motion sickness and general discomfort and penalises the filtered accelerations within the controller.

1-3 Objectives

The focus of the project is creating a lateral and longitudinal path following controller that increases comfort. The increase in comfort is made by decreasing the overall acceleration in the frequencies of motion sickness and general discomfort. The goal is to create a controller that could be implemented in a real vehicle. To implement the controller in a real vehicle safety is important. The vehicle should have low lateral deviations. If the lateral deviations are high the vehicle could leave the designated lane and causes accidents. The controller performance is tested on safety, comfort and solving time. In order to test the vehicle the following problems are addressed:

- Built a reference generator for the controller
- Create multiple trajectories and disturbances to test the controller
- Create a comfort oriented nonlinear model predictive controller
- Create an evaluation method for comfort
- Evaluated the proposed method of penalising discomfort by using filters

Table 1-2: The SAE levels of automation [4].

Monitoring of driving environment	Level of automation	Description
Human driver	0: Driver only	The human driver performs all aspects of the dynamic driving task
Human driver	1: Assisted automation	A driver assistance system performs either steering or acceleration/deceleration, while the human driver is expected to carry out the remaining aspects of the dynamic driving task
Human driver	2: Partial automation	One or more driver assistance systems perform both steering and acceleration/deceleration, while the human driver is expected to carry out all remaining aspects of the dynamic driving task
Automated driving system	3: Conditional automation	An automated driving system performs all aspects of the dynamic driving task (in conditions for which it was designed), but the human driver is expected to respond appropriately to a request to intervene
Automated driving system	4: High automation	An automated driving system performs all aspects of the dynamic driving task (in conditions for which it was designed), even if the human driver does not respond appropriately to a request to intervene
Automated driving system	5: Full automation	An automated driving system performs all aspects of the dynamic driving task under all roadway and environmental conditions

Chapter 2

Overview project

An autonomous vehicle consists of multiple components. Figure 2-1 presents a schematic overview of the simplified control architecture of the project. In order to understand how the controller works, a general understanding of the reference generator, controller and plant is needed.

In a autonomous vehicle, the path is generated by the reference generator. The reference generator creates the signals for the controller to follow. The controller gives commands to the vehicle, the commands could be throttle/brake and/or steering angle. The controller is made to follow the reference signals without creating large errors and high discomfort. In this chapter a general understanding of the blocks reference generator, controller and plant is made. In Chapter 3 the inner workings of the controller is described more in depth.

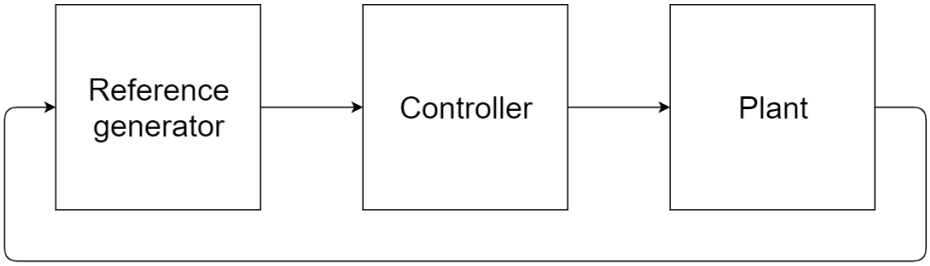

Figure 2-1: Schematic model of the automated vehicle

2-1 Controller

The controller creates commands for comfortable path-following control. The commands, given to the plant, should make the plant follow the reference signals safely while

minimizing discomfort. The commands for the plant are throttle/brake and steering angle. There are multiple ways to create the commands, Proportional-integral-derivative control (PID), Discrete linear quadratic regulator (LQR) and Model predictive control (MPC) could be used. A PID controller can handle one in- and output, even though both outputs, throttle/brake and steering angle, have influences on comfort. LQR and MPC can handle multiple in- and outputs.

The differences between LQR and MPC controller are described in paper [23]. The LQR bases the output on a feedback law, which places weights on the states and control input. While MPC uses an optimization problem to create the lowest cost over the whole time horizon. The advantages of the optimization problem instead of the feedback law is that the controller can react on future changes. A simple example could be braking before a corner. In MPC boundaries can be implemented. The choice is made to work with MPC for the project to achieve the highest comfort.

2-1-1 Model predictive control (MPC)

Model predictive control, as the name says, uses a model to predict the future states. The predicted states can be influenced by the control, in our case the steering angle and throttle/brake. For example, if the controller gives the throttle command the state for the predicted velocity will increase. How far the controller predicts is a design choice called the prediction horizon.

The predicted states and the reference signals are implemented in a cost function. The cost function is minimised by an optimization algorithm. To give an indication on how MPC works an example is given below [24], with the cost function being (2-1). The algorithm chooses the control values which minimizes the cost function and gives the first control output to the plant (vehicle). This process is repeated every time step.

$$\begin{aligned} \min_{\mathbf{u}} \sum_{\mathrm{k}=0}^{N-1} J \\ J = (\tilde{x}_{\mathrm{k}}^T Q \tilde{x} + \triangle u_{\mathrm{k}}^T R \triangle u_{\mathrm{k}}) + x_{\mathrm{N}}^T Q x_{\mathrm{N}} \end{aligned} \tag{2-1}$$

$$s.t. : x_{\mathrm{k}+1} = f(x_{\mathrm{k}}, u_{\mathrm{k}}) \quad k = 0, ..., N-1 \tag{2-2}$$

$$u_{\mathrm{k}+1} = u_k + \triangle u_{\mathrm{k}} \quad k = 0, ..., N-1 \tag{2-3}$$

$$u_{\mathrm{k}} \in [\bar{u}, \underline{u}] \tag{2-4}$$

$$x_{\mathrm{k}} \in [\bar{x}, \underline{x}] \tag{2-5}$$

$$x_0 = x_{\mathrm{current}} \tag{2-6}$$

$$\boldsymbol{u} = [u_0, \ldots, u_{N-1}] \tag{2-7}$$

The solution must be found within in the boundaries of the constraints (Equations (2-2), (2-3), (2-4), (2-6)). To predict the future states a model is used, see Equation (2-2). The control is given in Equation (2-3), the optimization algorithm uses the control as argument to minimize the cost function. The boundaries are given in Equations (2-4) and (2-5). The initial condition of the states are determined in Equation (2-6).

2-2 Reference generator

The reference generator creates signals about the path ahead for the controller to follow. A trajectory is made offline and uploaded to the reference generator. The reference generator will create signals based on the vehicles position to follow the trajectory. The reference signals are made for path following and are based on the middle of the lane. The reference generator has no extra functions than path following. For example, functions such as collision avoidance is not taken into consideration in the project.

2-2-1 Reference path

To create signals of the path ahead, the future position of the vehicle is calculated. The future position is based on the vehicle driving straight ahead from the current position ($\mathrm{k} = 0$). The future position of the vehicle is compared to the trajectory to define the reference signals. The future position of the vehicle is calculated as followed, with the symbols explained in Table 2-1:

$$\begin{bmatrix} X_{\mathrm{k+i}} \\ Y_{\mathrm{k+i}} \end{bmatrix} = \begin{bmatrix} X_{\mathrm{k}} \\ Y_{\mathrm{k}} \end{bmatrix} + \begin{bmatrix} \cos(\psi) \\ \sin(\psi) \end{bmatrix} uT_{\mathrm{s}}i \tag{2-8}$$

Table 2-1: Future position prediction

Symbols	Meaning
$X_{\mathrm{k+i}}$	Future world x coordinate
$Y_{\mathrm{k+i}}$	Future world y coordinate
X_{k}	Current world x coordinate
Y_{k}	Current world y coordinate
ψ	Angle vehicle in world coordinates
u	Longitudinal velocity
T_{s}	Time sample

With the future position of the vehicle known the closest point to the path can be calculated. The path consits of points which contain information, see the red points on Figure 2-2. The information in the points are the position (x and y coordinates), the angle of the path and the velocity. The distance from the future vehicle to the nearest point of the path is calculated with the euclidean distance, see Equation (2-9) [25].

$$\min(\sqrt{(X_{\mathrm{path}} - X_{\mathrm{k+i}})^2 + (Y_{\mathrm{path}} - Y_{\mathrm{k+i}})^2}) \tag{2-9}$$

Three points are taken to calculate the reference signals, the nearest point and the point before and after, see the red points on Figure 2-2. The points are translated to the future vehicle coordinate system, see the following equation [26]:

$$\begin{bmatrix} X_{\mathrm{new}} \\ Y_{\mathrm{new}} \end{bmatrix} = \begin{bmatrix} \cos(\psi) & -\sin(\psi) \\ \sin(\psi) & \cos(\psi) \end{bmatrix} \begin{bmatrix} X_{\mathrm{path,j}} - X_{\mathrm{k+i}} \\ Y_{\mathrm{path,j}} - Y_{\mathrm{k+i}} \end{bmatrix} \; for \; j = 1, 2, 3 \tag{2-10}$$

The lateral (y) error is defined as the error between the vehicles position and the closest point on the trajectory. The lateral error is based on the method in paper [27]. By choosing the closest point on the trajectory the lateral error stand perpendicular on the trajectory instead of the vehicle. The method is chosen due to always finding a solution. When the lateral error start 90 degrees from the vehicle there is not always a solution, see dotted line in Figure 2-3.

To find the closest point on the line a function is made, see Equations (2-11) and (2-12) [28]. The starting point of the lateral error can be on two lines, the first line is the line before the nearest point, the second after the nearest point. Therefore the calculation is done for both lines. The shortest distance will be taken as the lateral error.

$$P_{\text{veh}} = \begin{bmatrix} x_0 \\ y_0 \end{bmatrix}, \; P_1 = \begin{bmatrix} x_1 \\ y_1 \end{bmatrix}, \; P_2 = \begin{bmatrix} x_2 \\ y_2 \end{bmatrix} \tag{2-11}$$

$$|Y_{\text{error}}| = \frac{|(y_2 - y_1)x_0 - (x_2 - x_1)y_0 + x_2 y_1 - y_2 x_1|}{\sqrt{(y_2 - y_1)^2 + (x_2 - x_1)^2}} \tag{2-12}$$

The sign of the distance is still unknown since the vehicle can be on both sides of the line. The calculation of the sign for the y error is done by calculating the angle between the points and the vehicle. To calculate the other signals (ψ and velocity) interpolation between the points of the path is used. The starting position of the lateral error on the line is used for interpolation.

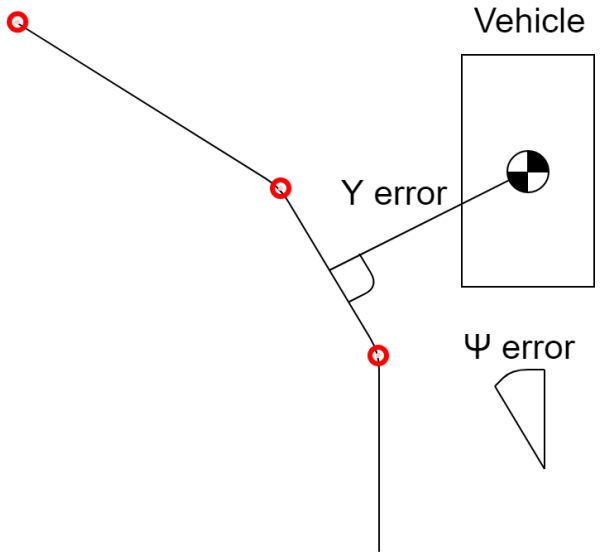

Figure 2-2: Reference signal example

2-3 Vehicle simulator

The simulations are done in Simulink [29]. To simulate the vehicle (plant) the same vehicle simulation model is used as in paper [30] and described accordingly. The plant

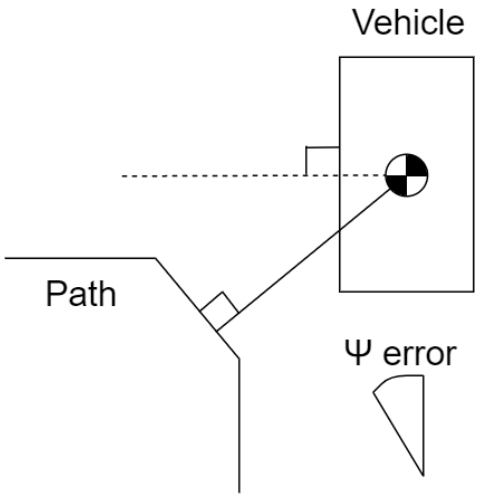

Figure 2-3: Reference controller

consists of 9 degrees of freedom which comes from translational motion (longitudinal, lateral and vertical), rotational motion (yaw, roll and pitch) and the suspension. To model the tire behaviour the Delft-tire 6.2 [31] with Magic Formula steady-state slip model is implemented. The tire model describes the nonlinear slip forces and moments. The relaxation behavior in the tires is implemented by empirical relations for the relaxation lengths. The steering of the plant has simplified dynamics. The steering is implemented with a transfer-function and time delay including the Ackerman geometry. The model is developed and therefore depended on MATLAB and SimMechanics (Now known as Simscape Multibody) [3, 32]. The vehicle model represent a Toyota Prius of the thrid generation. A simplified version of the test setup is shown in Figure 2-4.

The controller uses three control signals to control the plant. The control signals are used for steering and throttle/brake. The control signal for steering (δ) is based on the angle of the steering wheel [rad]. The control signals for throttle/brake ($c_{\mathrm{x,f}}$ and $c_{\mathrm{x,r}}$) are based on the force the wheels apply to the road [N]. The throttle/brake signals are converted to torque in the plant [Nm]. The rear wheels can only brake due to the Toyota Prius being a front wheel driven vehicle. The plant is not equipped with modern technology such as anti-lock braking system or electronic stability control. The trajectories driven are all in the 2D plane (horizontal), in the real world the vehicle moves horizontal and vertical.

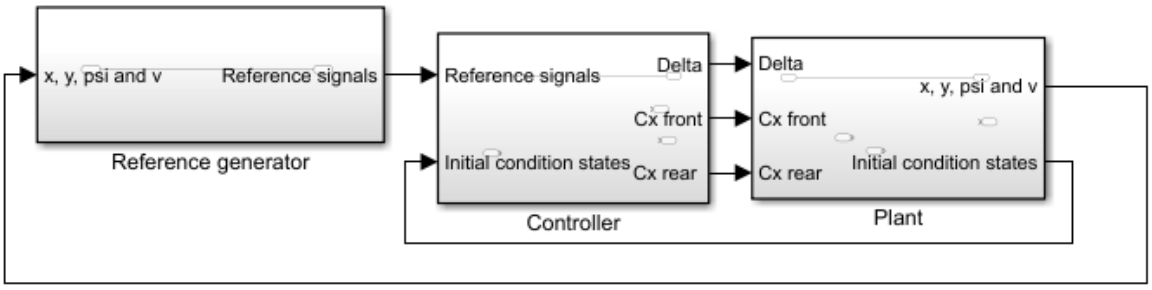

Figure 2-4: Simplified version of test setup

Chapter 3

Controller

The comfort oriented nonlinear MPC consists of multiple parts, that are, (i) cost function, (ii) model, and (iii) boundary conditions. The model creates predictions about the future states. The predicted states can be used in the cost function to track comfortable the reference signals. The predicted states can be bound in the MPC. These components will be detailed in this chapter.

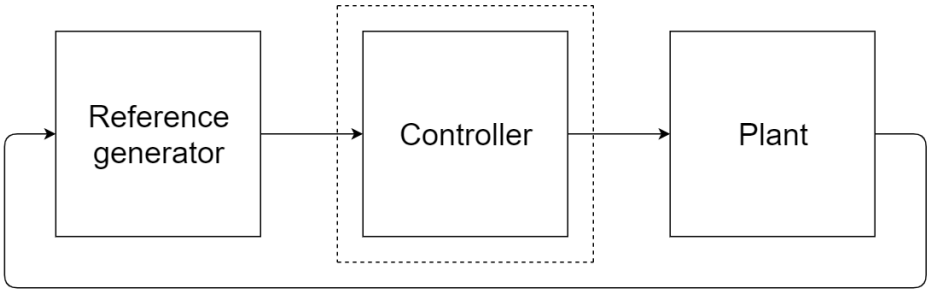

Figure 3-1: Schematic model of the automated vehicle, controller

3-1 Model

The model consists of two parts, the tire model and the vehicle model. The tire model describes the forces that come from the road tire contact. The vehicle model is used to simulate the influences of the control input, the steering angle and throttle/brake. See Appendix A-1 for the complete vehicle model.

3-1-1 Tire model

There are multiple models for describing the tire force. The tire behaviour is plotted in Figure 3-2, as can be seen is that the tire force acts linear until a certain force/side

slip angle is reached. After reaching the maximum of the linear force, the tire force becomes nonlinear. A model can be chosen to describe only the linear part or both parts, linear and nonlinear tire forces.

A model that describes both linear and nonlinear tire forces will be more complex. If the controller works well the nonlinear part of the tire forces is not reached, since the accelerations are kept low, and a linear tire model will be sufficient. The choice is made to work with a linear tire model. The linear tire model is given in the equations below, with the meaning in Table 3-1 [33, 34]:

$$\begin{aligned} F_{\mathrm{yf}} &= -C_{\alpha\mathrm{f}}\alpha_{\mathrm{f}} \\ F_{\mathrm{yr}} &= -C_{\alpha\mathrm{r}}\alpha_{\mathrm{r}} \end{aligned} \tag{3-1}$$

$$\begin{aligned} \alpha_{\mathrm{f}} &= \delta - \frac{v + l_f r}{u} \\ \alpha_{\mathrm{r}} &= \frac{v - l_r r}{u} \end{aligned} \tag{3-2}$$

Table 3-1: Linear tire model symbols

Symbols	Meaning
F_{yf}	Lateral force front
F_{yr}	Lateral force rear
$C_{\alpha\mathrm{f}}$	Cornering stiffness front
$C_{\alpha\mathrm{r}}$	Cornering stiffness rear
α_{f}	Slip angle front
α_{r}	Slip angle rear

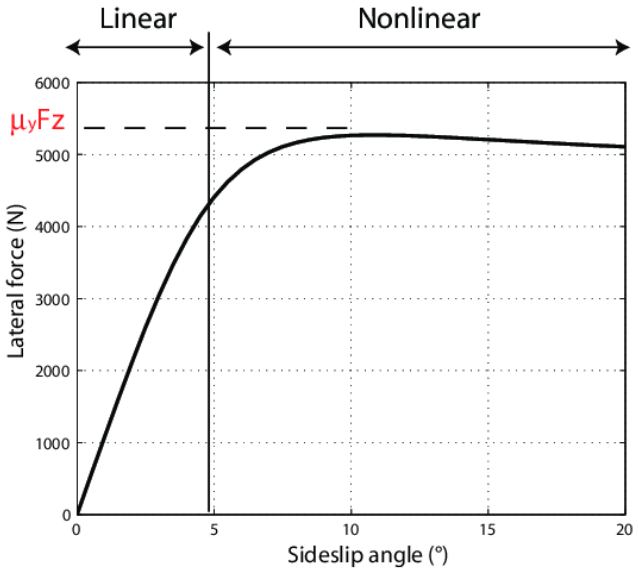

Figure 3-2: Lateral tire force [1]

3-1-2 Vehicle model

The controller is made for path-following, making the internal forces negligible. A bicycle model is used to represent the vehicle. The kinematic and dynamic bicycle model are both simplified versions of the real vehicle. The drawback from the kinematic model is that on a higher velocity the reference error will grow [35]. The kinematic bicycle model does not use tire forces, the dynamic bicycle model does use the tire forces. By using a tire model a better understanding of the vehicle's behaviour can be made. The dynamic bicycle model is used for the project. The model of the vehicle can be seen in Figure 3-3.

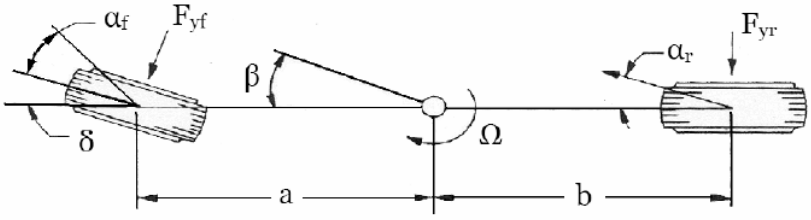

Figure 3-3: Bicycle model [2]

The throttle/brake is controlled with F_{xf} and F_{xr} and the steering angle with δ_{f}. The lateral tire forces are given by F_{y}, with F_{yf} being the front wheel and F_{yr} the rear wheel. L_{f} is the distance from the front wheel to the centre of gravity and L_{r} from the rear wheel to the centre of gravity, respectively a and b in Figure 3-3. The dynamic bicycle

model is given by [36], which can be derived from Figure 3-3:

$$m(\ddot{x} - \dot{y}\dot{\psi}) = -F_{\mathrm{xf}}\cos(\delta_{\mathrm{f}}) - F_{\mathrm{yf}}\sin(\delta_{\mathrm{f}}) - F_{\mathrm{xr}} \tag{3-3}$$

$$m(\ddot{y} + \dot{x}\dot{\psi}) = F_{\mathrm{yf}}\cos(\delta_{\mathrm{f}}) - F_{\mathrm{xf}}\sin(\delta_{\mathrm{f}}) + F_{\mathrm{yr}} \tag{3-4}$$

$$I_{\mathrm{z}}\ddot{\psi} = L_{\mathrm{f}}(F_{\mathrm{yf}}\cos(\delta_{\mathrm{f}}) - F_{\mathrm{xf}}\sin(\delta_{\mathrm{f}})) - L_{\mathrm{r}}F_{\mathrm{yr}} \tag{3-5}$$

Compact model

A compact version of the whole model implemented in the MPC is given below. The symbols are given in Table 3-2. The longitudinal control is divided by a constant value, in our case the mass of the vehicle. By dividing longitudinal control by the mass of the vehicle the difference in magnitude between the control values for longitudinal and lateral control becomes smaller. In the vehicle the longitudinal control value is converted to torque.

$$\dot{\boldsymbol{x}} = f(\boldsymbol{x}, \boldsymbol{u}) \tag{3-6}$$

$$\boldsymbol{x} = [\triangle\delta_{\mathrm{f}}, \triangle c_{\mathrm{x,f}}, \triangle c_{\mathrm{x,r}}, \dot{x}, \dot{y}, \dot{\psi}, y, \psi, \delta_{\mathrm{f}}, c_{\mathrm{x,f}}, c_{\mathrm{x,r}}] \tag{3-7}$$

$$\boldsymbol{u} = [\delta_{\mathrm{f}}, c_{\mathrm{x,f}}, c_{\mathrm{x,r}}] \tag{3-8}$$

$$c_{\mathrm{x,f}} = F_{\mathrm{xf}}/1590 \tag{3-9}$$

$$c_{\mathrm{x,r}} = F_{\mathrm{xr}}/1590 \tag{3-10}$$

Table 3-2: Compact model symbols

Symbols	Meaning
$\triangle\delta_{\mathrm{f}}$	Change in steering angle [rad]
$\triangle c_{\mathrm{x,f}}$	Change in longitudinal control front wheels [N/1590]
$\triangle c_{\mathrm{x,r}}$	Change in longitudinal control rear wheels [N/1590]
$\dot{x}$	Longitudinal velocity [m/s]
$\dot{y}$	Lateral velocity [m/s]
$\dot{\psi}$	Yaw rate [rad/s]
y	Lateral position [m]
ψ	Yaw angle [rad]
δ_{f}	Steering angle [rad]
$c_{\mathrm{x,f}}$	Longitudinal control front wheels [N/1590]
$c_{\mathrm{x,r}}$	Longitudinal control rear wheels [N/1590]

3-2 Cost function

As explained in Section 2-1-1 MPC minimizes an optimization problem. The optimization algorithm minimizes the cost function. The cost function consists of two parts: Tracking and comfort.

3-2-1 Tracking

To create a path following controller, the reference signals are implemented in the cost function. The signals from the reference generator are in the vehicle frame. The reference signals are the lateral deviation (y_{ref}), the difference in yaw angle (ψ_{ref}) and the desired velocity (v_{ref}). Implementing the reference signals into the cost function leads to the following cost function, with w being the weights:

$$y_{\text{penalty}}(k) = \|y(k) - y_{\text{ref}}(k)\|^2 w_{\text{y}} \tag{3-11}$$
$$\psi_{\text{penalty}}(k) = \|\psi(k) - \psi_{\text{ref}}(k)\|^2 w_{\psi} \tag{3-12}$$
$$v_{\text{penalty}}(k) = \|v(k) - v_{\text{ref}}(k)\|^2 w_{\text{v}} \tag{3-13}$$
$$J_{\text{tracking}}(k) = y_{\text{penalty}}(k) + \psi_{\text{penalty}}(k) + v_{\text{penalty}}(k) \tag{3-14}$$

The MPC tries to minimize the penalties by adjusting the control input, making the controller follow the reference signals. By penalizing the change in lateral and longitudinal control the tracking and comfort performance can be improved. Therefore, the following equations could be both under tracking and comfort.

$$\triangle\delta_{\text{penalty}}(k) = \|\delta(k) - \delta(k-1)\|^2 w_{\triangle\delta} \tag{3-15}$$
$$\triangle a_{\text{penalty,rear}}(k) = \|c_{\text{rear}}(k) - c_{\text{rear}}(k-1)\|^2 w_{\triangle c} \tag{3-16}$$
$$\triangle a_{\text{penalty,front}}(k) = \|c_{\text{front}}(k) - c_{\text{front}}(k-1)\|^2 w_{\triangle c} \tag{3-17}$$
$$J_{\text{increments}}(k) = \triangle\delta_{\text{penalty}}(k) + \triangle a_{\text{penalty,rear}}(k) + \triangle a_{\text{penalty,front}}(k) \tag{3-18}$$

3-2-2 Comfort

The controller is now able to track the reference signals. To achieve more comfort, terms can be implemented in the cost function. The proposed method to increase the comfort is penalizing the acceleration frequencies in which humans are sensitive for discomfort. A band pass filter for these frequencies is created. The transfer function for the low pass filter is Equation (3-19), and for the high pass filter is Equation (3-20), with ω being the frequency in Hz.

$$\frac{2\pi\omega}{s + 2\pi\omega} \tag{3-19}$$
$$\frac{s}{s + 2\pi\omega} \tag{3-20}$$

To create the band pass filter the two filters are multiplied. To use the band pass filter in the model, the filters are made into a discrete state space. The filters can be used as following:

$$z(k+1) = Az(k) + Ba(k) \tag{3-21}$$
$$a_{\text{filter}}(k) = Cz(k) + Da(k) \tag{3-22}$$

In Figure 3-4 the weights for the frequencies that create motion sickness and general discomfort are plotted, see Section 1-1. To penalise discomfort as precise as possible, the filter should follow the lines of the weights. The band pass filter chosen for motion sickness is 0.03-0.2 Hertz and for general discomfort 1-2 Hertz. In Figure 3-4 can be seen that the lines are closely together. More accurate filters can be chosen, however this leads to more states in the filter and increasing the complexity of the controller. The transfer functions for the filters are as following:

$$\text{Filter}_{\text{motion sickness}} = \frac{1.257s}{s^2 + 1.445s + 0.2369} \tag{3-23}$$

$$\text{Filter}_{\text{general discomfort}} = \frac{12.57s}{s^2 + 18.85s + 78.96} \tag{3-24}$$

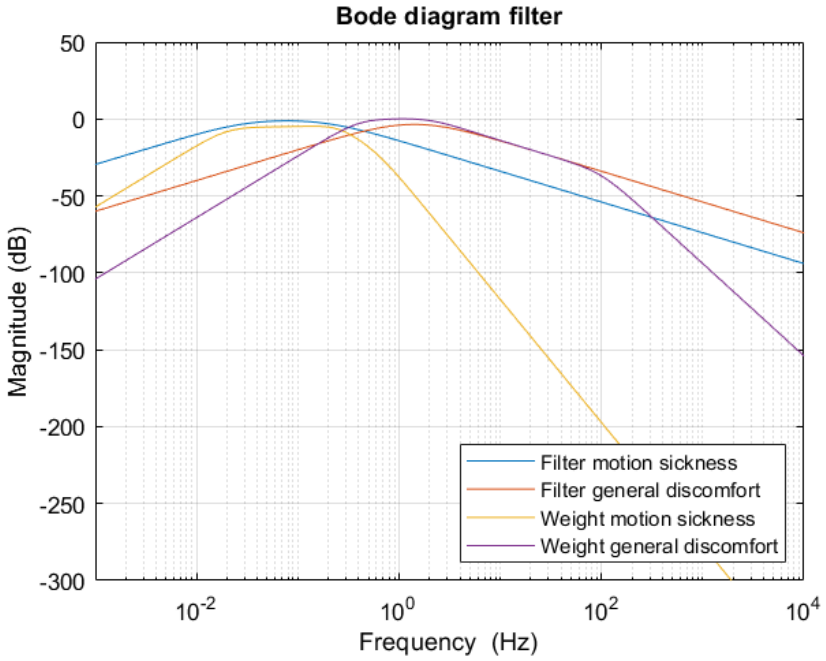

Figure 3-4: Filters from the controller compared to the weights of motion sickness and general discomfort

The cost function for lateral comfort consists of two parts, that are, the lateral acceleration filtered for motion sickness and for general discomfort, respectively. This leads to the following cost functions:

$$a_{\text{y,ms,penalty}}(k) = a_{\text{y,ms}}(k)^2 w_{\text{ay,ms}} \tag{3-25}$$

$$a_{\text{y,gd,penalty}}(k) = a_{\text{y,gd}}(k)^2 w_{\text{ay,gd}} \tag{3-26}$$

$$J_{\text{filter}}(k) = a_{\text{y,ms}}(k)^2 w_{\text{ay,ms}} + a_{\text{y,gd}}(k)^2 w_{\text{ay,gd}} \tag{3-27}$$

The same penalties as for lateral acceleration can be given for longitudinal acceleration:

$$a_{\mathrm{x,ms,penalty}}(k) = a_{\mathrm{x,ms}}(k)^2 w_{\mathrm{ax,ms}} \tag{3-28}$$
$$a_{\mathrm{x,gd,penalty}}(k) = a_{\mathrm{x,gd}}(k)^2 w_{\mathrm{ax,gd}} \tag{3-29}$$
$$J_{\mathrm{filter}}(k) = a_{\mathrm{x,ms}}(k)^2 w_{\mathrm{ax,ms}} + a_{\mathrm{x,gd}}(k)^2 w_{\mathrm{ax,gd}} \tag{3-30}$$

3-3 Constraints

An advantage from using MPC is that constraints can be implemented. In a vehicle there are constraints on the throttle/brake and steering wheel. The steering wheel constraints implemented in the controller are:

$$|\delta| \leq 30[\mathrm{deg}] \tag{3-31}$$
$$|\triangle\delta| \leq 30[\mathrm{deg/s}] \tag{3-32}$$

The constraints of the throttle/brake are set more loosely. The controller is made for comfort, using the throttle/brake aggressively will lead to discomfort. The controller will therefore behave conservative. The vehicle is front wheel driven, therefore (3-35) goes to zero and not a positive value. The front wheels have a higher constraint on braking. The higher value is chosen so that the front wheels will lose traction before the rear wheels does to keep the vehicle safe.

$$c_{\mathrm{x,front}} \leq 6.5[\mathrm{N}/1590] \tag{3-33}$$
$$c_{\mathrm{x,front}} \geq -4.0[\mathrm{N}/1590] \tag{3-34}$$
$$c_{\mathrm{x,rear}} \leq 0.0[\mathrm{N}/1590] \tag{3-35}$$
$$c_{\mathrm{x,rear}} \geq -2.5[\mathrm{N}/1590] \tag{3-36}$$
$$|\triangle c_{\mathrm{x,front}}| \leq 5[(\mathrm{N}/1590)/\mathrm{s}] \tag{3-37}$$
$$|\triangle c_{\mathrm{x,rear}}| \leq 5[(\mathrm{N}/1590)/\mathrm{s}] \tag{3-38}$$

The boundaries of the states which are not specified are from $-\infty$ to ∞.

Chapter 4

Evaluation

To test if the proposed method for comfort oriented nonlinear MPC works, a few different test scenarios are created. The tests should take multiple things into consideration: tracking abilities, solving time and comfort. In the real world disturbances are present, therefore disturbances are simulated and can be implemented on the test scenarios.

To evaluate the performance of the controller, the controller needs to be tuned for optimal performance. Due to the cost function consisting of multiple weights that depends on each other tuning can be difficult and time consuming, therefore an automatic tuning algorithm is written.

4-1 Evaluation

We evaluate the performance of the controller with respect to tracking, computation time and comfort.

4-1-1 Tracking and solving time

The safety of the controller is related to the lateral error. To be safe the lateral deviation should be low in order to not deviate from the lane. In the Netherlands the standard road is of size 2.75 meters [37]. In other countries the standard lane has more width. The vehicle simulated, see Section 2-3, is a Toyota Prius with a maximum track width of 1.519 meters [30]. Therefore, the vehicle could have a lateral deviation of around 0.61 meters while staying in the lane, to create a higher safety margin a more conservative value for the lateral deviation should be taken.

The solving time of the controller gives an indication whether the controller can be used in real time. The controller runs at a frequency of 25 Hertz, meaning every 0.04 seconds a new solution should be found. The controller can be implemented if the maximum

solving time is always below 0.04 seconds. Increasing the sample time can have a negative effect on performance. The calculations errors could grow, for an example see Section 5-2.

4-1-2 Comfort evaluation

To evaluate comfort of the controllers, we created comfort indicators. Since humans are sensitive for certain comfort frequencies, the accelerations are filtered for these frequencies. The frequencies are for motion sickness and general discomfort, see Section 1-1. From the filtered accelerations the overall acceleration is calculated, see Equation (8-3).

From the overall filtered acceleration an indication of comfort can be made. An indication can be given with the root-mean-square method (RMS) [12, 38]:

$$a_{\mathrm{RMS}} = \left[\frac{1}{T}\int_0^T a^2(t)dt\right]^{\frac{1}{2}} \tag{4-1}$$

The root-mean-square method is used over the whole simulation time. A second method which can be used is the maximum transit vibration value (MTVV) [39]:

$$a_{\mathrm{MTVV}}(t) = \left[\frac{1}{\tau}\int_{t-\tau}^{t} a^2(t)dt\right]^{\frac{1}{2}} \tag{4-2}$$

$$\mathrm{MTVV} = \max(a_{\mathrm{MTVV}}(t)) \tag{4-3}$$

The MTVV method finds the highest RMS acceleration of a small sample time within the simulation time. The MTVV test is done with the time period of one second ($\tau = 1$). An example of the RMS and MTVV method is given in Figure 4-1.

4-2 Test scenarios

To test the performance of the controller we built a few test scenarios. The test scenarios consist of different trajectories, velocities and disturbances.

4-2-1 Disturbances

In the real world a number of disturbances are effecting the performance of the vehicle. A few disturbances are implemented to see how the vehicle behaves.

Wind disturbance

Safety of the passengers has a high priority, therefore the vehicle should not swerve to another lane under wind disturbance. To test the performance crosswind is implemented. Crosswind is wind that comes from the side (lateral) of the vehicle. Crosswind

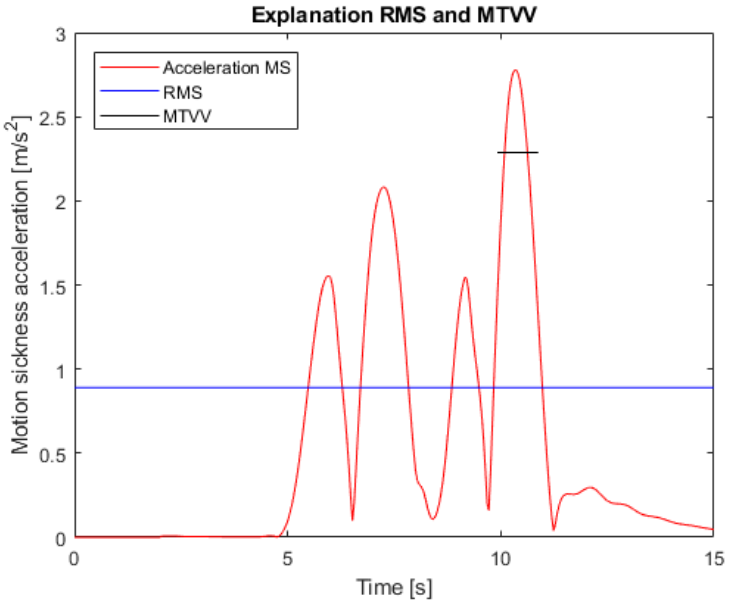

Figure 4-1: Example of the RMS and MTVV performance indicators

is implemented according to the papers [40, 41]. The wind disturbance is simulated with a wind velocity of 10m/s. The crosswind leads to a force and a moment on the vehicle, which are described by the following equations:

$$F_{\mathrm{w}} = \frac{2.5\pi}{2} v_{\mathrm{w}}^2 \tag{4-4}$$

$$M_{\mathrm{w}} = \left(2.5\frac{\pi}{2} - 3.3\frac{\pi^3}{8}\right) v_{\mathrm{w}}^2 + \frac{l_{\mathrm{f}} - l_{\mathrm{r}}}{2} F_{\mathrm{w}} \tag{4-5}$$

The forces are implemented on the center of gravity of the vehicle. The influence on the vehicle is shown in Figure 4-2, with V_x being the drive direction. The crosswind will be implemented as a step input.

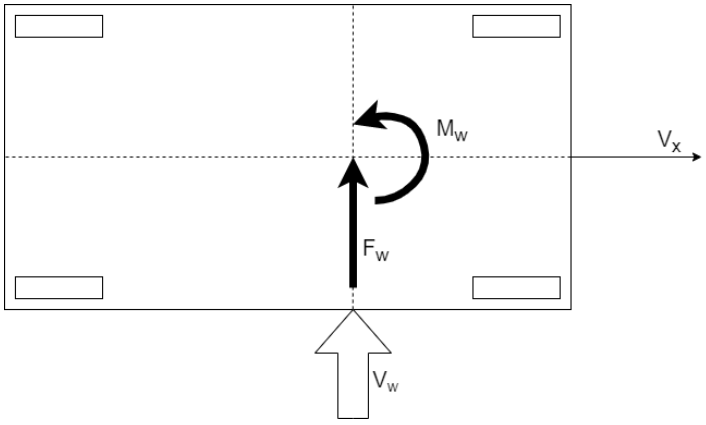

Figure 4-2: Implementation of wind disturbance

Sensor noise

The controller will get the information of the initial states from the sensors. The sensors could be inaccurate. On the initial states of y, ψ and $\dot{x}$ white noise is added to simulate sensor noise, see Figure 4-3.

The white noise is added with the block "Band-Limited White Noise" in Simulink [3], see Figure 4-3. The sample time of the block is set on the same sample time of the controller (0.04 second), the noise power is set on 0.005. The conversion block will multiple the noise with a conversion factor. The conversion factor is depended on the state the noise is added, see Table 4-1.

Table 4-1: Conversion factors for sensor noise

Conversion y	0.10 [m]
Conversion ψ	0.05 [rad]
Conversion $\dot{x}$	5 [km/hour]

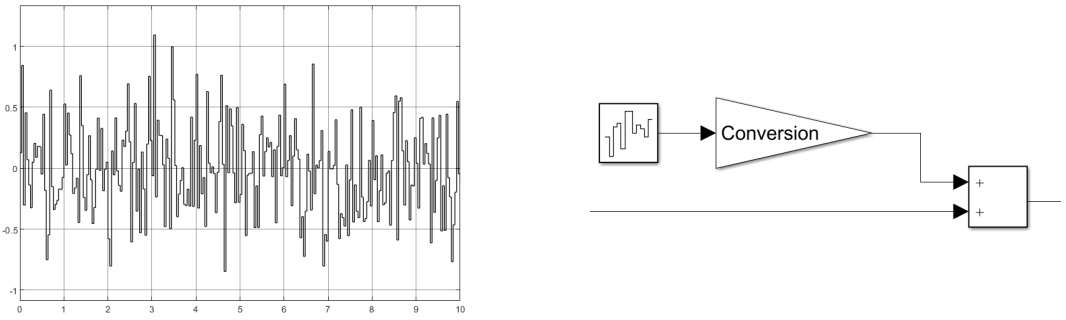

Figure 4-3: White noise implementation in Simulink [3]

Road friction change

In the real world the friction of the road can change, for example due to rain. The friction change can lead to dangerous scenarios, such as spinning out of the corner due to the lost of traction. Normal driving conditions the μ is around one. But for driving on wet asphalt the μ can go to 0.5 and with ice conditions to 0.1 [42]. The different road friction can be simulated to show the behaviour of the vehicle.

4-2-2 Trajectory

The controller is designed to safely and comfortably track a path or a velocity profile. Therefore, we test the controller on the following trajectories.

Double lane change (ISO 3888)

The double lane change is a manoeuvre to test the lateral control of the vehicle in an emergency. The test is included in the international standard organization under ISO 3888. To pass the double lane change, the vehicle must stay within the boundaries [43], see Figure 4-4.

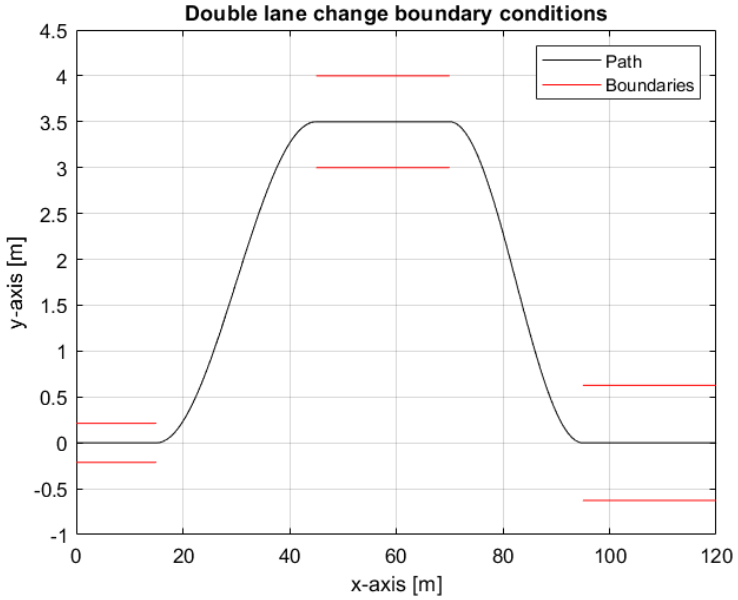

Figure 4-4: Double lane change with boundary conditions

Velocity profile

To test the longitudinal control, we built a velocity profile. The velocity profile is driven on a straight path. The velocity profile has both parts accelerating and decelerating, see Figure 4-5.

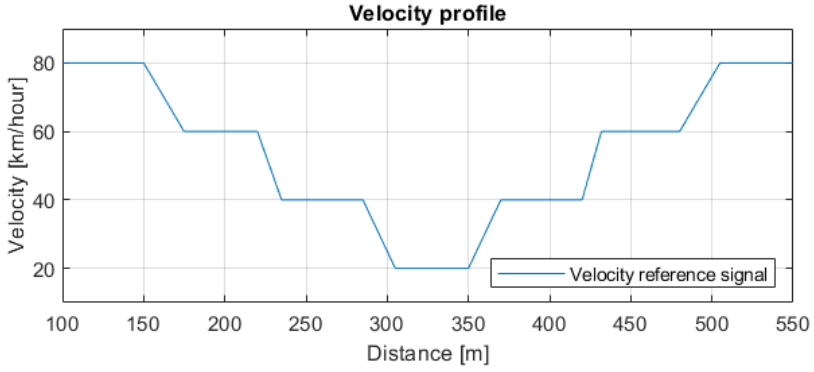

Figure 4-5: Velocity profile on straight path

Sine wave

To create a test which creates a lot of motion sickness we built a sine-wave path. The frequency of the sine-wave path is chosen to be 0.2 Hz, which is in the motion sickness frequency. The path can be seen in Figure 4-6. The sine-wave path is made with the following equation:

$$Y_{\text{position}} = 1.5\sin(0.4\pi(t-5)) \tag{4-6}$$

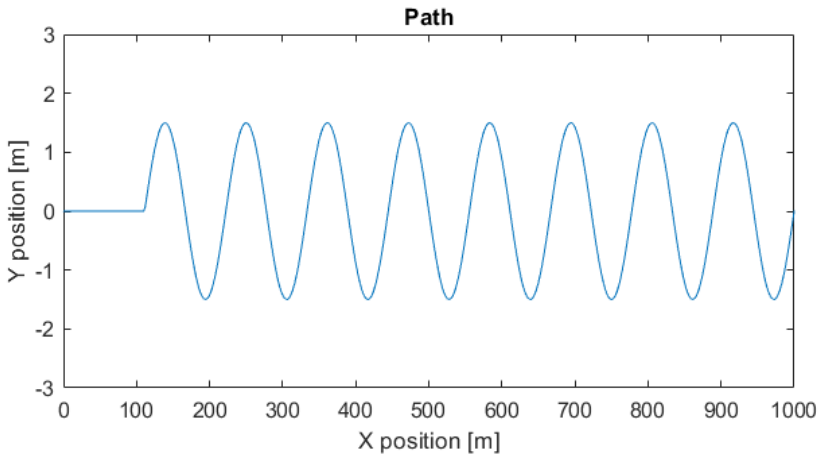

Figure 4-6: Path based on a sine wave

4-3 Tuning

To tune the weights of the controller, an algorithm is written inspired by other algorithms for automatic tuning [44, 45]. A self-made grid search algorithm is used to find the optimal solution. A pseudo code is written in the case of two variable weights to show how the algorithm works, see Algorithm 1.

To test every combination of the two variable weights, two loops are created, see code line 9 and 10. The pseudo code has four different values to test for each of the variable weights, which leads to 4^2 different combinations. From all the different combinations the optimal weights are found and new values are selected, see code line 18-33. The selecting of the new values are done in a similar way as in Figures 4-7a and 4-7b. The start of the arrow represents the optimal weight, in Figure 4-7a weight three and in Figure 4-7b weight four. The process is repeated a number of times.

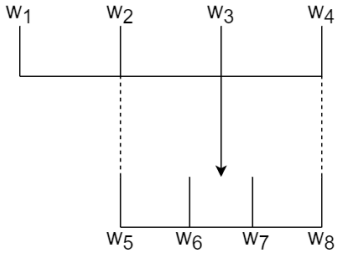

(a) selecting new weights from within the boundary weights

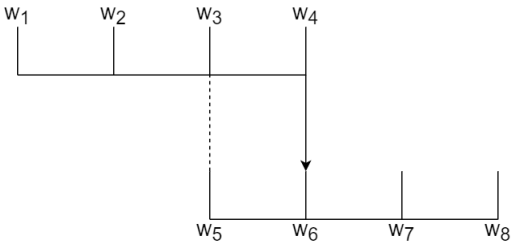

(b) selecting new weights from the boundary weights

Figure 4-7: Selecting new weights

There is a chance that the problem is non-convex and the tuning algorithm will optimize to a local minimum. The same problem arises when tuning by hand unless every possible combination is tried. Trying every possible combination is impossible to do due to time restrictions. The tuning is done for all the controllers under the same constraints.

4-4 System

The simulations are done in Matlab/Simulink [3, 29]. Simulink has a fixed step size of 10^{-3} second, while using the ode4 solver (Runge-Kutta). Due to initializing Simulink, the controller is activated after 2 seconds. The simulation are done on an Intel I5-9300H processor with 8 GB RAM and runs on Windows. The solver used for the model predictive controller is FORCES PRO [46, 47].

Algorithm 1 Algorithm for automatic tuning of the weights

1: **procedure** TUNING WEIGHTS
2: $y = w_{\mathrm{a}}x_1 + w_{\mathrm{b}}x_2$
3: $w_{\mathrm{a},1}$ = *Boundary condition 1*; $w_{\mathrm{a},1}$ = *Boundary condition 2*
4: $w_{\mathrm{b},1}$ = *Boundary condition 1*; $w_{\mathrm{b},1}$ = *Boundary condition 2*
5: $i = 1$
6: **while** $i \neq N + 1$ **do**
7: $w_{\mathrm{a}} = linspace(w_{\mathrm{a},1}, w_{\mathrm{a},4}, 4)$; $w_{\mathrm{b}} = linspace(w_{\mathrm{b},1}, w_{\mathrm{b},4}, 4)$
8: $j = 1$; $k = 1$;
9: **while** $j \neq 5$ **do**
10: **while** $k \neq 5$ **do**
11: *Run simulation with values* $w_{\mathrm{a}}(j)$ $w_{\mathrm{a}}(k)$
12: *Save data*
13: $k = ++$
14: **end while**
15: $j = ++$; $k = 1$
16: **end while**
17: *Find optimal weights*
18: **if** $w_{\mathrm{a,optimal}} = w_{\mathrm{a},1}$ **then**
19: $w_{\mathrm{a},1} = w_{\mathrm{a},1} - 2(w_{\mathrm{a},2} - w_{\mathrm{a},1})$; $w_{\mathrm{a},4} = w_{\mathrm{a},2}$
20: **if** $w_{\mathrm{a},1}<0$ **then**
21: $w_{\mathrm{a},1} = 0$
22: **end if**
23: **end if**
24: **if** $w_{\mathrm{a,optimal}} = w_{\mathrm{a},2}$ **then**
25: $w_{\mathrm{a},1} = w_{\mathrm{a},1}$; $w_{\mathrm{a},4} = w_{\mathrm{a},3}$
26: **end if**
27: **if** $w_{\mathrm{a,optimal}} = w_{\mathrm{a},3}$ **then**
28: $w_{\mathrm{a},1} = w_{\mathrm{a},2}$; $w_{\mathrm{a},4} = w_{\mathrm{a},4}$
29: **end if**
30: **if** $w_{\mathrm{a,optimal}} = w_{\mathrm{a},4}$ **then**
31: $w_{\mathrm{a},1} = w_{\mathrm{a},3}$; $w_{\mathrm{a},4} = w_{\mathrm{a},4} + 2(w_{\mathrm{a},4} - w_{\mathrm{a},3})$
32: **end if**
33: *Repeat step 16-40 for* w_{b}
34: i=++
35: **end while**
36: **end procedure**

Chapter 5

Filter evaluation and implementation

A filter can process a signal by removing unwanted parts of a signal. In the case of improving the comfort the filter should process the signal to keep only the important frequencies (i.e., motion sickness and general discomfort), as Section 1-1 discusses. To increase comfort in a driving vehicle, a filter was implemented in the cost function (Section 3-2-2).

To see what influences the behaviour of the filter, offline tests are done. The test data is created by a vehicle driving the double lane change and saving the accelerations. With the data, tests can be done on the filters without taking the vehicle into consideration. From the test results a conclusion can be made on how to implement the filter.

The filters implemented in the controller are for motion sickness 0.03-0.2 Hz and for general discomfort 1-2 Hz, see Section 3-2-2. The filters are compared to the continuous filtered accelerations for the same frequencies.

5-1 Initializing filter

The influences on how to initialize the filter are researched. The two different ways of initializing are: initialize with zero or using a feedback loop to initialize with the calculated states of the previous time step. The test is done with a time horizon of 1 second and a sampling time of 0.04 seconds.

Initialize with zero

In the following results the states of the filter are initialized with zero ($z(1) = 0$) on every new time step of the MPC.

$$z(k+1) = Az(k) + Ba(k) \tag{5-1}$$
$$a_{\text{filter}}(k) = Cz(k) + Da(k) \tag{5-2}$$

The results of step 5 and 25 are plotted in Figure 5-2. The performance of the controller is measured in the difference between the control filter and the continuous filter. If the error between the lines are small, the filter has a good performance.

Initialize filter with previous time step

To increase the performance of the filter, the states of the last time step can be used to initialize the filter of the current time, see Figure 5-1. The filter equations are given in Equations (5-1) and (5-2), with z being the states. The result can be seen in Figure 5-3.

Figure 5-1: Initialize with states of the previous time step

5-1-1 Discussion

If the filter states are initialized with zero, the filter needs time to find the correct states. While finding the correct states the error is larger, as can be seen in the larger error on step 5 compared to step 25. On a low frequency finding the states takes a longer time than on a high frequency, this leads to a larger error on step 25 for motion sickness than for general discomfort.

Comparing Figures 5-2 and 5-3 can be seen that the performances of the filter increases when the filter is initialized with the previous time step. Implementing the filter in the controller will be done with initializing the filter with the previous time step, to create a more accurate filtered acceleration.

5-2 Sample time

The effect of the sample time is showed with the controller initialized by the previous state of the filter. The time horizon is kept constant, see Table 5-1. The sum of the root-mean-square is taken for all steps on the prediction horizon each sampling time and plotted, see Figure 5-4. If the sample time is lower for the same time horizon, the filter can estimated more accurately the filtered acceleration. By using a low sample

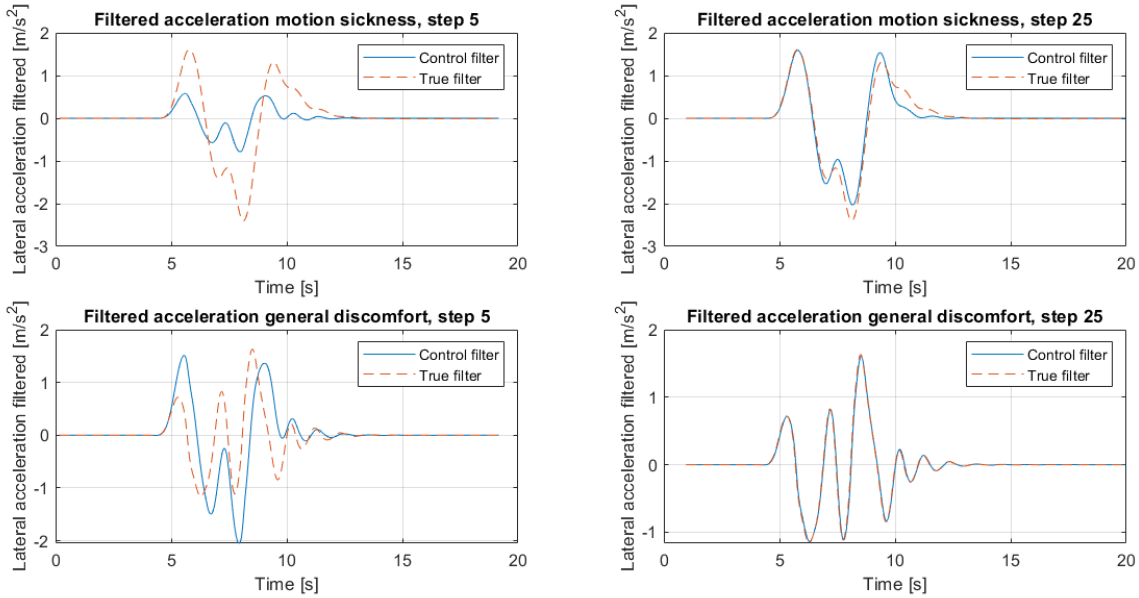

Figure 5-2: Initialize with zero

time the MPC needs to calculate more steps on the same time horizon, which makes the problem more computationally expensive compared to the lower time steps. In the controller is chosen for a time step of 0.04 second, see Section 4-1-1.

Table 5-1: Test setup for Figure 5-4

Sample time [s]	Steps	Time horizon [s]
0.02	50	1
0.04	25	1
0.10	10	1

5-3 Time horizon

The MPC can be used with different time horizons. Before using different time horizons, a test on the performance of the filter is done. The tested values are given in Table 5-2. The results of the test is given in Figure 5-5. The root-mean-square is calculated over all the steps, meaning that a time horizon of 1 second has 25 values for the calculation of the root-mean-square and 2 seconds has 50 steps. The short time horizon is more influenced by outliers on the calculation of the root-mean-square error due to having less values to calculate the root-mean-square.

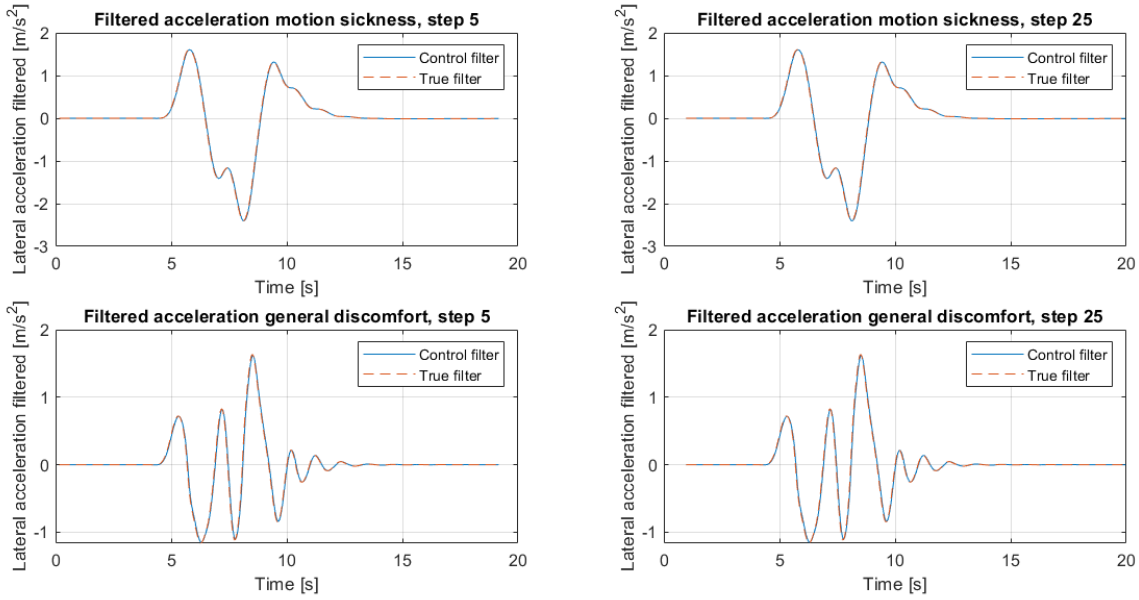

Figure 5-3: Initialize filter with previous time step

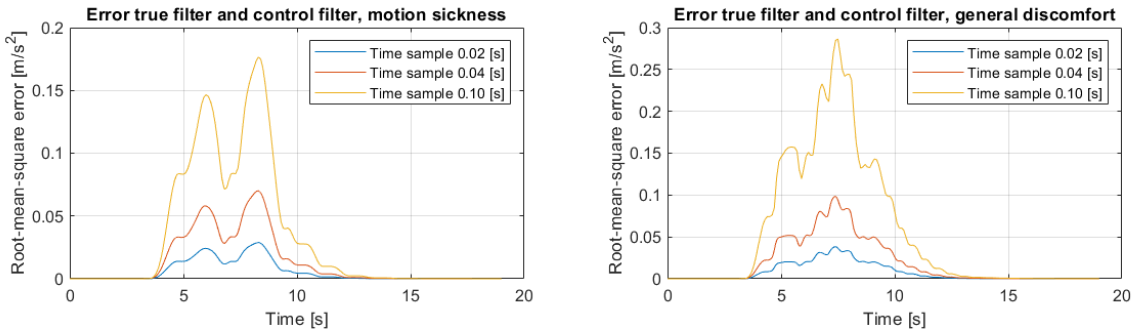

Figure 5-4: Influence sample time on filter

5-4 Filtered signal behaviour

By implementing a filter the signals are processed further. The filter takes a longer time to describe the full effects of the filtered signals compared to the input signal. Therefore, the filtered signals behaviour is influenced for a longer time after a change in input signal. The long influence of the filter time wise could have a great influence on the performance of the controller. If the controller is unable to predict the behaviour of the filtered accelerations correctly due to time constraints, the performance could be lower. To see the behaviour of the filtered signals, a test is made in Simulink. The test is done on frequency of 25 Hertz, sample time of 0.04 seconds.

The filter is tested with a change in value for one time step, see Figure 5-6. The disadvantage from the filter can be seen in the figure. The MPC needs a longer time horizon to fully understand the behaviour of the filtered acceleration. In the figure a time horizon of 1 second is shown between the red dotted lines. On time step one of

Table 5-2: Test setup for Figure 5-5

Sample time [s]	Steps	Time horizon [s]
0.04	25	1
0.04	50	2
0.04	75	3

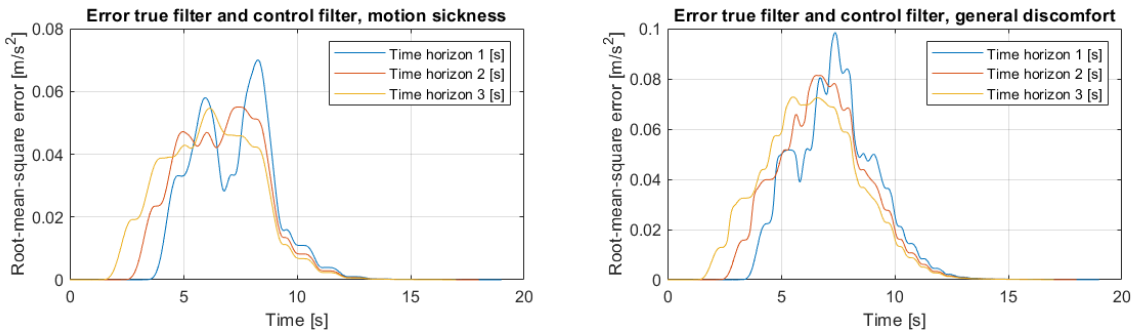

Figure 5-5: Influence time horizon on filter

the time horizon a change in the input signal is made. As can be seen in the figure the time horizon does not include the whole behaviour of the filtered signals. Therefore, the part after the second dotted line is not taken into consideration in the cost function due to the limit on the time horizon. The effect of the motion filter carries on for longer than the effect of the general discomfort filter, due to the difference in frequency. The frequency of motion sickness is low compared to general discomfort.

5-5 Summary

To increase the performance of the controller the states of the filter should be initialized with the states of the last time step. This will give the filter "memory" of the driven road. The sample time has influences on the performance, the lower the sample time the more accurate the filter can calculate the filtered acceleration. The filtered accelerations take a longer time to show the full behaviour, see Figure 5-6.

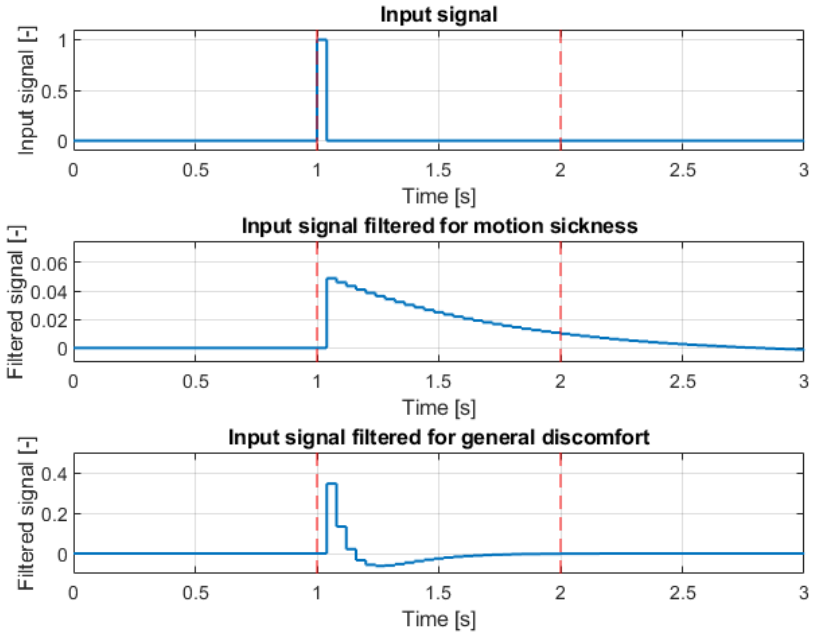

Figure 5-6: Filtered signal behaviour

Chapter 6

Lateral influences on the combined controller

To increase comfort lateral acceleration can be filtered and penalised for motion sickness and general discomfort, see Section 3-2-2. The method is researched in three controllers, the motion sickness controller, the general discomfort controller and a combined motion sickness and general discomfort controller. The method is compared to three other controllers, each with a different cost function. The differences in the controllers come from different cost functions and the implementation of the filters. In the end a conclusion can be made about the advantages and disadvantages of the filters.

The motion sickness filter will have a positive influence on comfort by keeping the accelerations in the frequency of motion sickness down. Since the motion sickness filter will only penalise the motion sickness frequency, accelerations in other frequencies can grow which could lead to a low performance in general discomfort. The general discomfort filter will have similar effects as described above for the motion sickness filter, only the frequencies will differ.

The motion sickness filter uses a low frequency filter, the low frequency filter will react slower on high frequency changes. As an example the controller will react poorly on wind disturbance. However, the filter will be less influenced by high frequency noise. Where the motion sickness filter lacks due to the slow behaviour the general discomfort filter can perform, due to the fast response of the high frequency filter.

A compact version of the results are given in the following chapters. For the complete results see Appendix B.

6-1 Adding penalties

Multiple terms can be added in the cost function to increase comfort performance. In the results below each comfort term is tested by increasing the weight from zero, while

the other terms are kept constant, see Table 6-1. The description of the comfort terms can be found in Section 3-2, the variable terms are: $w_{\triangle\delta}$, w_{ay} , $w_{\text{ay,ms}}$, $w_{\text{ay,gd}}$. The test is done on the double lane change of 60 km/hour. The double lane change manoeuvre is chosen due to creating uncomfortable accelerations.

Both lateral and longitudinal accelerations have influences on comfort, see Section 1-1. To test only the lateral control, the longitudinal penalties are set high to create similar longitudinal performance over all the controllers. In the end both lateral and longitudinal control should be tuned to create maximal comfort, see Chapter 8. The comfort in the plots are shown to be the mean comfort over the terms of RMS and MTVV for motion sickness and general discomfort, see Section 4-1-2.

Table 6-1: Weights applied on the controllers, w_{var} is a variable weight

Controller	J_1	J_2	J_3	J_4
w_{y}	50	50	50	50
w_{ψ}	800	800	800	800
w_{v}	3.0e05	3.0e05	3.0e05	3.0e05
$w_{\triangle\delta}$	w_{var}	0	0	0
$w_{\triangle\text{a}}$	5000	5000	5000	5000
w_{ay}	0	w_{var}	0	0
$w_{\text{ay,ms}}$	0	0	w_{var}	0
$w_{\text{ay,gd}}$	0	0	0	w_{var}

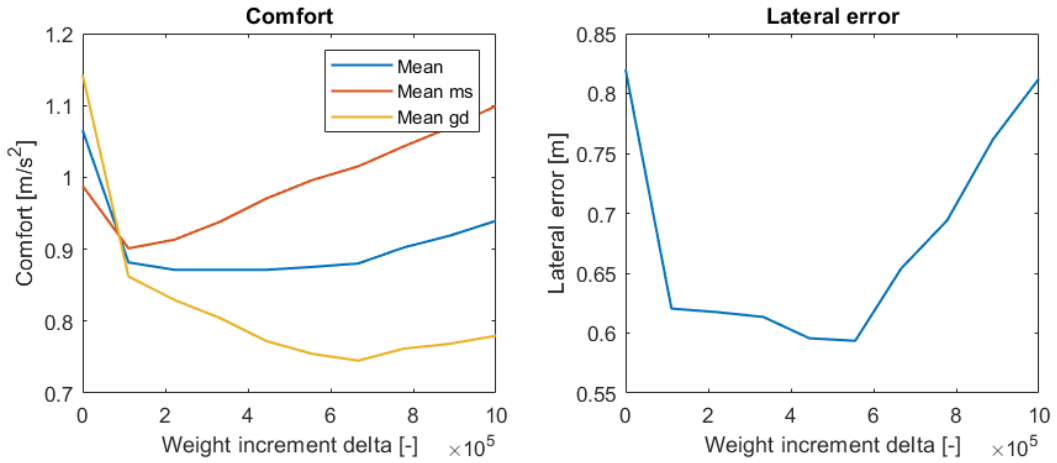

Figure 6-1: Effect of changing weight $\triangle\delta$

Discussion

In Figures 6-1 till 6-4 can be seen that each term can improve the comfort. The weight of $\triangle\delta$ can have a positive effect on both comfort and lateral error. The terms which penalises the lateral acceleration (filtered and unfiltered) all increases the lateral error. Combining the penalty $w_{\triangle\delta}$ with a penalty on lateral acceleration (filtered or unfiltered) will lead to more comfort.

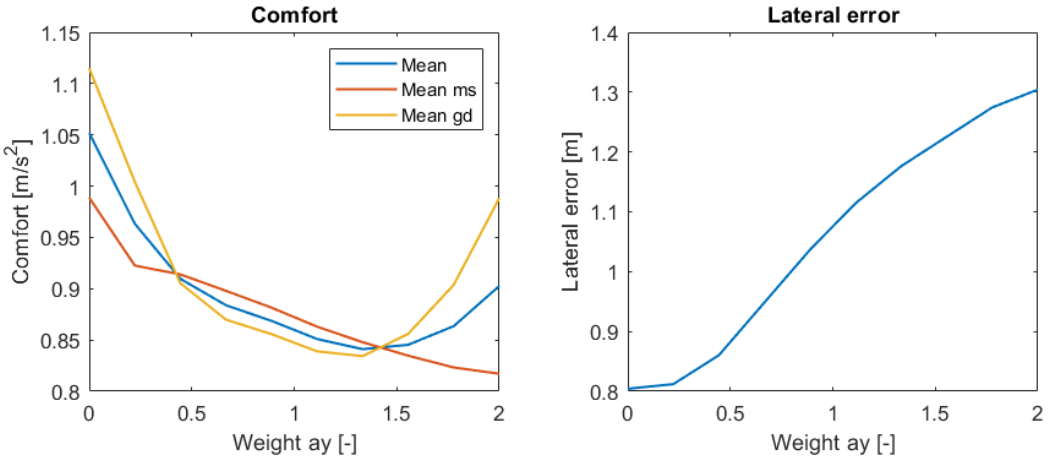

Figure 6-2: Effect of changing weight ay

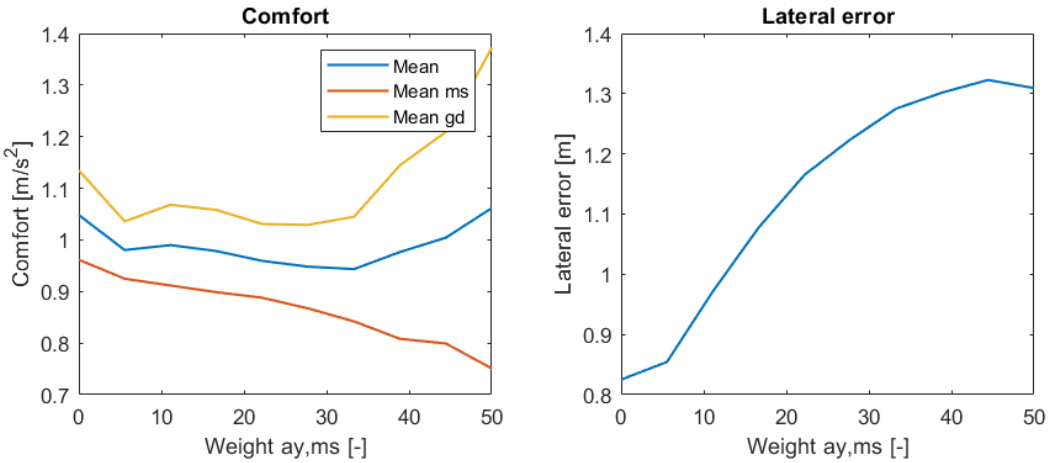

Figure 6-3: Effect of changing weight ay, ms

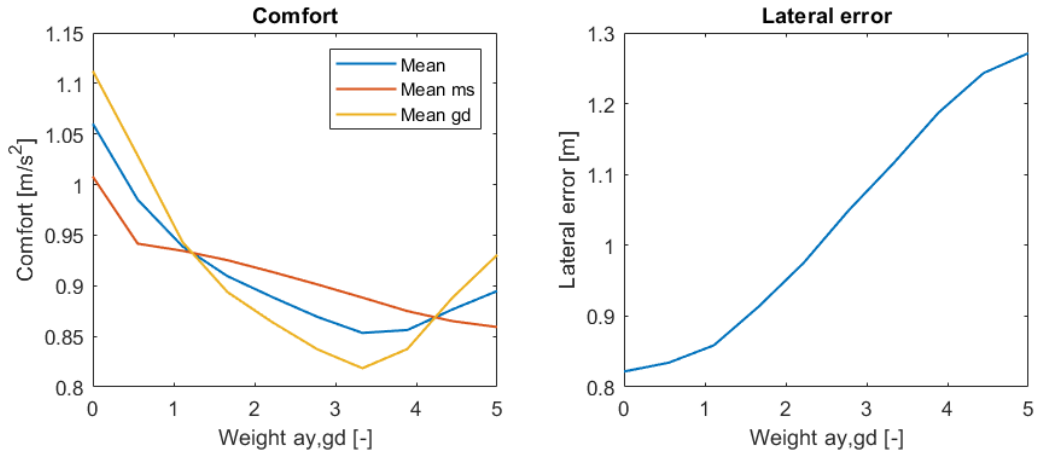

Figure 6-4: Effect of changing weight ay, gd

On the higher weights the discomfort can grow. A possible reason could be bad tuning. For example in the case of weight increment δ the vehicle's settling time and overshooting increases, see Figure 6-5.

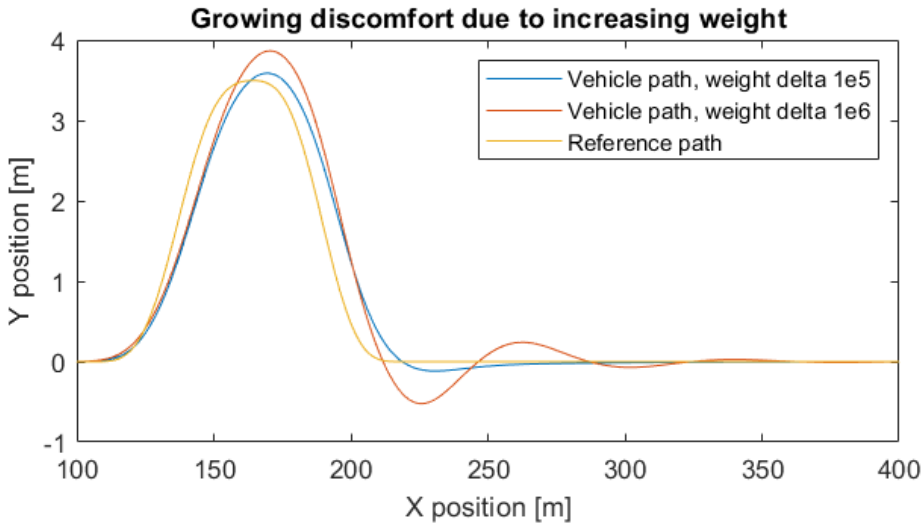

Figure 6-5: Growing discomfort due to increasing the weight on increment delta

6-2 Double lane change

The controllers which penalise the filtered acceleration can be more effective in creating comfort due to penalising the motion sickness or general discomfort directly. Six controllers are tuned and compared, see Table 6-2. In controllers J_1, J_2 and J_6 the filters are not present. In controller J_3 only the motion sickness filter is implemented and in controllers J_4 and J_5 both filters are implemented, see Table 6-2. The tuning is done with the tuning algorithm in Section 4-3 and processed further by hand for optimal performance in terms of comfort. The scenario of the double lane change at 80 km/hour is chosen as test setup due to generating high accelerations, see Section 4-2-2.

Table 6-2: Weights applied on the controllers

Controller	J_1	J_2	J_3	J_4	J_5	J_6
w_{y}	50	50	50	50	50	50
w_{ψ}	2.70e3	7.62e3	4.50e3	9.72e3	3.50e3	2.71e4
w_{v}	3.00e5	3.00e5	3.00e5	3.00e5	3.00e5	3.00e5
$w_{\triangle\delta}$	1.07e6	3.00e6	2.57e6	2.95e6	1.27e6	0
$w_{\triangle\mathrm{a}}$	5000	5000	5000	5000	5000	5000
w_{ay}	x	19.7	0	0	0	x
$w_{\mathrm{ay,ms}}$	x	x	149.1	0	75	x
$w_{\mathrm{ay,gd}}$	x	x	x	83.4	7.6	x

x means the term is not implemented in the controller

Table 6-3: Double lane change 80 km/hour

Controller	J_1	J_2	J_3	J_4	J_5	J_6
Time horizon [s]	1	1	1	1	1	1
RMS ms $[m/s^2]$	0.738	0.66	0.636	0.67	0.644	0.761
Improvement [%]	–	**10.6**	[**13.9**]	**9.2**	[**12.8**]	-3.1
RMS gd $[m/s^2]$	0.701	0.654	0.687	0.65	0.677	1.29
Improvement [%]	–	**6.7**	**2**	(**7.3**)	(**3.4**)	-84.5
MTVV ms $[m/s^2]$	1.49	1.35	1.3	1.37	1.32	1.51
Improvement [%]	–	**9.3**	[**12.3**]	**7.9**	[**11.5**]	-1.4
MTVV gd $[m/s^2]$	1.25	1.15	1.22	1.13	1.21	2.1
Improvement [%]	–	**7.5**	**2.2**	(**9.3**)	(**3.3**)	-68.1
mean comfort $[m/s^2]$	1.04	0.954	0.962	0.955	0.961	1.42
Improvement [%]	–	**8.6**	**7.8**	**8.5**	**7.9**	-35.6
y error max $[m]$	0.3	0.299	0.3	0.3	0.3	0.292

Increase performance due to motion sickness filter, [ ]
Increase performance due to general discomfort filter, ( )
Improvement compared to the baseline controller, J_1 –
Bold is a positive effect

Discussion

The results of the double lane change are given in Table 6-3. Controllers J_2 and J_4 have the highest performance in terms of general discomfort, with a small advantage for J_4. By penalising the motion sickness directly controller J_3 has the highest performance in motion sickness comfort. Combining both motion sickness and general discomfort filter in one controller leads to a performance between the controllers for motion sickness and general discomfort, see controller J_5. An advantage of penalising both motion sickness and general discomfort in one controller is that the ratio between the weights of the two filters can be selected. Therefore, the passengers could select the ratio between the weights on motion sickness and general discomfort to create a controller which fits to the needs of the passengers.

The motion sickness filter uses a low frequency filter, by increasing the time horizon the controller could increase the performance of the predictions about motion sickness behaviour. By increasing the performance of the predictions more motion sickness comfort could be achieved. In Section 6-3 results are created with a longer time horizon.

An advantage/disadvantage from penalising lateral acceleration (filtered and unfiltered) is that the longitudinal behaviour is influenced by the lateral acceleration terms. To keep the lateral acceleration low, the controller wants to brake. A direct effect of a lower velocity is a lower lateral acceleration in a corner. However, the braking behaviour can also lead to discomfort due to the longitudinal accelerations. In the results of Table 6-3 the vehicle has a constant velocity. The effect of braking is described in Section 6-4, these effects can lead to more comfort if tuned right. In Chapter 8 the lateral and longitudinal control are tuned together to find the optimal results.

6-3 Motion sickness

Motion sickness is generated in the lower frequencies, see Section 1-1. Due to the low frequency motion sickness has a large time period. The controller can create more accurate predictions of the motion sickness with a longer time horizon. The controller tested is controller J_3, with different time horizons. For the different time horizons the controller is re-tuned.

6-3-1 Double lane change with different time horizons

The results of increasing the time horizon can be found in Table 6-4. The longer time horizon improves the total comfort by creating less general discomfort. For the motion sickness comfort the results are similar with different time horizons. Increasing the sample time leads to a decrease in performance due to the growing errors within the controller. Increasing the time horizon without increasing the sample time creates a more complex problem due to the increase of the number of calculations. When increasing the time horizon a trade off between complexity (solving time) and sample time should be made.

The controllers are tuned for the highest comfort without crossing the lateral boundaries. To achieve more comfort in motion sickness soft/hard boundary constraints could be implemented. The highest lateral error is only reached at a few sections of the track, see Figure 6-6. The controller would be able to have a larger lateral error on the other parts of the path without crossing the boundaries.

While tuning for a time horizon of 10 seconds, no tuning was found within the boundaries of the double lane change. The tuning was done with a sample time of 0.20 seconds. Reasons for not finding a tuning could be that the reference generator performances goes down with a longer time horizon. Another reason could be an increase in error within the MPC due to using larger sample time.

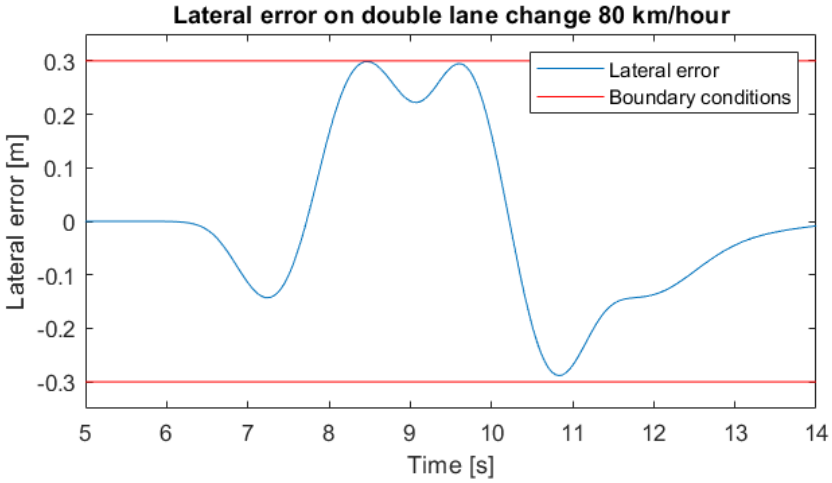

Figure 6-6: Lateral error controller J_3, without soft or hard constraints

Table 6-4: Double lane change 80 km/hour, different time horizons

Controller	J_3	J_3	J_3	J_3
Time horizon $[s]$	1	2	2	5
Sample time $[s]$	0.04	0.04	0.10	0.10
RMS ms $[m/s^2]$	0.667	0.673	0.678	0.667
Improvement [%]	–	-0.9	[-1.7]	0
RMS gd $[m/s^2]$	0.721	0.56	0.568	0.545
Improvement [%]	–	**22.2**	[**21.1**]	**24.3**
MTVV ms $[m/s^2]$	1.3	1.32	1.33	1.3
Improvement [%]	–	-1	[-1.6]	**0.1**
MTVV gd $[m/s^2]$	1.22	0.971	0.993	0.959
Improvement [%]	–	**20.4**	[**18.6**]	**21.4**
mean comfort $[m/s^2]$	0.978	0.88	0.891	0.869
Improvement [%]	–	**10**	[**8.9**]	**11.2**
y error max $[m]$	0.3	0.298	0.297	0.298

Decrease improvement due increase in sample time [ ]
The improvements are compared to the first result column (–)
Bold is a positive effect

6-3-2 Sine wave

In the real world there are roads which creates more motion sickness than the double lane change, for example a mountain road with a lot of curves. To show more potential of the motion sickness filter a sine wave is made in the frequency of motion sickness, see Section 4-6. The sine wave is driven at 80 km/hour. The motion sickness filter (J_3) works well on the sine wave, the root-mean-square and maximum-transit-vibration-value for motion sickness decreases by respectively 17.6% and 17.2% compared to the basic controller (J_1). A positive side effect is that the controller for motion sickness (J_3) also decreases the general discomfort, compared to controller J_1 with 18% (RMS) and 17.2% (MTVV). The results are taken from one period of the sine wave.

The motion sickness filter has a high performance on other velocities as well. To show the performance on an other velocity the controller needs to be re-tuned. If the controller is not re-tuned the lateral error grows on lower driven velocities, see appendix Table B-4. The sine wave is recreated on the velocity of 60 km/hour, using the same formula as in Section 4-6. The sine wave has a similar frequency of 0.2 Hz as in the sine wave of 80 km/hour. Controllers J_1 and J_3 are re-tuned on the double lane change with a maximum lateral error of 0.3 meters. One period of the sine wave is taken for the results. As can be seen in Table 6-6 the motion sickness filter leads to high comfort.

Increasing acceleration terms on the sine wave

In the future the controllers might be able to have dynamic weights, the weights could change depending on the scenario ahead. The comfort on the sine wave could be increased by increasing the weights on lateral acceleration (filtered and unfiltered).

Table 6-5: One period of the sine wave at 80 km/hour

Controller	J_1	J_2	J_3	J_4	J_5	J_6
Time horizon [s]	1	1	1	1	1	1
RMS ms $[m/s^2]$	0.93	0.83	0.767	0.847	0.793	0.931
Improvement [%]	–	**10.7**	[**17.6**]	**8.9**	**14.7**	0
RMS gd $[m/s^2]$	0.413	0.366	0.339	0.374	0.35	0.459
Improvement [%]	–	**11.3**	[**18**]	**9.5**	**15.3**	-11.1
MTVV ms $[m/s^2]$	1.22	1.1	1.01	1.12	1.05	1.23
Improvement [%]	–	**10.4**	[**17.2**]	**8.6**	**14.4**	-0.1
MTVV gd $[m/s^2]$	0.528	0.482	0.442	0.495	0.459	0.609
Improvement [%]	–	**8.7**	[**16.2**]	**6.2**	**13**	-15.4
mean comfort $[m/s^2]$	0.774	0.694	0.64	0.709	0.663	0.806
Improvement [%]	–	**10.3**	[**17.2**]	**8.4**	**14.4**	-4.1
y error max $[m]$	0.174	0.178	0.25	0.162	0.216	0.386

Positive influence due to the motion sickness filter [ ]
The improvements are compared to the first result column (–)
Bold is a positive effect

The results are given in Figure 6-7. As can be seen in the figure the motion sickness filter has the highest comfort on the sine wave.

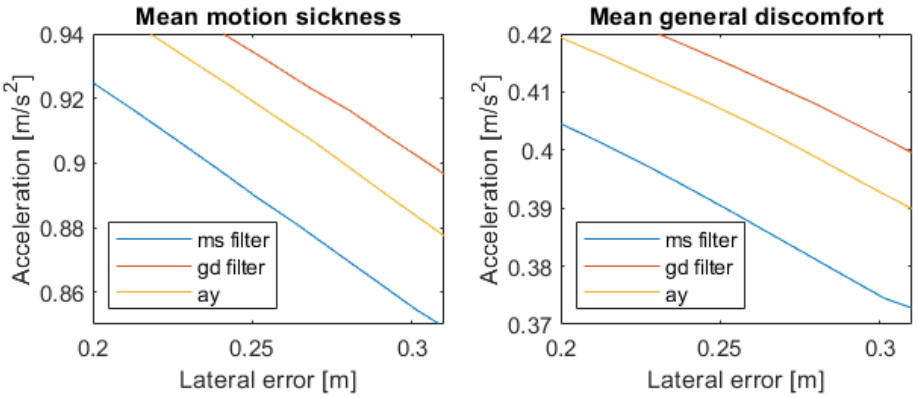

Figure 6-7: Comfort on the sine wave while increasing the weights on the acceleration terms (filtered and unfiltered), higher weight is higher lateral error

Table 6-6: Sine wave at 60 km/hour

Controller	J_1	J_3
RMS ms $[m/s^2]$	0.931	0.737
Improvement [%]	–	[**20.9**]
RMS gd $[m/s^2]$	0.443	0.324
Improvement [%]	–	[**26.9**]
MTVV ms $[m/s^2]$	1.22	0.971
Improvement [%]	–	[**20.4**]
MTVV gd $[m/s^2]$	0.493	0.423
Improvement [%]	–	[**14.1**]
mean comfort $[m/s^2]$	0.772	0.614
Improvement [%]	–	[**20.5**]
y error max $[m]$	0.255	0.324

Improvement due to the motion sickness filter [ ]
The controllers are re-tuned for the velocity of 60 km/hour
The improvement is compared to the first result column (–)
Bold is a positive effect

6-4 Longitudinal influence due to lateral acceleration penalty

By penalising the lateral acceleration, the vehicle wants to slow down to keep the lateral acceleration low in the corners. The lateral acceleration can be calculated from Equation (6-1) [15, 16, 17], with the meaning of the symbols given in Table 6-7:

$$a_{\mathrm{l}} = \frac{d\theta}{dt} v = \kappa \cdot v^2 = \frac{1}{\rho} v^2 \tag{6-1}$$

Table 6-7: Velocity profile

Symbols	Meaning
a_l	Lateral acceleration
θ	Vehicle orientation
ρ	Curvature radius
v	Longitudinal velocity
κ	Curvature

As seen in the equation the velocity influences directly the lateral acceleration. In the results of Section 6-2 the longitudinal penalties were set high to counter changes in longitudinal behaviour and test the lateral performance. To show the longitudinal behaviour the longitudinal penalties are decreased. The test is done on the double lane change at 80 km/hour, which creates high lateral accelerations and therefore effect the longitudinal behaviour.

6-4-1 Velocity increase

The velocity is influenced by the lateral acceleration weights (filtered and unfiltered) and the velocity weights. When setting the velocity and lateral acceleration weights to zero, or almost zero, to test the behaviour the vehicle's velocity goes up, see Figure 6-9. An explanation of the behaviour comes from the cost function. If the vehicle's velocity goes up, the vehicle can cover more ground. In Figure 6-8 can be seen that the path which covers more ground has a lower angle, the lower angle can lead to a positive influence on the cost of increment δ and ψ angle. In both paths the lateral error is the same. The effects can be different with different trajectories. Due to the increase in velocity the longitudinal error increases which leads to a poor tracking performance, the longitudinal error is not penalised within the controller.

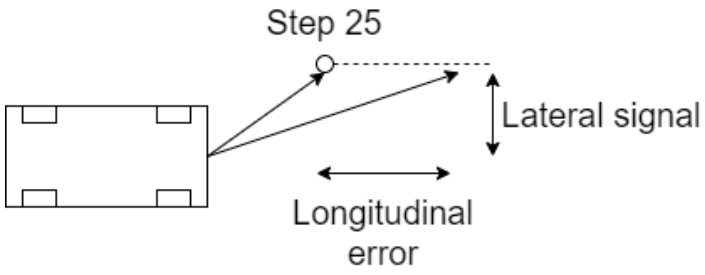

Figure 6-8: Minimizing cost due to increasing velocity and therefore travelled path, positive influences on increment δ and ψ angle cost

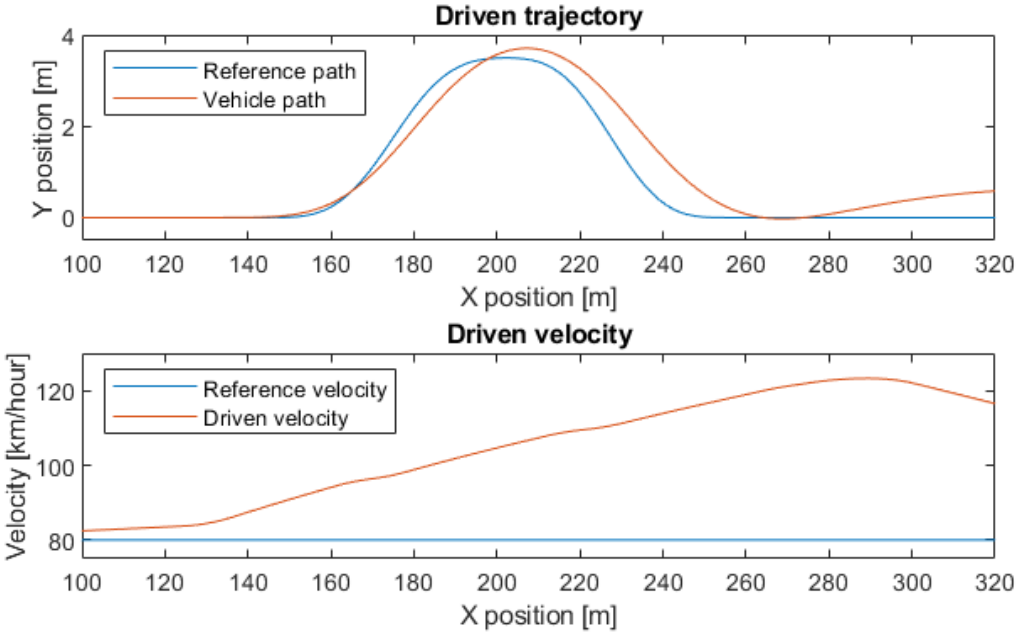

Figure 6-9: No penalties on the velocity weights leads to an increase in driven velocity

6-4-2 Influence lateral acceleration

To test the influences of the lateral acceleration terms (filtered and unfiltered) on longitudinal control, a penalty on the velocity terms must be applied in order to track the path well. The influences of the lateral acceleration terms will be limited due to the influences of increasing the velocity described in Section 6-4-1. The weights are kept constant except for the lateral acceleration terms, see Table 6-8. In Figure 6-10 a penalty is given on lateral acceleration with different weights from 0-30. The same is done for general discomfort in Figure 6-12. For motion sickness other weights are taken to show the effect (0-120), see Figure 6-11.

By penalising the lateral acceleration or the lateral general discomfort acceleration the driven velocity is kept lower than when no penalty is applied, see Figures 6-10 and 6-12. The lower velocity leads to a lower lateral acceleration. In case of the motion sickness filter can be seen that the velocity is not lower all the time, see Figure 6-11. The effect comes from overshooting and can be countered by tuning the longitudinal weights. The effect of overshooting can happen to all the controllers due to bad tuning.

In Figures 6-10, 6-11 and 6-12 can be seen that the longitudinal control changes to create a lower velocity. The changes in longitudinal control will lead to longitudinal accelerations, which could create discomfort. When tuning the controller both longitudinal and lateral control needs to be tuned.

Table 6-8: Weights applied on the controllers, w_{var} is a variable weight

Weights	Value		
w_{y}	50	50	50
w_{ψ}	3750	3750	3750
w_{v}	10	10	10
$w_{\triangle\delta}$	2.50e6	2.50e6	2.50e6
$w_{\triangle\text{a}}$	1	1	1
w_{ay}	w_{var}	0	0
$w_{\text{ay,ms}}$	0	w_{var}	0
$w_{\text{ay,gd}}$	0	0	w_{var}
w_{ax}	0	0	0
$w_{\text{ax,ms}}$	0	0	0
$w_{\text{ax,gd}}$	0	0	0

6-4-3 Discussion

In Section 6-4-1 can be seen that the velocity increases. The increase in velocity has a negative effect on comfort due to the increase in lateral and longitudinal acceleration. The effect could be countered by creating a more advanced reference generator and controller. The reference generator could create longitudinal position signals in order to penalise the longitudinal error, see Figure 6-8. Penalising both the lateral and longitudinal position leads to a cost on velocity. The cost on velocity happens due to minimizing the distances between the points and the vehicle within a time step. The

controller could be upgraded by taking into account the shift of the reference points due to a varying velocity. Shifting the reference points within the controller would make the problem more complex.

As can be seen in Section 6-4-2 the vehicle wants to slow down to keep the lateral acceleration down. The effect of slowing down before the corner could lead to an increase of comfort. The effect is, due to the problem described in Section 6-4-1, of low nature but could be beneficial in the future when the accelerating problem is fixed.

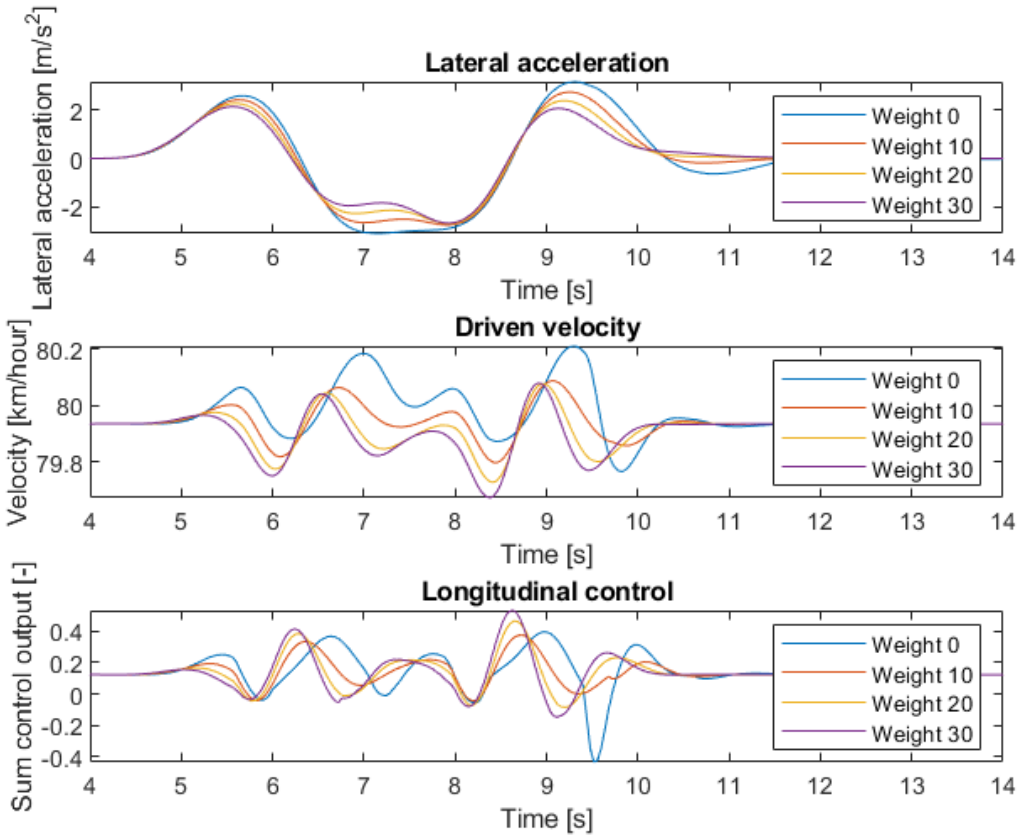

Figure 6-10: Longitudinal influences by penalising lateral acceleration with different weights on the double lane change of 80 km/hour

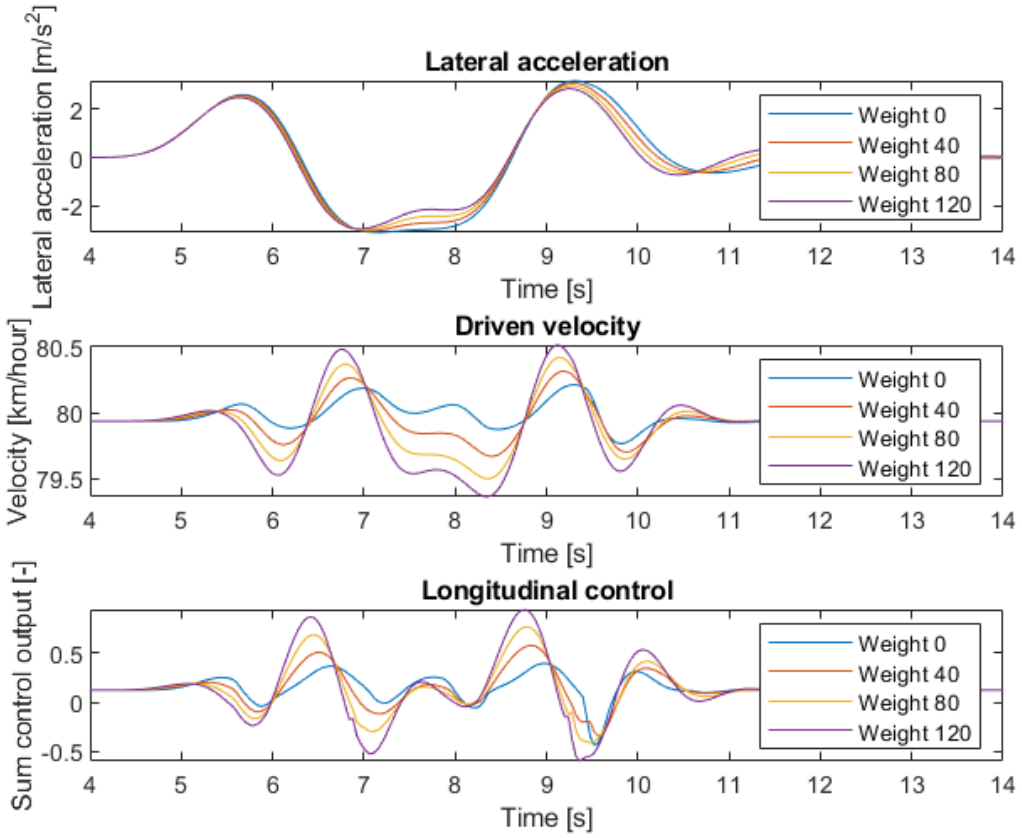

Figure 6-11: Longitudinal influences by penalising lateral motion sickness acceleration with different weights on the double lane change of 80 km/hour

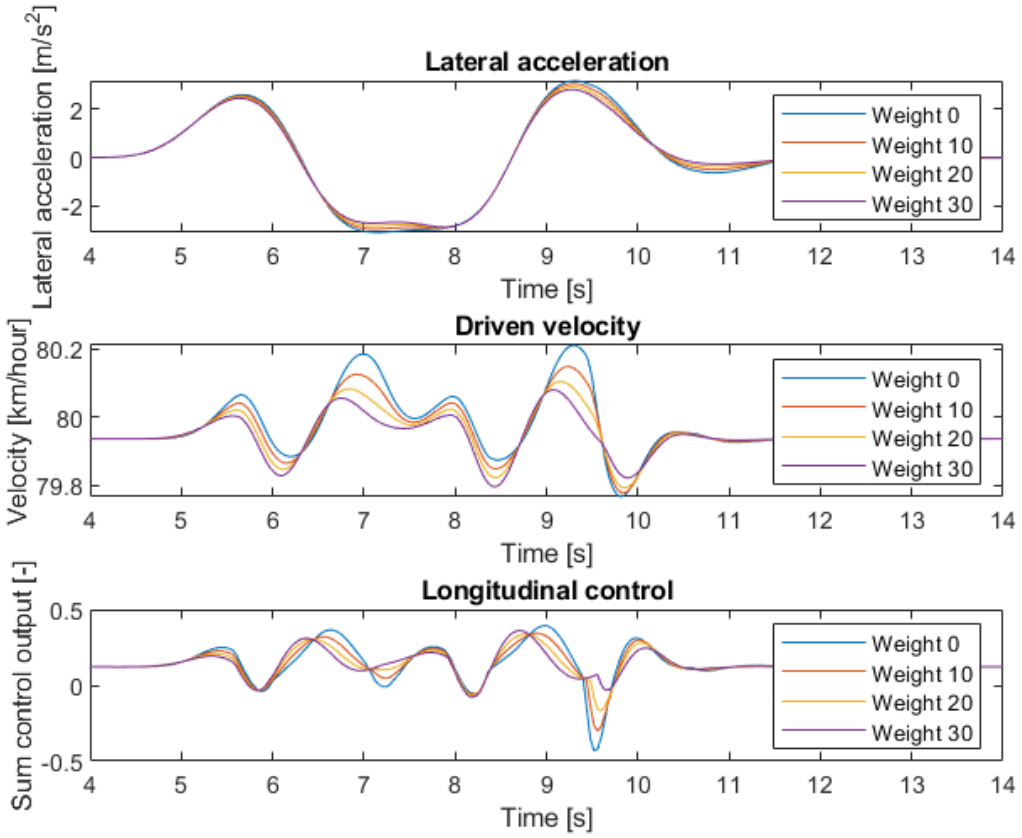

Figure 6-12: Longitudinal influences by penalising lateral general discomfort acceleration with different weights on the double lane change of 80 km/hour

6-5 Disturbance

When the controller is tested in a real vehicle, disturbances are present. The disturbances can have a negative effect on comfort and safety. The controllers are tested on three types of disturbances: wind disturbance, lower friction and sensor noise, see Section 4-2-1. The disturbances will give an indication where the controllers lacks in performance. The tuning of Section 6-2 is used. In the controller the disturbances are not modeled, therefore, the controller does not have extra tools to counter the disturbances.

6-5-1 Lower friction

The tire forces are influenced by the road friction [48]. Controllers which have lower accelerations will be less effected by a lower friction. The performance of controllers J_2-J_5 will increase compared to J_1. The test is done on the double lane change at 80 km/hour due to creating high lateral accelerations. The controllers are tested on safety and comfort in wet road conditions.

Table 6-9: Double lane change 80 km/hour with $\mu = 0.5$

Controller	J_1	J_2	J_3	J_4	J_5	J_6
Time horizon [s]	1	1	1	1	1	1
RMS ms $[m/s^2]$	0.735	0.674	0.664	0.682	0.662	0.751
Improvement [%]	–	**8.3**	**9.7**	**7.2**	**10**	-2.2
RMS gd $[m/s^2]$	0.691	0.669	0.686	0.672	0.678	1.22
Improvement [%]	–	**3.2**	**0.8**	**2.8**	**1.9**	-77.2
MTVV ms $[m/s^2]$	1.48	1.37	1.36	1.39	1.35	1.5
Improvement [%]	–	**7.2**	**8.2**	**6.1**	**8.8**	-1.2
MTVV gd $[m/s^2]$	1.22	1.18	1.22	1.18	1.21	2.01
Improvement [%]	–	**2.6**	-0.2	**3.2**	**0.8**	-65.5
mean comfort $[m/s^2]$	1.03	0.975	0.982	0.98	0.974	1.37
Improvement [%]	–	**5.4**	**4.7**	**4.9**	**5.5**	-33.1
y error max $[m]$	[0.387]	0.273	0.29	0.273	0.292	[0.371]

Without penalising a form of lateral acceleration, large lateral error [ ]
The improvements are compared to the first result column (–)
Bold is a positive effect

Discussion

The controllers which penalises the lateral acceleration (filtered and unfiltered) increase the comfort compared to controller J_1, see Table 6-9. In comparison with Section 6-2 the improvement decreases. The decrease comes from controller J_1 being unable to follow the track within the limits, in this case maximum lateral error of 0.3 meter. The controller J_1 can therefore drive a smoother trajectory. Controller J_6 is also unable to

stay within the lateral limits of track. Controllers J_2 till J_5 stay within the boundaries and create comfort.

6-5-2 Wind disturbance

The wind disturbance will have a direct influence on the lateral error by applying force to the side of the vehicle. The controller with motion sickness filter will take a longer time to react due to the low frequency filter, the controllers which penalise lateral acceleration directly or general discomfort (J_2 and J_4) can respond faster.

Table 6-10: Double lane change 80 km/hour with wind disturbance

Controller	J_1	J_2	J_3	J_4	J_5	J_6
Time horizon [s]	1	1	1	1	1	1
RMS ms $[m/s^2]$	0.739	0.661	0.634	0.671	0.644	0.782
Improvement [%]	–	**10.6**	**14.2**	**9.2**	**12.9**	-5.8
RMS gd $[m/s^2]$	0.715	0.651	0.689	0.647	0.673	1.86
Improvement [%]	–	**9**	**3.6**	**9.5**	**5.9**	-160
MTVV ms $[m/s^2]$	1.5	1.35	1.29	1.37	1.31	1.52
Improvement [%]	–	**10**	**13.7**	**8.6**	**12.4**	-1.6
MTVV gd $[m/s^2]$	1.3	1.14	1.2	1.12	1.18	3.33
Improvement [%]	–	**12.5**	**7.3**	**13.9**	**9.5**	-156
mean comfort $[m/s^2]$	1.06	0.949	0.955	0.951	0.951	1.87
Improvement [%]	–	**10.7**	**10.1**	**10.5**	**10.5**	-76.3
y error max $[m]$	0.504	[0.609]	[0.688]	[0.553]	0.499	0.473

Large lateral error due to penalties on acceleration [ ]
The improvements are compared to the first result column (–)
Bold is a positive effect

Discussion

In Table 6-10 can be seen that the lateral error becomes unsafe for all the controllers. Controllers J_2 till J_4 have the highest lateral error. The lateral error grows when filters are implemented with an exception of controller J_5. Controller J_5 has filters and achieves a low lateral error, similar to controller J_1. The lateral error of J_5 is kept low due to the lower cost on the filtered acceleration, see Appendix B-1-5.

An reason for the large lateral error of the controllers which penalises the lateral acceleration (filtered or unfiltered) can come from the mismatch between the true and predicted lateral acceleration due to presence of wind disturbance. The first lateral acceleration is calculated with the states given from the vehicle plant effected from the wind disturbance. The calculated lateral acceleration after the first state does not contain any wind disturbance and leads to an incorrect prediction of the lateral acceleration compared to the true lateral acceleration. When the controller can calculated the lateral acceleration correctly the comfort could increase further, a disturbance observer

could help in case of the wind disturbance. The lateral acceleration is calculated with the state space which can be found in A-1. Similar effects can happen to the other predicted states of the controllers.

Another disadvantage from having to penalise the low frequency of the lateral acceleration, is the slow change of the filtered acceleration, see Figure 6-13. The motion sickness filter does react slower than the general discomfort filter on a fast change, in this scenario a step input to simulate the wind disturbance. The controller with the motion sickness filter will take a longer time to react to the sudden changes, the longer reaction time leads to a longer time converging to the new value. The general discomfort controller, J_4, has the lowest lateral error of the controllers which penalises the lateral acceleration (filtered or unfiltered) due to the high frequency filter and therefore quick response.

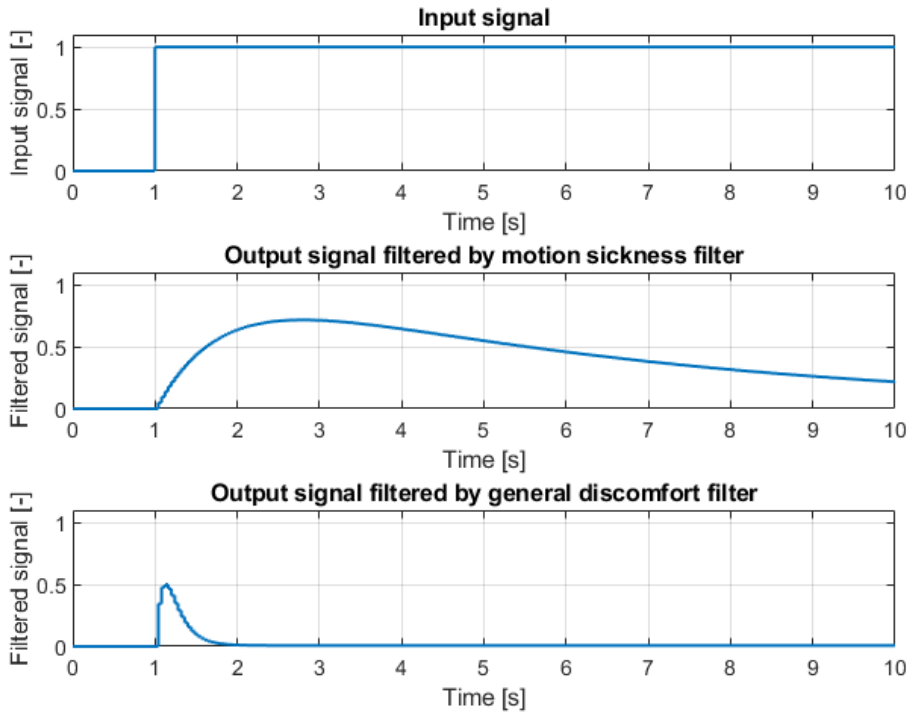

Figure 6-13: Filter response to a step input, filters from Section 3-2-2

6-5-3 Sensor noise

By testing only the lateral control in this chapter, the noise is implemented on the lateral error and psi angle and not on the velocity. The noise is of high frequency of 25 Hz, the same frequency as the controller. The test is done on the double lane change with a velocity of 80 km/hour.

Table 6-11: Double lane change 80 km/hour with sensor noise

Controller	J_1	J_2	J_3	J_4	J_5	J_6
Time horizon [s]	1	1	1	1	1	1
RMS ms $[m/s^2]$	0.728	0.651	0.625	0.661	0.634	0.704
Improvement [%]	–	**10.6**	**14.1**	**9.3**	**12.9**	**3.4**
RMS gd $[m/s^2]$	0.684	0.659	0.669	0.662	0.671	2.11
Improvement [%]	–	**3.7**	**2.2**	**3.3**	**1.9**	-209
MTVV ms $[m/s^2]$	1.46	1.33	1.28	1.35	1.3	1.41
Improvement [%]	–	**9.2**	**12.5**	**7.8**	**11.4**	**3.8**
MTVV gd $[m/s^2]$	1.22	1.19	1.25	1.19	1.23	3.83
Improvement [%]	–	**2.4**	-2.6	**2.4**	-0.6	-214
mean comfort $[m/s^2]$	1.02	0.958	0.957	0.966	0.957	2.01
Improvement [%]	–	**6.5**	**6.6**	**5.7**	**6.5**	-96.5
y error max $[m]$	0.258	0.262	0.309	0.263	0.265	0.32

Low influence sensor noise on motion sickness
The improvements are compared to the first result column (–)
Bold is a positive effect

Discussion

When sensor noise is implemented the motion sickness terms stay high compared to controller J_1, see Table 6-11. The motion sickness is of a low frequency and will be less influenced by high frequency noise. In Figure 6-14 can be seen the difference in influences, the motion sickness graph has a maximum value of 0.0882 and the general discomfort graph of 0.5164. In the figure the noise is directly filtered, in the vehicle the noise goes through the controller first which process the signals further.

The improvement of general discomfort decreases for the controllers which penalises the lateral acceleration directly or filtered for general discomfort, compared to when no sensor noise is applied. The controller can respond quickly to the noise due to the high frequency filter (or no filter). The quick response has a negative effect on general discomfort.

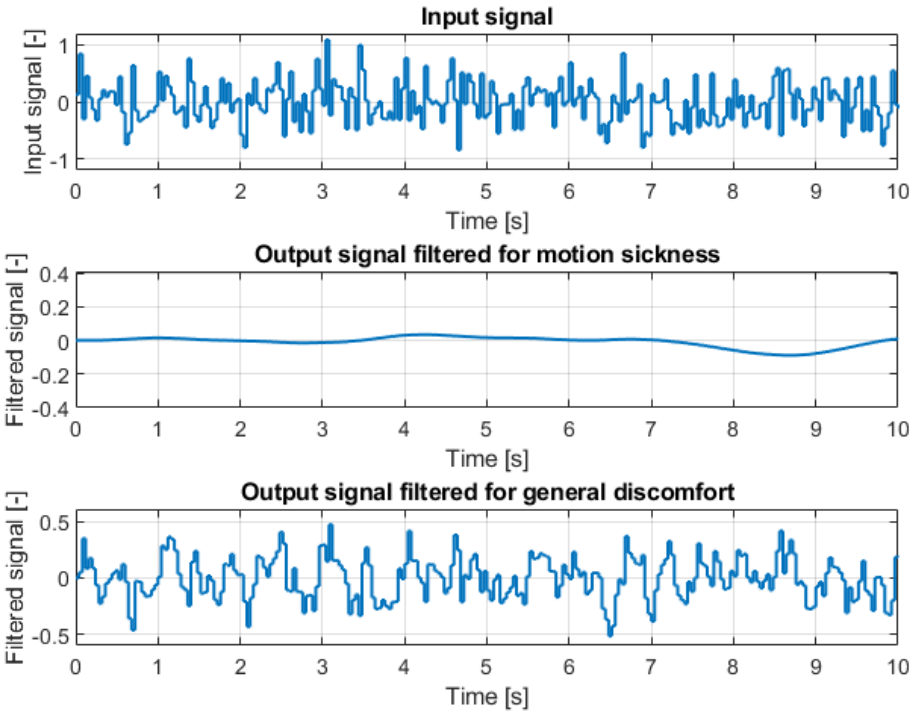

Figure 6-14: Influences noise on motion sickness and general discomfort using the weights from Section 1-1

6-6 Influences of the time horizon

In Section 6-3 can be seen the positive influence of increasing the time horizon for the motion sickness filter. To see the effect on the other controllers the time horizon is increased from one second to two seconds, the controllers are re-tuned for the new time horizon. The increase in time horizon with the same sample time creates more steps to calculate within the controller, the problem becomes more complex.

The results can be found in Table 6-12. In the results can be found that increasing the time horizon can decrease general discomfort up to 20.5%. The effect of increasing the time horizon has almost no influences on motion sickness comfort for the controllers which penalise the lateral acceleration (filtered and unfiltered).

Table 6-12: Double lane change 80 km/hour with different time horizons

Controller	J_1	J_1	J_2	J_2	J_4	J_4
Time horizon [s]	1	2	1	2	1	2
Sample time [s]	0.04	0.04	0.04	0.04	0.04	0.04
RMS ms $[m/s^2]$	0.738	0.704	0.66	0.657	0.67	0.674
Improvement [%]	–	**4.7**	–	**0.5**	–	-0.6
RMS gd $[m/s^2]$	0.701	0.557	0.654	0.532	0.65	0.537
Improvement [%]	–	**20.5**	–	**18.7**	–	**17.3**
MTVV ms $[m/s^2]$	1.49	1.43	1.35	1.35	1.37	1.38
Improvement [%]	–	**4.1**	–	-0.1	–	-0.9
MTVV gd $[m/s^2]$	1.25	0.997	1.15	0.951	1.13	0.952
Improvement [%]	–	**20.1**	–	**17.6**	–	**15.8**
mean comfort $[m/s^2]$	1.04	0.921	0.954	0.873	0.955	0.886
Improvement [%]	–	**11.7**	–	**8.6**	–	**7.2**
y error max $[m]$	0.3	0.299	0.299	0.3	0.3	0.3

Controllers of time horizon 2 seconds are re-tuned for the scenario
The improvements are compared to the same controller with time horizon of 1 second (–)
Bold is a positive effect

6-7 Solving time

An important part for a controller is the solving time, the solving time is the time the controller takes for calculating the control output. The controller runs on 25 Hz, the controller should find a solution within 0.04 seconds. The test of the double lane change on 80 km/hour is repeated elevens times and the maximum and mean solving time are saved. The tuning is the same as in Section 6-2, with a time horizon of 1 second. The controllers are able to find a solution within the sample time (<0.04 second). The results can be found in Table 6-13.

Table 6-13: Solving times on the double lane change

Controller	J_1	J_2	J_3	J_4	J_5	J_6
Maximum of maximums* [s]	0.0131	0.0117	0.0257	0.0225	0.0176	0.0385
Mean of maximums* [s]	0.0125	0.0115	0.014	0.017	0.0145	0.0379
Mean of means** [s]	0.00799	0.00812	0.00929	0.0113	0.0111	0.0147

Each controller is simulated 11 times, * Maximum of each simulation, ** Mean of each simulation

6-8 Summary

The performance of the controllers J_2 - J_5 are quite similar on the double lane change, when no disturbance is present. The benefit for penalising the lateral acceleration (filtered and unfiltered) is around 8% on mean comfort compared to J_1.

The most important result is the reduction in motion sickness. In Section 6-3-2 the controllers are tested on a scenario which creates motion sickness. A large increase in comfort was created by using the motion sickness filter. The improvement on mean comfort of the motion sickness controller increased to 17.2% compared to controller J_1. The motion sickness filter, when used in the right scenario, could help with dealing with motion sickness and lead to a more comfortable drive.

The general discomfort filter achieves a small increase in performance in the general discomfort frequency compared to penalising the lateral acceleration directly. Under disturbances the only advantage from penalising general discomfort is on wind disturbance, creating a lower lateral error than the other methods of penalising the lateral acceleration. When penalising lateral acceleration (filtered or unfiltered) the lateral error is too high for safe driving under wind disturbance.

Implementing both the general discomfort filter and motion sickness filter can have a positive effect due to choosing the weight ratio. A ratio can be selected between motion sickness and general discomfort filter to achieve the most comfort according to the passengers.

The penalty on lateral acceleration of controller J_2-J_5 affects longitudinal control, see Section 6-4. A problem arises due to not penalising the longitudinal position. The controller wants to increase the velocity, see Section 6-4-1. The increasing velocity problem could be countered in the future by creating a more advanced reference generator/controller. When the velocity problem is dealt with the controller could slow down before entering the corner to achieve lower lateral accelerations, leading to an increase in comfort. To achieve high comfort choosing the correct weights for longitudinal control is important, which will be further handled in Chapter 8.

When applying disturbances different results are found. For lower friction, penalising lateral acceleration (filtered and unfiltered) helps to stay on track. The effect of the lower lateral deviation comes from generating lower accelerations and therefore lower tire forces. When applying wind disturbance the penalty on lateral acceleration (filtered and unfiltered) leads to an increase in the lateral error. The lateral error increases and causes unsafe road behaviour. Besides the unsafe road behaviour due to the wind disturbance, the controllers which penalise lateral acceleration (filtered or unfiltered) ensure high comfort. When penalising a form of lateral acceleration the motion sickness comfort is kept high under sensor noise. Therefore, implementing a penalty on lateral acceleration (filtered or unfiltered) is recommended when sensor noise is present.

Increasing the time horizon while keeping the sample time constant leads to an increase in comfort and complexity. The general discomfort performance increases for the controllers. The disadvantage is an increase of the number of calculations within the controller, which leads to longer solving time. The solving time of all the controllers

with time horizon of one second are within bounds (< 0.04 second). The controller can be implemented in a real vehicle.

Chapter 7

Longitudinal influences on the combined controller

In the previous chapter the results of penalising the filtered lateral acceleration is researched. In a vehicle both lateral and longitudinal accelerations lead to discomfort. Therefore, combining them could lead to the best overall option to counter discomfort. This chapter shows the effects of penalising longitudinal acceleration. The longitudinal discomfort can be countered the same as the lateral discomfort, by penalising the filtered accelerations. The filters for longitudinal accelerations are the same as for lateral accelerations (motion sickness and general discomfort), see Section 3-2-2.

By creating a test scenario which leads to high accelerations the terms can be tested. The test scenario, velocity profile, can be found in Section 4-2-2. The test scenario is used in the whole chapter. The effect of the longitudinal terms in normal day driving would be lower than the results shown in this chapter. The question is if implementing these terms could create a real benefit to the controller. When implementing the longitudinal acceleration terms the complexity of the problem rises.

The velocity profile has multiple high frequency changes. The general discomfort filter will perform well due to the high frequency filter and the motion sickness filter will perform less due to the low frequency filter. In Section 6-5-3 can be seen that the motion sickness is less effected by noise, which will be the same for longitudinal control.

7-1 Adding penalties

To prove that penalising the lateral accelerations (filtered and unfiltered) generates comfort, the penalties are tested one by one. The weights of the other terms are kept constant, see Table 7-1. The velocity test is done on the braking section of the scenario, see Section 4-2-2 (till approximated 325 meters).

Table 7-1: Weights applied on the controllers, w_{var} is a variable weight

Controller	J_1	J_2	J_3	J_4
w_{y}	50	50	50	50
w_{ψ}	3750	3750	3750	3750
w_{v}	10	10	10	10
$w_{\triangle\delta}$	2.90e6	2.90e6	2.90e6	2.90e6
$w_{\triangle\text{a}}$	w_{var}	0	0	0
w_{ax}	0	w_{var}	0	0
$w_{\text{ax,ms}}$	0	0	w_{var}	0
$w_{\text{ax,gd}}$	0	0	0	w_{var}

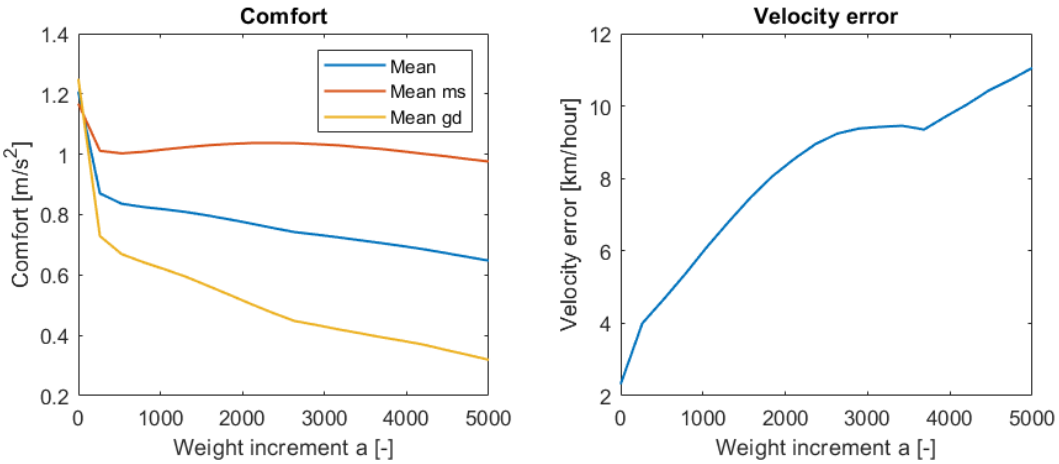

Figure 7-1: Effect of changing weight $\triangle a$

As can be seen in Figures 7-1 till 7-4 the terms all increase comfort. The increase in comfort leads to an increase in velocity error.

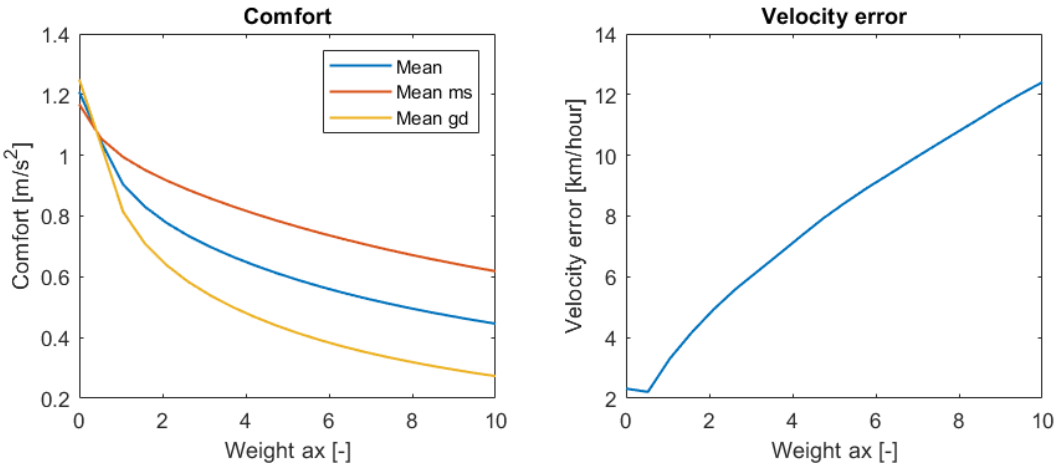

Figure 7-2: Effect of changing weight ax

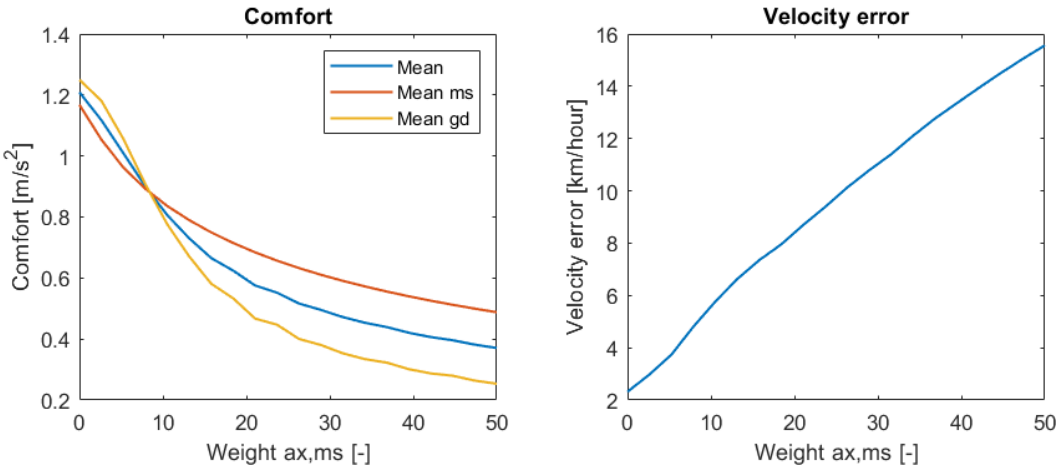

Figure 7-3: Effect of changing weight ax, ms

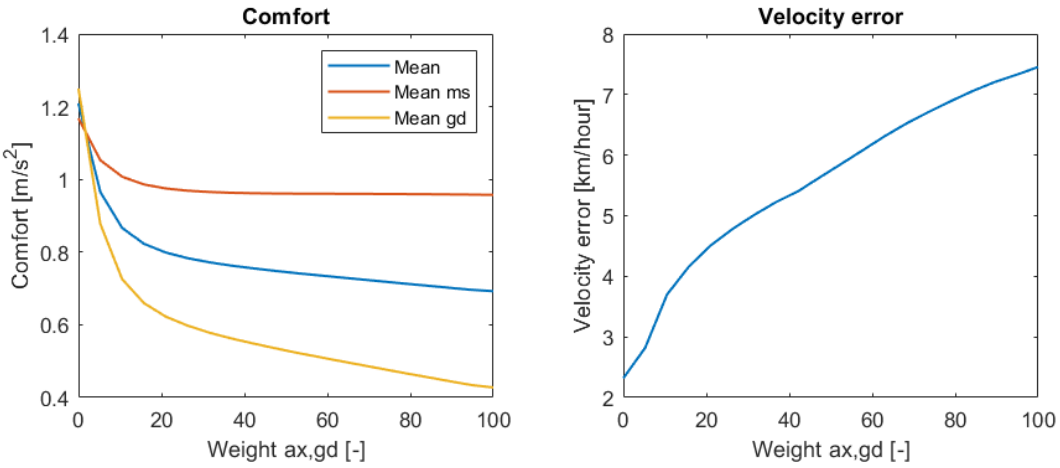

Figure 7-4: Effect of changing weight ax, gd

7-2 Velocity profile

To compare the method of filtering longitudinal acceleration, 6 controllers are tuned and compared, see Table 7-2. In controllers J_1, J_2 and J_6 the filters are not present. In controller J_3 only the motion sickness filter is implemented and in controllers J_4 and J_5 both filters are implemented, see Table 7-2. The vehicle drives on a straight path, therefore, the lateral weights do not affect the results. All the controllers have no lateral deviation. The controllers are tuned to have a maximum velocity error of 5 km/hour while braking. The scenario can be found in Section 4-2-2.

Table 7-2: Weights applied on the controllers

Controller	J_1	J_2	J_3	J_4	J_5	J_6
w_{y}	50	50	50	50	50	50
w_{ψ}	3750	3750	3750	3750	3750	3750
w_{v}	10	10	10	10	10	10
$w_{\triangle\delta}$	2.90e6	2.90e6	2.90e6	2.90e6	2.90e6	2.90e6
$w_{\triangle\mathrm{a}}$	653	2.0	342	0.0072	0.0068	0
w_{ax}	x	2.12	0	0	0	x
$w_{\mathrm{ax,ms}}$	x	x	1.775	0	1.78	x
$w_{\mathrm{ax,gd}}$	x	x	x	30.9	19.05	x

x means the term is not implemented in the controller

Table 7-3: Velocity profile

Controller	J_1	J_2	J_3	J_4	J_5	J_6
Time horizon [s]	1	1	1	1	1	1
RMS ms $[m/s^2]$	0.67	0.593	0.616	0.64	0.608	0.709
Improvement [%]	–	**11.5**	**8**	**4.5**	**9.2**	-5.8
RMS gd $[m/s^2]$	0.357	0.354	0.345	0.338	0.335	0.676
Improvement [%]	–	**1**	**3.4**	[**5.3**]	[**6.3**]	-89.3
MTVV ms $[m/s^2]$	1.37	1.26	1.3	1.31	1.27	1.63
Improvement [%]	–	**7.8**	**4.5**	**4.1**	**6.8**	-19.7
MTVV gd $[m/s^2]$	0.937	0.958	0.909	0.866	0.902	1.74
Improvement [%]	–	-2.2	**3**	[**7.6**]	[**3.7**]	-86.3
mean comfort $[m/s^2]$	0.832	0.791	0.794	0.789	0.779	1.19
Improvement [%]	–	**5**	**4.7**	**5.3**	**6.4**	-43.1
v error max acc. $[km/hour]$	8.58	7.36	8.04	7.06	7.2	7.56
v error max brak. $[km/hour]$	5	4.99	5	5	5	2.32

Improvement due to the general discomfort filter [ ]
The improvements are compared to the first result column (–)
Bold is a positive effect

Discussion

The improvements in terms of mean comfort are small, for controller J_2 till J_5 around $\pm 5\%$ compared to J_1, see Table 7-3. The increase in comfort could grow, if the velocity error can grow. Due to safety being a high priority the velocity error is kept low.

Controller J_2 has the highest performance in motion sickness instead of controller J_3 which is implemented with the motion sickness filter. The improvement on mean comfort due to the motion sickness filter is less than the improvement due to the weight of $\triangle a$, which can be seen by the ratio of the two weights ($w_{\triangle \mathrm{a}}$ and $w_{\mathrm{ax,ms}}$). The effect has to do with the velocity scenario having a sudden change in velocity, or high frequency acceleration change, and the motion sickness filter is of a low frequency. The difference in frequency makes the motion sickness weight perform less well and shift the focus on the increment term, $w_{\triangle \mathrm{a}}$, to achieve the highest overall comfort. As can be seen in Appendix B-2-1 only controller J_1 and J_3 has a high cost on the increment. The general discomfort filter which is implemented in controller J_4 and J_5 achieves the highest performance in general discomfort.

When driving in the real world the reference generator can create a smooth velocity profile. A smooth velocity profile will create lower accelerations therefore lower improvements on comfort compared to Table 7-3. The reference generator will create an uncomfortable velocity profile when needed, which happens in emergency scenarios. In the case of an emergency scenario following the reference signal should be done with a low error, meaning safety over comfort. Implementing the longitudinal acceleration terms in a normal day driving scenario could be not worth it.

7-3 Disturbance

In the real world disturbances are present, to see how the longitudinal control reacts on disturbance two scenarios are tested. The two scenarios are sensor noise and lower friction which can be found in Section 4-2-1. These scenarios are tested on the velocity profile which can be found in Section 4-2-2. In the controller the disturbances are not modeled, therefore, the controller does not have extra tools to counter the disturbances.

7-3-1 Friction change

If the friction of the road changes, for example due to rain, the controller still needs to be safe. How the controllers react and which of the controllers are the least influenced by the change of road friction is researched. The road friction is changed from 1 to 0.5 μ, see Section 4-2-1.

Discussion

The vehicle is a front wheel driven vehicle, meaning the vehicle can only accelerate with the front wheels. The front wheels lose traction in the low friction scenario, the traction is not lost while braking due to using all the four wheels. In Figure 7-5 the different longitudinal tire forces in dry and wet road conditions are shown for the right front tire under acceleration conditions. In the figure can be seen where the tire loses the grip on the road. The comfort is influenced by when the wheel spin starts and ends, creating differences in comfort. The longitudinal acceleration has a direct influences on when the wheel spin starts, see Equation (7-1) [49]. Where F_{f} is the traction force, μ the road friction and F_{n} the normal force.

$$F_{\mathrm{f}} = \mu F_{\mathrm{n}} \tag{7-1}$$

Controller J_2 has the highest performance due to penalising the full frequency of the acceleration. By penalising only certain frequencies the accelerations can grow outside these frequencies. If the acceleration leads to tire forces bigger than the traction force the wheel starts to spin.

Configuration adjustment lower friction

When rain is detected by the vehicle the performance can be increased by adjusting the constraints in the MPC. The constraints can be set more conservative for the longitudinal control. In the new results, see Table 7-5, the longitudinal control value is constraint to be maximum 3.0. The tires do not lose traction, in Figure 7-6 the force of the tire under the new constraint is compared to the old constraint. Controller J_5 performs well under the new constraints, by keeping both the general discomfort and motion sickness low.

Table 7-4: Velocity profile with $\mu = 0.5$, Longitudinal control value constraint by maximum of 6.5

Controller	J_1	J_2	J_3	J_4	J_5	J_6
Time horizon [s]	1	1	1	1	1	1
RMS ms $[m/s^2]$	0.633	0.554	0.58	0.611	0.58	0.65
Improvement [%]	–	[**12.5**]	**8.4**	**3.4**	**8.4**	-2.6
RMS gd $[m/s^2]$	0.367	0.302	0.333	0.342	0.331	0.663
Improvement [%]	–	[**17.9**]	**9.3**	**6.9**	**10**	-80.5
MTVV ms $[m/s^2]$	1.48	1.26	1.3	1.43	1.29	1.6
Improvement [%]	–	[**14.9**]	**11.8**	**3.4**	**12.8**	-8.5
MTVV gd $[m/s^2]$	1.23	0.917	0.995	1.2	1.13	1.9
Improvement [%]	–	[**25.5**]	**19.1**	**2.4**	**8**	-54.5
mean comfort $[m/s^2]$	0.928	0.758	0.803	0.896	0.833	1.2
Improvement [%]	–	[**18.3**]	**13.4**	**3.4**	**10.2**	-29.9
v error max acc. $[km/hour]$	12.2	11.7	11.8	11.6	11.4	12.4
v error max brak. $[km/hour]$	5	4.99	5	5	5	3.75

Improvement due to penalising the whole acceleration frequency [ ]
The improvements are compared to the first result column (–)
Bold is a positive effect

7-3-2 Sensor noise

Section 6-5-3 shows that the motion sickness filter is less affected by the high-frequency noise compared to the general discomfort filter. Both the general discomfort and penalising the lateral acceleration are more effected by noise. Implementing a penalty on longitudinal acceleration, unfiltered of filtered for motion sickness, does improve the motion sickness.

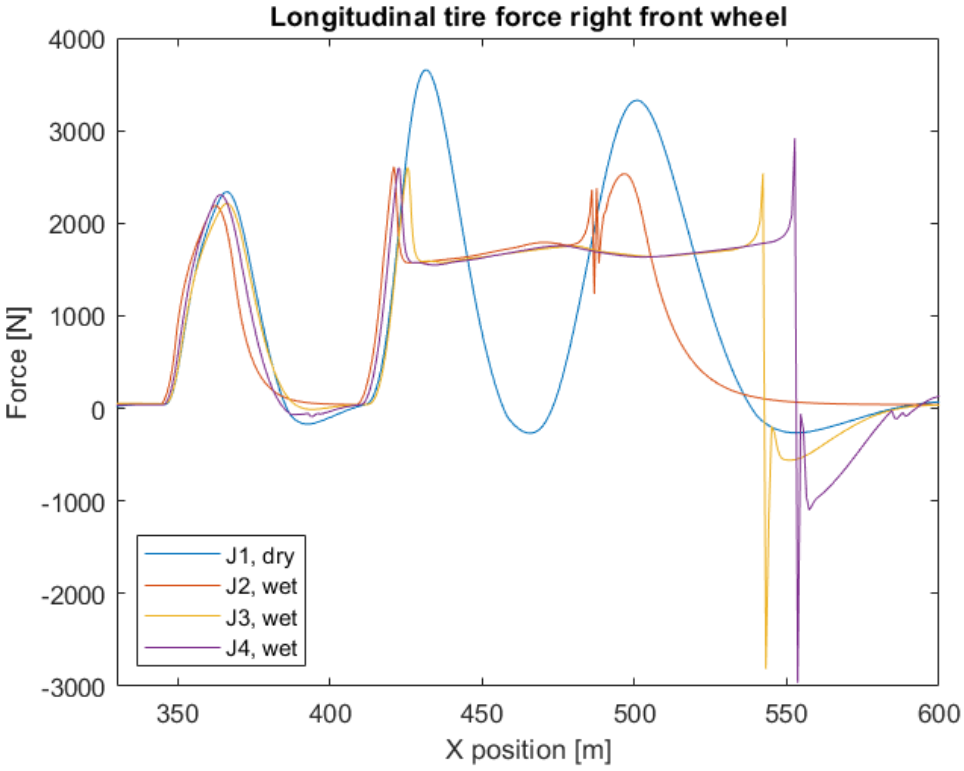

Figure 7-5: Comparison controllers J_2 - J_4 on wet road conditions while losing traction, compared to dry road condition with controller J_1

Table 7-5: Velocity profile with $\mu = 0.5$, Longitudinal control value constraint by maximum of 3.0

Controller	J_1	J_2	J_3	J_4	J_5	J_6
Time horizon [s]	1	1	1	1	1	1
RMS ms $[m/s^2]$	0.622	0.567	0.582	0.603	0.577	0.656
Improvement [%]	–	**8.9**	**6.4**	**3.2**	**7.2**	-5.3
RMS gd $[m/s^2]$	0.312	0.305	0.302	0.291	0.288	0.554
Improvement [%]	–	**2.2**	**3.2**	**6.6**	**7.7**	-77.5
MTVV ms $[m/s^2]$	1.37	1.26	1.3	1.31	1.27	1.6
Improvement [%]	–	**7.9**	**4.5**	**4.1**	**6.9**	-17.4
MTVV gd $[m/s^2]$	0.939	0.917	0.911	0.821	0.826	1.36
Improvement [%]	–	**2.3**	**2.9**	**12.5**	**12**	-45.2
mean comfort $[m/s^2]$	0.81	0.762	0.775	0.757	0.741	1.04
Improvement [%]	–	**5.9**	**4.3**	**6.6**	**8.5**	-28.9
v error max acc. $[km/hour]$	11.3	10.5	10.8	10.2	10.2	11.2
v error max brak. $[km/hour]$	5	4.99	5	5	5	3.75

The improvements are compared to the first result column (–)
Bold is a positive effect

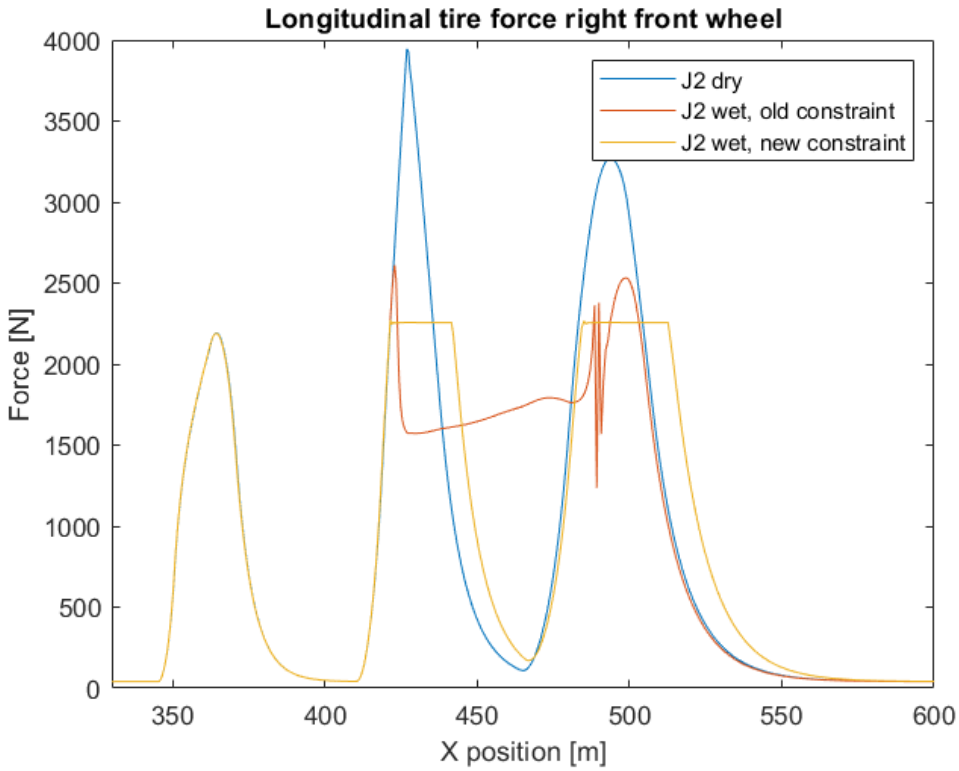

Figure 7-6: Comparison controllers J_2 on dry and wet road conditions, old constraint is longitudinal control maximum 6.5, new constraint maximum 3.0

Table 7-6: Velocity profile with sensor noise

Controller	J_1	J_2	J_3	J_4	J_5	J_6
Time horizon [s]	1	1	1	1	1	1
RMS ms $[m/s^2]$	0.663	0.62	0.613	0.678	0.645	0.808
Improvement [%]	–	**6.4**	**7.6**	-2.2	**2.8**	-21.9
RMS gd $[m/s^2]$	0.353	0.423	0.344	0.368	0.378	0.842
Improvement [%]	–	-20	**2.3**	-4.3	-7.3	-139
MTVV ms $[m/s^2]$	1.31	1.27	1.26	1.31	1.28	1.62
Improvement [%]	–	**3.3**	**4.3**	**0.4**	**2.6**	-23.4
MTVV gd $[m/s^2]$	0.942	0.951	0.916	0.819	0.892	1.54
Improvement [%]	–	-1	**2.7**	**13.1**	**5.3**	-64
mean comfort $[m/s^2]$	0.817	0.816	0.782	0.793	0.798	1.2
Improvement [%]	–	**0.2**	**4.3**	**3**	**2.3**	-47.3
v error max acc. $[km/hour]$	8.38	8.17	8	7.66	7.58	8.79
v error max brak. $[km/hour]$	4.92	5.37	4.98	6.02	5.89	4.54

The improvements are compared to the first result column (–)
Bold is a positive effect

7-4 Influences time horizon

To test the influence of a longer time horizon on longitudinal control, the controllers are compared with a different time horizon. The controllers compared are J_2, J_3 and J_4. The controllers all penalises longitudinal acceleration differently. The results can be found in Table 7-7. An increase is made in comfort, the motion sickness and the general discomfort decreases while increasing the time horizon. Controller J_3 has the highest decrease in RMS motion sickness. Keep in mind that the controllers in the results are compared to them self with a different time horizon. For example, controller J_3 with time horizon of 2 seconds has online an improvement of 1.8% compared to controller J_2 with time horizon of 2 seconds on RMS for motion sickness. When the calculating power of the vehicle goes up, the solving time goes down, increasing the time horizon from one to two seconds will be beneficial for comfort.

Table 7-7: Double lane change 80 km/hour with different time horizons

Controller	J_2	J_2	J_3	J_3	J_4	J_4
Time horizon [s]	1	2	1	2	1	2
Sample time [s]	0.04	0.04	0.04	0.04	0.04	0.04
RMS ms $[m/s^2]$	0.593	0.553	0.616	0.543	0.64	0.599
Improvement [%]	–	**6.7**	–	**11.8**	–	**6.4**
RMS gd $[m/s^2]$	0.354	0.262	0.345	0.267	0.338	0.288
Improvement [%]	–	**25.9**	–	**22.6**	–	**14.9**
MTVV ms $[m/s^2]$	1.26	1.14	1.3	1.15	1.31	1.23
Improvement [%]	–	**9.6**	–	**12**	–	**6.3**
MTVV gd $[m/s^2]$	0.958	0.696	0.909	0.704	0.866	0.728
Improvement [%]	–	**27.3**	–	**22.5**	–	**15.9**
mean comfort $[m/s^2]$	0.791	0.662	0.794	0.666	0.789	0.711
Improvement [%]	–	**16.2**	–	**16.1**	–	**9.8**
v error max acc. $[km/hour]$	7.36	7.33	8.04	7.78	7.06	7.5
v error max brak. $[km/hour]$	4.99	5	5	5	5	5

The improvements are compared to the same controller with time horizon of 1 second (–)
Bold is a positive effect

7-5 Solving time

As in Section 6-7 for the lateral control, the solving time is now checked for longitudinal control. The tuning and scenario is the same as in Section 7-2, with a time horizon of one second. The results can be found in Table 7-8. The controllers all find a solution within the sample time (<0.04 second).

Table 7-8: Solving times on the double lane change

Controller	J_1	J_2	J_3	J_4	J_5	J_6
Maximum of maximums* [s]	0.0102	0.00657	0.0212	0.0153	0.019	0.0387
Mean of maximums* [s]	0.00714	0.00625	0.0135	0.00878	0.0161	0.0379
Mean of means** [s]	0.00502	0.00483	0.00659	0.00502	0.00918	0.0126

Each controller is simulated 11 times, * Maximum of each simulation, ** Mean of each simulation

7-6 Summary

Implementing longitudinal acceleration terms (filtered and unfiltered) leads to an increase in comfort. The improvement on mean comfort is $\pm 5\%$ due to penalising the longitudinal acceleration (filtered and unfiltered) compared to J_1. In the velocity scenario the longitudinal acceleration goes up to 5.3 m/s^2 for controller J_1, therefore the scenario leads to aggressive accelerations.

In a normal situation the high longitudinal accelerations are not necessary by creating a velocity profile which takes comfort into account. The increase would be lower than the 5% in normal day driving. In an emergency situation high longitudinal accelerations could happen, in that case the controller should closely follow the signals. Therefore, the comfort terms would be kept off or low in order to keep the velocity error low. The effect of combining the lateral and longitudinal acceleration terms are further researched in Chapter 8.

In the lower friction case the comfort increase further for controllers J_2, J_3 and J_5. However, the performance is influenced when the wheels start to lose and gain traction. Losing traction could lead to unsafe scenarios, creating more conservative constraints for longitudinal control the controller will not lose traction. To decrease motion sickness under sensor noise, a penalty should be implemented for either the motion sickness filter or the longitudinal acceleration.

Increasing the time horizon is beneficial for comfort, both the general discomfort and motion sickness decreases. When increasing the time horizon the complexity of the problem grows due to more steps being calculated. The maximum solving time of the controllers with time horizon of one second are lower than 0.04 seconds. The controllers could be implemented in real time in a vehicle.

Chapter 8

Results combined lateral and longitudinal control

To create a controller which can drive on all scenarios, the lateral and longitudinal control are combined. The controller should be able to follow a trajectory and velocity profile safely. Five controllers are tuned and compared.

In the aggressive scenario of Chapter 7 the influence was $\pm 5\%$ on the mean comfort. Since the controller is not made for emergency handling the velocity profile would not be aggressive and the influence of the longitudinal acceleration would be lower. In Sections 8-2 and 8-3 can be found that the longitudinal terms have a small influence on comfort in the tested scenarios.

The motion sickness filter will decrease motion sickness, when a scenario is created which generates a lot of motion sickness the controller will out perform the rest. Implementing the motion sickness filter in a real vehicle could help with roads which generates a lot of motion sickness, for example mountain roads. The general discomfort filter will help with keeping the general discomfort low.

8-1 Double lane change with velocity shift

To create a scenario where the controller can be tuned for lateral and longitudinal control, the scenario in Figure 8-1 is created. The scenario is a combination of the double lane change with a velocity change. The scenario tests both lateral and longitudinal control. The maximum lateral error allowed is 0.325 meter. The velocity is tuned to have a max error of 2.5 km/hour. In controllers J_1 and J_2 the filters are not present. In controller J_3 only the motion sickness filter is implemented and in controllers J_4 and J_5 both filters are implemented, see Table 8-11.

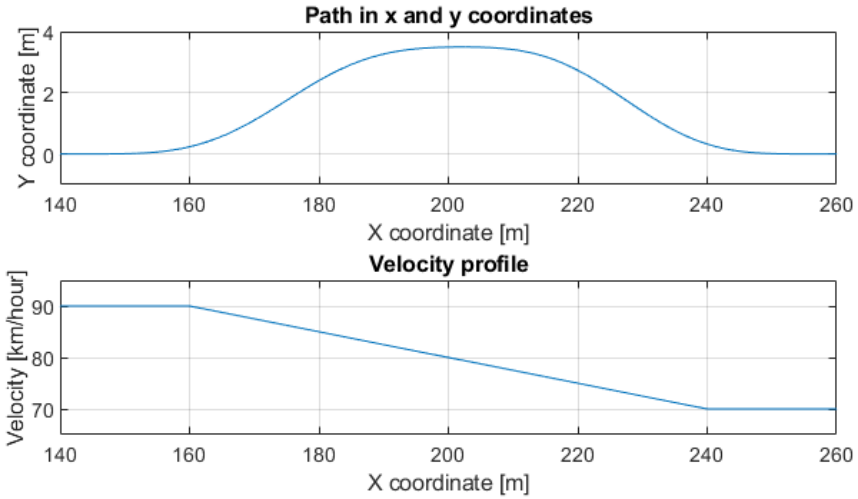

Figure 8-1: Double lane change with velocity shift

Table 8-1: Weights applied on the controllers

Controller	J_1	J_2	J_3	J_4	J_5
w_{y}	50	50	50	50	50
w_{ψ}	2700	7620	4500	9720	3500
w_{v}	21	42	57	42	27
$w_{\triangle\delta}$	2.42e6	3.15e6	4.40e6	2.95e6	1.80e6
$w_{\triangle\mathrm{a}}$	280	605	790	610	439
w_{ay}	x	30.7	0	0	0
$w_{\mathrm{ay,ms}}$	x	x	255	0	100
$w_{\mathrm{ay,gd}}$	x	x	x	130	21
w_{ax}	x	0	0	0	0
$w_{\mathrm{ax,ms}}$	x	x	0	0	0
$w_{\mathrm{ax,gd}}$	x	x	x	0	0

x means the term is not implemented in the controller

Discussion

In the results of Table 8-2 controllers J_2 and J_4 perform well in terms of comfort with a small advantage over controllers J_3 and J_5. The velocity error is kept low for all the controllers to achieve the most comfort. The lateral errors are all at boundary conditions. In Figure 8-2 the accelerations are plotted for motion sickness and general discomfort, which shows similar information as Table 8-2.

Table 8-2: Double lane change with velocity change

Controller	J_1	J_2	J_3	J_4	J_5
Time horizon [s]	1	1	1	1	1
RMS ms $[m/s^2]$	0.881	0.748	0.747	0.757	0.748
Improvement [%]	–	**15.1**	**15.2**	**14.1**	**15.1**
RMS gd $[m/s^2]$	0.703	0.641	0.698	0.628	0.674
Improvement [%]	–	**8.7**	**0.7**	**10.7**	**4.1**
MTVV ms $[m/s^2]$	1.75	1.51	1.55	1.53	1.53
Improvement [%]	–	**13.8**	**11.6**	**12.8**	**13.1**
MTVV gd $[m/s^2]$	1.38	1.34	1.36	1.33	1.39
Improvement [%]	–	**3.3**	**1.4**	**3.7**	-0.1
mean comfort $[m/s^2]$	1.18	1.06	1.09	1.06	1.08
Improvement [%]	–	**10.2**	**7.7**	**10.1**	**8.3**
v error max $[km/hour]$	0.75	0.78	0.779	0.779	0.79
y error max $[m]$	0.325	0.325	0.325	0.324	0.324

The improvements are compared to the first result column (–)
Bold is a positive effect

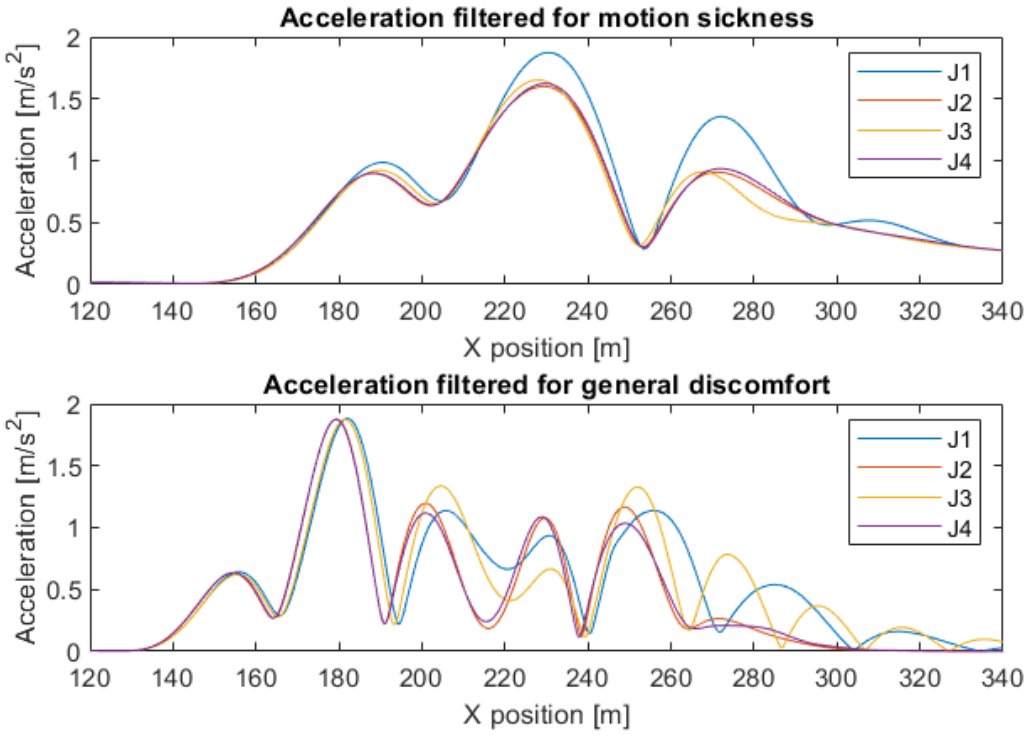

Figure 8-2: Accelerations from double lane change with velocity shift, J_1 has high motion sickness discomfort, J_1 and J_3 high general discomfort

8-2 Motion sickness

From Section 6-3-2 can be seen that the motion sickness filter performs well compared to the other controllers in a scenario where a lot of motion sickness is generated. The controller is tested on a sine-wave path while changing the velocity, see Figure 8-3. The scenario is driven until the vehicle reaches 600 meters. Both sine waves, path and velocity, are within the frequencies of motion sickness (± 0.2 and ± 0.1 Hz), see the following equations:

$$Y_{\text{position}} = 1.5 \sin(0.4\pi(t-5)) \tag{8-1}$$

$$V_{\text{velocity}} = (2.5/3.6)\sin(0.2\pi(t-5)) + (80/3.6) \tag{8-2}$$

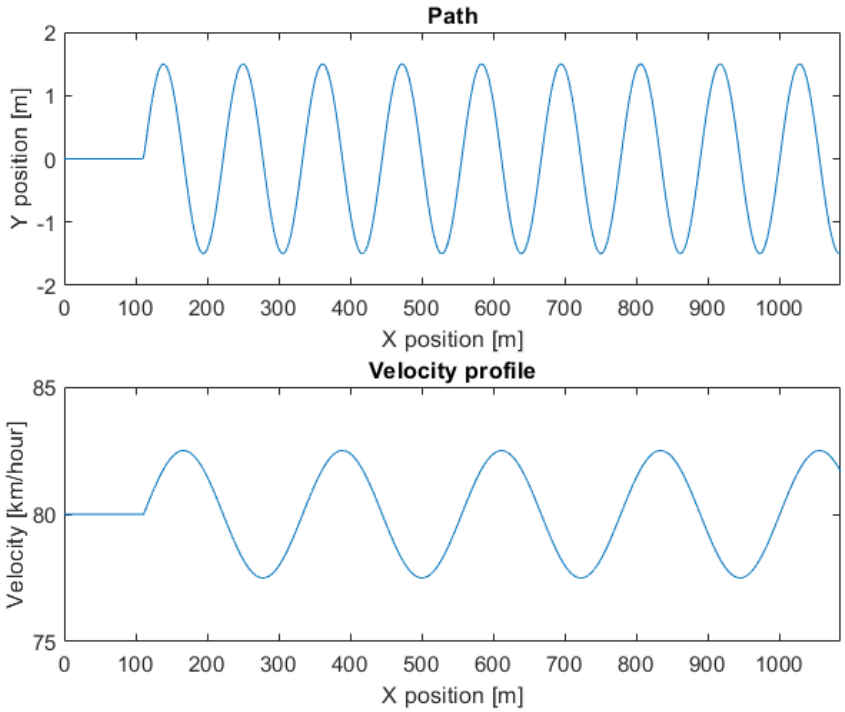

Figure 8-3: Sine wave for lateral and longitudinal control

Discussion

In Table 8-3 the results can be found. As expected the motion sickness filter leads to a decrease in motion sickness. To increase the performance further extra terms can be implemented in the longitudinal control, such as a motion sickness filter. In Chapter 7 penalty on longitudinal acceleration directly has a larger impact on motion sickness. Due to a different velocity scenario in the sine wave both methods are tested in Section 8-2-1.

Table 8-3: Sine wave for lateral and longitudinal control

Controller	J_1	J_2	J_3	J_4	J_5
Time horizon [s]	1	1	1	1	1
RMS ms $[m/s^2]$	1.28	0.988	0.887	1.01	0.961
Improvement [%]	–	**22.9**	[**30.7**]	**21.2**	[**24.9**]
RMS gd $[m/s^2]$	0.673	0.53	0.513	0.534	0.532
Improvement [%]	–	**21.4**	**23.8**	**20.7**	**21**
MTVV ms $[m/s^2]$	1.91	1.48	1.33	1.52	1.43
Improvement [%]	–	**22.6**	[**30.4**]	**20.7**	[**25**]
MTVV gd $[m/s^2]$	1.25	1.08	1.12	1.04	1.12
Improvement [%]	–	**13.5**	**10.2**	**16.8**	**9.9**
mean comfort $[m/s^2]$	1.28	1.02	0.963	1.02	1.01
Improvement [%]	–	**20.3**	**24.7**	**19.9**	**20.8**
v error max $[km/hour]$	0.53	0.495	0.513	0.493	0.5
y error max $[m]$	0.836	0.312	0.273	0.359	0.294

Improvement due to motion sickness filter [ ]
The improvements are compared to the first result column (–)
Bold is a positive effect

8-2-1 Longitudinal control

For tuning the longitudinal control, the test setup of Figure 8-1 is used. The lateral control is kept the same, in the longitudinal control a term is added. The term is tuned until the velocity error grows till 5 km/hour. To test if these terms leads to more comfort in motion sickness, scenario in Figure 8-3 is used.

Discussion

The results can be found in Table 8-5. In the results can be seen that the longitudinal tuning has a low influence on performance. The velocity error grows while the comfort performance stays similar. Adding the extra terms for longitudinal acceleration (filtered and unfiltered) leads to extra states and a more complex problem while creating only a small advantage.

Table 8-4: Weights applied on the controllers

Controller	J_3	$J_{3,\mathrm{ms,x}}$	$J_{3,\mathrm{ax}}$
w_{y}	50	50	50
w_{ψ}	4500	4500	4500
w_{v}	57	57	57
$w_{\triangle\delta}$	4400000	4400000	4400000
$w_{\triangle\mathrm{a}}$	790	790	790
w_{ay}	0	0	0
$w_{\mathrm{ay,ms}}$	255	255	255
$w_{\mathrm{ay,gd}}$	x	x	x
w_{ax}	0	0	45
$w_{\mathrm{ax,ms}}$	0	105	0
$w_{\mathrm{ax,gd}}$	x	x	x

x means the term is not implemented in the controller

Table 8-5: Sine wave with different longitudinal terms

Controller	J_3	$J_{3,\mathrm{ms,x}}$	$J_{3,\mathrm{ax}}$
Time horizon [s]	1	1	1
RMS ms $[m/s^2]$	0.887	0.876	0.869
Improvement [%]	–	**1.3**	**2.1**
RMS gd $[m/s^2]$	0.513	0.506	0.5
Improvement [%]	–	**1.4**	**2.6**
MTVV ms $[m/s^2]$	1.33	1.28	1.28
Improvement [%]	–	**3.6**	**4**
MTVV gd $[m/s^2]$	1.12	1.11	1.11
Improvement [%]	–	**1.3**	**1.2**
mean comfort $[m/s^2]$	0.963	0.943	0.938
Improvement [%]	–	**2.1**	**2.6**
v error max $[km/hour]$	0.513	1.82	1.97
y error max $[m]$	0.273	0.271	0.269

$J_{3,\mathrm{ms,x}}$ penalises the longitudinal filtered acceleration for motion sickness
$J_{3,\mathrm{ax}}$ penalises the longitudinal acceleration
The improvements are compared to the first result column (–)
Bold is a positive effect

8-3 General discomfort

To decrease the general discomfort, the filtered longitudinal acceleration for general discomfort can be penalised. In Chapter 7 could be seen that penalising the longitudinal acceleration for general discomfort works. To compare the influence of longitudinal control, controller J_4 is penalised three different ways on longitudinal control. One is the controller J_4 from Section 8-2. The other two have a penalty on the longitudinal acceleration, unfiltered or filtered for general discomfort.

The same scenario as in Figure 8-1 is taken. The velocity error can grow till around 5 km/hour. The effect of the filters are shown in Figures 8-4 and 8-5, with the same tuning for lateral control as in Section 8-1. As can be seen in the figures the comfort decrease while the lateral error becomes smaller. Due to the decrease in lateral error from the longitudinal comfort terms, extra weight can be implemented on the lateral comfort terms. The extra weight could lead to an increase in comfort. The controllers are re-tuned after finding the minimum lateral error. The results are found in Table 8-6, with the tuning in Table 8-7.

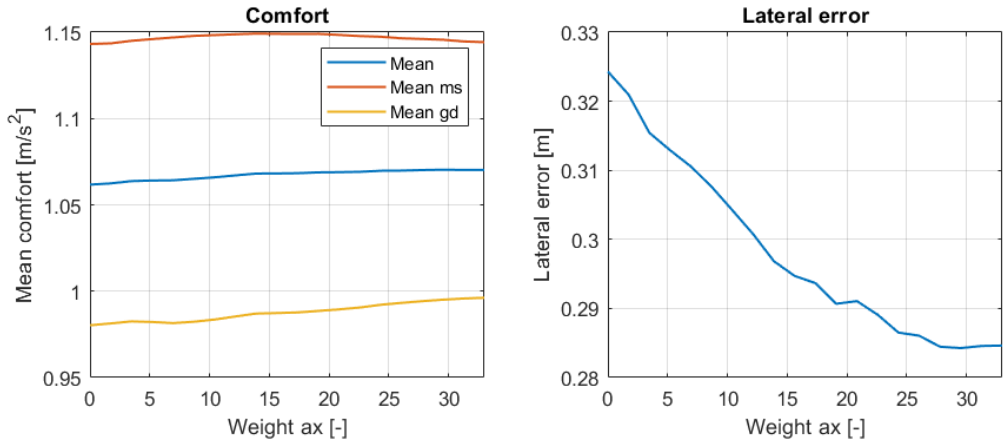

Figure 8-4: Effect of changing weight ax

Discussion

The advantage of penalising an extra term in longitudinal control is an increase in comfort. Compared to the lateral control the influence is low. The general discomfort filter can help with creating more comfort in the frequencies of general discomfort, with $\pm 3\%$ decrease in general discomfort compared to the baseline controller. Longitudinal control could be used to create safer controllers by creating smaller lateral errors, see Figures 8-4 and 8-5.

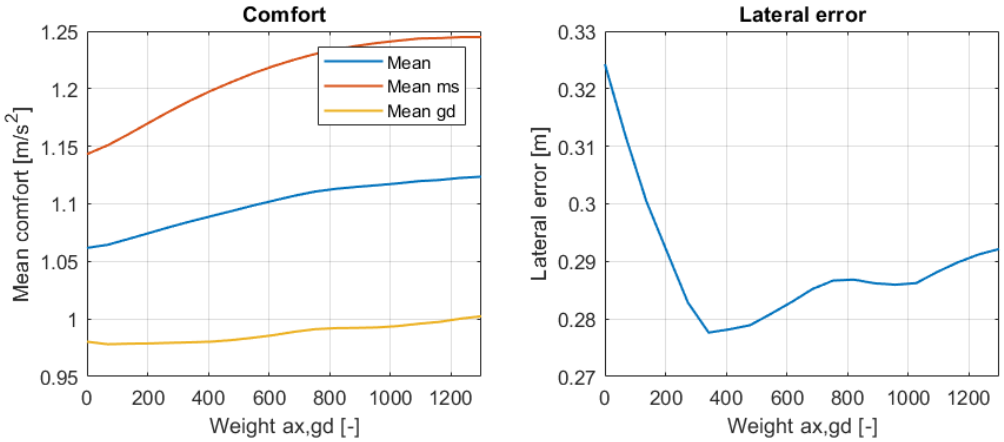

Figure 8-5: Effect of changing weight ax, gd

Table 8-6: Double lane change with velocity shift

Controller	J_4	$J_{4,\mathrm{gd,x}}$	$J_{4,\mathrm{ax}}$
Time horizon [s]	1	1	1
RMS ms $[m/s^2]$	0.757	0.773	0.727
Improvement [%]	–	-2.2	**3.9**
RMS gd $[m/s^2]$	0.628	0.607	0.643
Improvement [%]	–	**3.3**	-2.5
MTVV ms $[m/s^2]$	1.53	1.58	1.53
Improvement [%]	–	-3	-0.2
MTVV gd $[m/s^2]$	1.33	1.3	1.3
Improvement [%]	–	**2.8**	**2.8**
mean comfort $[m/s^2]$	1.06	1.06	1.05
Improvement [%]	–	-0.1	**1.1**
v error max $[km/hour]$	0.779	1.76	4.67
y error max $[m]$	0.324	0.325	0.324

$J_{4,\mathrm{gd,x}}$ penalises the longitudinal filtered acceleration for general discomfort
$J_{4,\mathrm{ax}}$ penalises the longitudinal acceleration
The improvements are compared to the first result column (–)
Bold is a positive effect

Table 8-7: Weights applied on the controllers

Controller	J_4	$J_{4,\mathrm{gd,x}}$	$J_{4,\mathrm{ax}}$
w_{y}	50	50	50
w_{ψ}	9720	9720	9720
w_{v}	42	42	42
$w_{\triangle\delta}$	2950000	2950000	2950000
$w_{\triangle\mathrm{a}}$	610	610	610
w_{ay}	0	0	0
$w_{\mathrm{ay,ms}}$	0	0	0
$w_{\mathrm{ay,gd}}$	130	150	148
w_{ax}	0	0	30
$w_{\mathrm{ax,ms}}$	0	0	0
$w_{\mathrm{ax,gd}}$	0	342	0

8-4 Disturbances

Due to the limited influences of the longitudinal acceleration control terms (filtered and unfiltered), the terms are not implemented in the following section. The tuning and test scenario is the same as in Section 8-2. Multiple disturbances are tested on the vehicle (wind, lower friction and sensor noise). In the controller the disturbances are not modeled, therefore, the controller does not have extra tools to counter the disturbances.

8-4-1 Friction change

The friction is set from $\mu = 1$ to $\mu = 0.5$ to simulated wet road conditions. The results are given in Table 8-8. The tire forces are influenced by the friction coefficient [48]. By keeping the accelerations low in all frequencies the comfort will stay high, and the tire forces low. By penalising the lateral acceleration directly or using the general discomfort filter the overall acceleration is kept low. The overall acceleration in this section is calculated with the unfiltered accelerations, see the following equation:

$$a_{\mathrm{w}} = \sqrt{a_{\mathrm{y}}^2 + a_{\mathrm{x}}^2} \tag{8-3}$$

By penalising only the motion sickness frequency the overall acceleration can increase due to the increase of acceleration in other frequencies. In Figure 8-6 the overall accelerations are plotted, controllers J_1 and J_3 have the highest overall accelerations on multiple points, which leads to the lowest mean comfort see Table 8-8. Controller J_3 creates a large lateral error which leads to unsafe behaviour. Controller J_3 could be made safe by implementing a small penalty on general discomfort and therefore keeping the overall acceleration down.

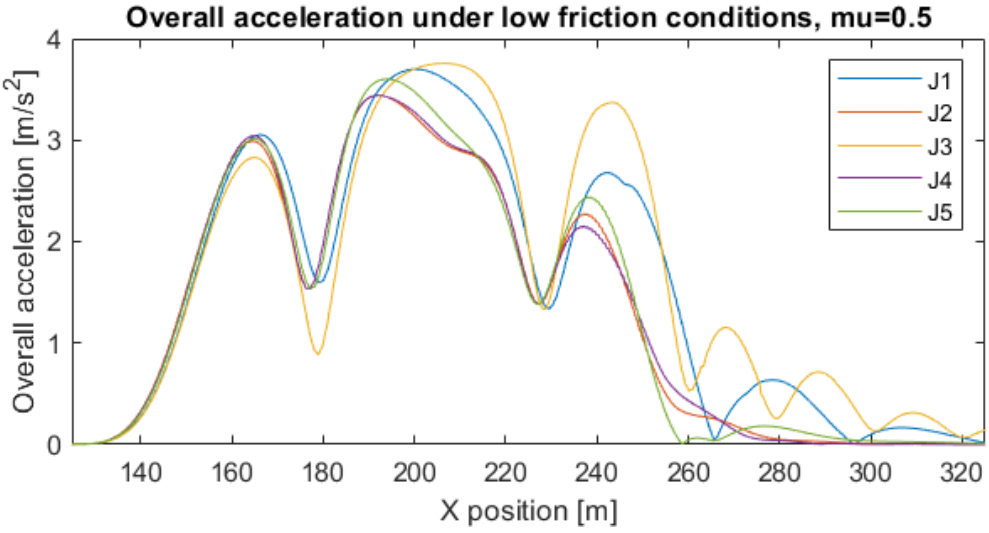

Figure 8-6: Overall acceleration on low friction scenario

Table 8-8: Double lane change with velocity change, friction change to $\mu = 0.5$

Controller	J_1	J_2	J_3	J_4	J_5
Time horizon [s]	1	1	1	1	1
RMS ms $[m/s^2]$	0.883	0.774	0.813	0.78	0.788
Improvement [%]	–	**12.4**	**8**	**11.7**	**10.8**
RMS gd $[m/s^2]$	0.699	0.659	0.743	0.655	0.687
Improvement [%]	–	**5.7**	-6.3	**6.3**	**1.7**
MTVV ms $[m/s^2]$	1.76	1.59	1.7	1.6	1.64
Improvement [%]	–	**9.9**	**3.2**	**9.3**	**7.1**
MTVV gd $[m/s^2]$	1.36	1.4	1.36	1.42	1.41
Improvement [%]	–	-2.3	**0.5**	-3.9	-3.3
mean comfort $[m/s^2]$	1.18	1.1	1.15	1.11	1.13
Improvement [%]	–	**6.2**	**1.9**	**5.5**	**4**
v error max $[km/hour]$	0.749	0.779	0.777	0.778	0.789
y error max $[m]$	0.321	0.224	0.423	0.227	0.215

The improvements are compared to the first result column (–)
Bold is a positive effect

8-4-2 Wind disturbance

The implementation of wind disturbance can be found in Section 4-2-1. The penalties on lateral acceleration have a negative reaction on wind disturbances in terms of lateral error, see Table 8-9. The controllers can not be implemented at this point when wind disturbances is present. A disturbance observer could help deal with this problem. In Section 6-5-2 more information is given for the wind disturbance problem.

8-4-3 Sensor noise

The implementation of sensor noise can be found in Section 4-2-1. All the controllers which penalises a form of the lateral acceleration (filtered and unfiltered) perform well in terms of comfort, see Table 8-10. Implementing a form of penalty on lateral acceleration during sensor noise is recommended.

Table 8-9: Double lane change with velocity change under wind disturbance

Controller	J_1	J_2	J_3	J_4	J_5
Time horizon [s]	1	1	1	1	1
RMS ms $[m/s^2]$	0.88	0.744	0.732	0.753	0.741
Improvement [%]	–	**15.5**	**16.9**	**14.4**	**15.8**
RMS gd $[m/s^2]$	0.701	0.643	0.695	0.633	0.668
Improvement [%]	–	**8.3**	**0.9**	**9.7**	**4.8**
MTVV ms $[m/s^2]$	1.76	1.5	1.51	1.52	1.5
Improvement [%]	–	**14.8**	**14.5**	**13.8**	**14.8**
MTVV gd $[m/s^2]$	1.37	1.35	1.34	1.34	1.38
Improvement [%]	–	**1.9**	**2.6**	**2.3**	-0.2
mean comfort $[m/s^2]$	1.18	1.06	1.07	1.06	1.07
Improvement [%]	–	**10.2**	**9.4**	**10**	**9.1**
v error max $[km/hour]$	0.748	0.768	0.774	0.762	0.782
y error max $[m]$	0.385	[0.814]	[1.05]	[0.768]	[0.736]

Large lateral error due to penalising accelerations [ ]
The improvements are compared to the first result column (–)
Bold is a positive effect

Table 8-10: Double lane change with velocity change with sensor noise

Controller	J_1	J_2	J_3	J_4	J_5
Time horizon [s]	1	1	1	1	1
RMS ms $[m/s^2]$	0.893	0.757	0.759	0.765	0.758
Improvement [%]	–	**15.3**	**15**	**14.4**	**15.2**
RMS gd $[m/s^2]$	0.751	0.712	0.761	0.709	0.74
Improvement [%]	–	**5.1**	-1.3	**5.6**	**1.5**
MTVV ms $[m/s^2]$	1.79	1.53	1.58	1.55	1.55
Improvement [%]	–	**14.4**	**11.7**	**13.5**	**13.6**
MTVV gd $[m/s^2]$	1.51	1.51	1.5	1.51	1.54
Improvement [%]	–	**0.3**	**1**	**0.4**	-1.8
mean comfort $[m/s^2]$	1.24	1.13	1.15	1.13	1.15
Improvement [%]	–	**8.8**	**7**	**8.4**	**7.3**
v error max $[km/hour]$	1.17	1.2	1.21	1.2	1.2
y error max $[m]$	0.367	0.307	0.36	0.31	0.301

Low influence sensor noise on motion sickness
The improvements are compared to the first result column (–)
Bold is a positive effect

8-5 Combinations acceleration terms filtered and unfiltered

When penalising filtered accelerations, the acceleration itself needs to be calculated. Therefore, penalising for example motion sickness and lateral acceleration in one controller does not lead to extra states to calculate. Therefore, two controllers will be compared which have a combination of filtered and unfiltered penalties on the lateral acceleration (J_7 and J_8).

Table 8-11: Weights applied on the controllers

Controller	J_2	J_3	J_4	J_7	J_8
w_{y}	50	50	50	50	50
w_{ψ}	7620	4500	9720	6.7e03	9.3e03
w_{v}	42	57	42	53	44
$w_{\triangle\delta}$	3150000	4400000	2950000	5000000	4.5e06
$w_{\triangle\mathrm{a}}$	605	790	610	758	741
w_{ay}	30.7	0	0	22	38
$w_{\mathrm{ay,ms}}$	x	255	0	154	0
$w_{\mathrm{ay,gd}}$	x	x	130	x	12
w_{ax}	0	0	0	0	0
$w_{\mathrm{ax,ms}}$	x	0	0	0	0
$w_{\mathrm{ax,gd}}$	x	x	0	x	0

x means the term is not implemented in the controller

As can be seen in Table 8-12 the results between the controllers are similar. The motion sickness filter does decrease the RMS motion sickness performance compared to J_2. The general discomfort filter does decrease the general discomfort performance compared to J_2. The differences between the controllers are small.

Table 8-12: Double lane change, different controllers

Controller	J_2	J_3	J_4	J_7	J_8
Time horizon [s]	1	1	1	1	1
RMS ms $[m/s^2]$	0.748	0.747	0.757	0.746	0.75
Improvement [%]	–	[**0.2**]	-1.1	[**0.3**]	-0.2
RMS gd $[m/s^2]$	0.641	0.698	0.628	0.648	0.632
Improvement [%]	–	-8.8	(**2.1**)	-1.1	(**1.5**)
MTVV ms $[m/s^2]$	1.51	1.55	1.53	1.52	1.52
Improvement [%]	–	[-2.6]	-1.1	[-0.8]	-0.4
MTVV gd $[m/s^2]$	1.34	1.36	1.33	1.33	1.32
Improvement [%]	–	-1.9	(**0.5**)	**1.1**	(**1.5**)
mean comfort $[m/s^2]$	1.06	1.09	1.06	1.06	1.05
Improvement [%]	–	-2.8	-0.1	-0.1	**0.5**
v error max $[km/hour]$	0.78	0.779	0.779	0.788	0.799
y error max $[m]$	0.325	0.325	0.324	0.325	0.325

Motion sickness filter implemented [ ]
General discomfort filter implemented ( )
The improvements are compared to the first result column –
Bold is a positive effect

8-6 Solving time

To test if the controller could be implemented, the solving time is measured. The tuning and scenario of Section 8-2 are used with a time horizon of 1 second. Since the longitudinal accelerations (filtered and unfiltered) are not penalized, the controllers are tested without the terms implemented, see Table 8-14. The test is simulated eleven times and the maximum and mean solving times are saved. The results can be found in Table 8-13. All the controllers are within sampling time (<0.04 second).

Table 8-13: Solving times on the double lane change with velocity change

Controller	J_1	J_2	J_3	J_4	J_5
Maximum of maximums* [s]	0.00849	0.01	0.0119	0.0264	0.0149
Mean of maximums* [s]	0.00825	0.00953	0.0116	0.017	0.0133
Mean of means** [s]	0.0062	0.00707	0.00784	0.01	0.00961

Each controller is simulated 11 times, * Maximum of each simulation, ** Mean of each simulation

Table 8-14: Weights applied on the controllers

Controller	J_1	J_2	J_3	J_4	J_5
w_{y}	50	50	50	50	50
w_{ψ}	2700	7620	4500	9720	3500
w_{v}	21	42	57	42	27
$w_{\triangle\delta}$	2.42e6	3.15e6	4.40e6	2.95e6	1.80e6
$w_{\triangle\mathrm{a}}$	280	605	790	610	439
w_{ay}	x	30.7	0	0	0
$w_{\mathrm{ay,ms}}$	x	x	255	0	100
$w_{\mathrm{ay,gd}}$	x	x	x	130	21
w_{ax}	x	x	x	x	x
$w_{\mathrm{ax,ms}}$	x	x	x	x	x
$w_{\mathrm{ax,gd}}$	x	x	x	x	x

x means the term is not implemented in the controller

8-7 Summary

The motion sickness filter improves the motion sickness comfort. If the motion sickness controller (J_3) is implemented in a scenario which creates a lot of motion sickness the controller will out perform the other methods, see Section 8-2. The mean comfort of the controller with the motion sickness filter improves with 24.7% compared to the basic controller (J_1). The highest decrease for RMS motion sickness is 30.7% compared to the basic controller (J_1). The general discomfort filter does decrease general discomfort. The highest improvement of the general discomfort filter is on the scenario of Figure 8-1 with a decrease of 10.7% on the RMS for general discomfort compared to the basic controller (J_1).

The longitudinal acceleration terms (filtered and unfiltered) have only a small effect. Implementing the terms makes the controller more complex. The terms could have a positive effect on the lateral error, see Section 8-3. If the controller should be safer the terms could help by keeping the lateral deviation low. The longitudinal control could have more effect when the problem described in Section 6-4-1 is solved. The problem is an increase in velocity to minimize the lateral cost, causing the controller to increase velocity before a corner when low longitudinal weights were given.

To keep a high performance under low friction the overall acceleration should be kept low. This can be done by penalising the accelerations directly or using a correct filter. Under wind disturbances penalising a form of lateral acceleration is not recommended due to an increase of lateral error, further research is recommended. When sensor noise is applied penalising a form of lateral acceleration is recommended (filtered or unfiltered), which keeps the comfort high.

The maximum solving time of the controllers are low enough to be implemented in a real vehicle (< 0.04 seconds).

Chapter 9

Conclusion and future work

9-1 Conclusion

To minimize discomfort, accelerations in the frequency of motion sickness and general discomfort must be minimized. Therefore, an MPC is built which filters the predicted accelerations for motion sickness and general discomfort and penalises them. Since the MPC can use both the steering wheel and throttle/brake, the longitudinal and lateral accelerations can be penalised. The MPC uses the Forces pro solver [46, 47], the solver is able to find a solution within the sample time, the test is done with a time horizon of one second and a sampling time of 0.04 seconds.

The penalties on the filtered accelerations for motion sickness and general discomfort prove to work. When driving on a road which creates high motion sickness, the motion sickness filter can bring the discomfort down (both general discomfort and motion sickness). In Section 8-2 the motion sickness controller drives on a sine wave of the frequency of motion sickness, the root-mean-square of motion sickness decreases with 30.7% and the root-mean-square of general discomfort with 23.8% compared to the basic controller. The improvements of the general discomfort filter are of lower nature. In Section 8-2 the root-mean-square for general discomfort on the double lane change decreases with 10.7% compared to the basic controller. The comfort can be further increased by increasing the time horizon. However, increasing the time horizon leads to a more complex problem.

Implementing the filters on the longitudinal acceleration does not lead to a significant increase in comfort. Even if the velocity signal is made aggressive the improvement of mean comfort is around $\pm 5\%$. In normal day driving the velocity profile would be less aggressive and the increase in comfort would be lower. Implementing one filter on the longitudinal acceleration leads to an increase of 4 states, and implementing both filters to 7 states. Therefore, implementing the filters lead to a more complex problem without generating significant improvements in comfort. The filters can have a positive effect on safety by creating a lower lateral deviation, see Section 8-3.

A drawback from using the filters is a large lateral error under wind disturbance which leads to unsafe road behaviour. When implementing the controller in a real vehicle the lateral error should be kept low to stay within the lane. When sensor noise is applied the controllers are able to keep the motion sickness low. The motion sickness is less effected by the high frequency noise due to the difference in the frequencies. When driving on low friction the overall acceleration should be kept low on all frequencies. Through using the motion sickness filter the controller could generate high accelerations in other frequencies and increasing the overall acceleration. Therefore, penalising the acceleration directly is effective due to keeping accelerations low in all frequencies.

In the end passengers should decide what kind of controller should be implemented. If the passengers find motion sickness or general discomfort more important, the passengers should select the controller which minimizes the selected comfort, or a certain ratio between motion sickness and general discomfort.

9-2 Future work

The filters do have positive effect on comfort. Implementing the filters in a vehicle could increase the comfort for the passengers. To create even more comfort and safety there are still topics to be researched further.

9-2-1 Tuning

The tuning of the controllers can become time consuming. In the case of Chapter 8 each controller has multiple weights which all need to be tuned. To make the problem easier a nonlinear tuning optimization algorithm should be written. The grid search approach is time consuming, the number of simulations grows exponential with every new variable weight.

Another problem with tuning is that for every person comfort is different. Different weights could be set for motion sickness and/or for general discomfort. Multiple controllers could be made in the future where the passengers can select their optimal mode for the vehicle and road ahead.

9-2-2 Safety controller

The controllers made in this thesis are controllers which use a bicycle model with a linear tire model and are maximized for comfort. The controllers will not be optimal when pushing the vehicle to the handling limits. When reaching the handling limits tire forces becomes nonlinear and will behave differently than in the current model. The comfort terms will have a negative effect on emergency handling due to increasing the lateral error. Therefore, a safety controller is proposed. The safety controller should be able to gain control of the vehicle in emergency scenarios and handle the vehicle accordingly.

9-2-3 Disturbance observer

The controllers that penalise the accelerations have a high lateral error under wind disturbance, which leads to unsafe behaviour. A decrease in lateral error could be made by implementing a disturbance observer. A disturbance observer could also increase the performance under sensor noise.

9-2-4 Soft/hard boundary constraints

The controllers reaches the lateral limits on only a few points of the track. By creating soft or hard constraints on the lateral deviation the comfort terms could be increased and therefore the comfort. The controllers will be able to have larger lateral errors on other parts of the path without crossing the constraints.

9-2-5 Velocity problem

If there are no or low penalties on the velocity weights, the controller wants to accelerate when a curvature is present, see Section 6-4-1. The controller does not penalise the longitudinal position and has constant reference terms. Due to not penalising the longitudinal position the controller does not care where the vehicle is as long as the lateral error is minimized on the time step. The reference terms in the controller should change when the velocity changes this will lead to a more complex problem.

9-2-6 Real world test

To see how well the controller really works, tests needs to be done on a real vehicle. Real people could give an indication of the increase or decrease of comfort. With simulations only an idea of comfort and tracking can be given. The real world will differ from the simulations.

Appendix A

Vehicle model

A-1 Dynamic bicycle model

$$m(\ddot{x} - \dot{y}\dot{\psi}) = -F_{\mathrm{xf}}\cos(\delta_{\mathrm{f}}) - F_{\mathrm{yf}}\sin(\delta_{\mathrm{f}}) - F_{\mathrm{xr}} \tag{A-1}$$

$$m(\ddot{y} + \dot{x}\dot{\psi}) = F_{\mathrm{yf}}\cos(\delta_{\mathrm{f}}) - F_{\mathrm{xf}}\sin(\delta_{\mathrm{f}}) + F_{\mathrm{yr}} \tag{A-2}$$

$$I_{\mathrm{z}}\ddot{\psi} = L_{\mathrm{f}}(F_{\mathrm{yf}}\cos(\delta_{\mathrm{f}}) - F_{\mathrm{xf}}\sin(\delta_{\mathrm{f}})) - L_{\mathrm{r}}F_{\mathrm{yr}} \tag{A-3}$$

Which leads to:

$$\ddot{x} = -\frac{1}{m}F_{\mathrm{xf}}\cos(\delta_{\mathrm{f}}) - \frac{1}{m}F_{\mathrm{yf}}\sin(\delta_{\mathrm{f}}) - \frac{1}{m}F_{\mathrm{xr}} + \dot{y}\dot{\psi} \tag{A-4}$$

$$\ddot{y} = \frac{1}{m}F_{\mathrm{yf}}\cos(\delta_{\mathrm{f}}) - \frac{1}{m}F_{\mathrm{xf}}\sin(\delta_{\mathrm{f}}) + \frac{1}{m}F_{\mathrm{yr}} - \dot{x}\dot{\psi} \tag{A-5}$$

$$\ddot{\psi} = \frac{1}{I_{\mathrm{z}}}L_{\mathrm{f}}(F_{\mathrm{yf}}\cos(\delta_{\mathrm{f}}) - F_{\mathrm{xf}}\sin(\delta_{\mathrm{f}})) - \frac{1}{I_{\mathrm{z}}}L_{\mathrm{r}}F_{\mathrm{yr}} \tag{A-6}$$

The longitudinal control value is divided by mass to create a smaller number, in the vehicle the number converted back:

$$c_{\mathrm{x,f}} = \frac{F_{\mathrm{xf}}}{m} \tag{A-7}$$

$$c_{\mathrm{x,r}} = \frac{F_{\mathrm{xr}}}{m} \tag{A-8}$$

Which leads to:

$$\ddot{x} = -c_{\mathrm{x,f}}\cos(\delta_{\mathrm{f}}) - \frac{1}{m}F_{\mathrm{yf}}\sin(\delta_{\mathrm{f}}) - c_{\mathrm{x,r}} + \dot{y}\dot{\psi} \tag{A-9}$$

$$\ddot{y} = \frac{1}{m}F_{\mathrm{yf}}\cos(\delta_{\mathrm{f}}) - c_{\mathrm{x,f}}\sin(\delta_{\mathrm{f}}) + \frac{1}{m}F_{\mathrm{yr}} - \dot{x}\dot{\psi} \tag{A-10}$$

$$\ddot{\psi} = \frac{1}{I_{\mathrm{z}}}L_{\mathrm{f}}(F_{\mathrm{yf}}\cos(\delta_{\mathrm{f}}) - c_{\mathrm{x,f}}\, m\sin(\delta_{\mathrm{f}})) - \frac{1}{I_{\mathrm{z}}}L_{\mathrm{r}}F_{\mathrm{yr}} \tag{A-11}$$

With the tire forces:

$$F_{\mathrm{yf}} = -C_{\alpha\mathrm{f}}\alpha_{\mathrm{f}} \tag{A-12}$$
$$F_{\mathrm{yr}} = -C_{\alpha\mathrm{r}}\alpha_{\mathrm{r}} \tag{A-13}$$
$$\alpha_{\mathrm{f}} = \frac{\dot{y} + L_{\mathrm{f}}\dot{\psi}}{\dot{x}} - \delta_{\mathrm{f}} \tag{A-14}$$
$$\alpha_{\mathrm{r}} = \frac{\dot{y} - L_{\mathrm{r}}\dot{\psi}}{\dot{x}} \tag{A-15}$$
$$F_{\mathrm{yf}} = -C_{\alpha\mathrm{f}}(\frac{\dot{y} + L_{\mathrm{f}}\dot{\psi}}{\dot{x}} - \delta_{\mathrm{f}}) \tag{A-16}$$
$$F_{\mathrm{yr}} = -C_{\alpha\mathrm{r}}(\frac{\dot{y} - L_{\mathrm{r}}\dot{\psi}}{\dot{x}}) \tag{A-17}$$

Which leads to:

$$\ddot{x} = -c_{\mathrm{x,f}}\cos(\delta_{\mathrm{f}}) - \frac{1}{m}(-C_{\alpha\mathrm{f}}(\frac{\dot{y} + L_{\mathrm{f}}\dot{\psi}}{\dot{x}} - \delta_{\mathrm{f}}))\sin(\delta_{\mathrm{f}}) - c_{\mathrm{x,r}} + \dot{y}\dot{\psi} \tag{A-18}$$
$$\ddot{y} = \frac{1}{m}(-C_{\alpha\mathrm{f}}(\frac{\dot{y} + L_{\mathrm{f}}\dot{\psi}}{\dot{x}} - \delta_{\mathrm{f}}))\cos(\delta_{\mathrm{f}}) - c_{\mathrm{x,f}}\sin(\delta_{\mathrm{f}}) + \frac{1}{m}(-C_{\alpha\mathrm{r}}(\frac{\dot{y} - L_{\mathrm{r}}\dot{\psi}}{\dot{x}})) - \dot{x}\dot{\psi} \tag{A-19}$$
$$\ddot{\psi} = \frac{1}{I_{\mathrm{z}}}L_{\mathrm{f}}((-C_{\alpha\mathrm{f}}(\frac{\dot{y} + L_{\mathrm{f}}\dot{\psi}}{\dot{x}} - \delta_{\mathrm{f}}))\cos(\delta_{\mathrm{f}}) - c_{\mathrm{x,f}}\ m\sin(\delta_{\mathrm{f}})) - \frac{1}{I_{\mathrm{z}}}L_{\mathrm{r}}(-C_{\alpha\mathrm{r}}(\frac{\dot{y} - L_{\mathrm{r}}\dot{\psi}}{\dot{x}})) \tag{A-20}$$

which leads to:

$$\ddot{x} = -c_{\mathrm{x,f}}\cos(\delta_{\mathrm{f}}) + \frac{1}{m}C_{\alpha\mathrm{f}}(\frac{\dot{y} + L_{\mathrm{f}}\dot{\psi}}{\dot{x}})\sin(\delta_{\mathrm{f}}) - \frac{1}{m}C_{\alpha\mathrm{f}}\delta_{\mathrm{f}}\sin(\delta_{\mathrm{f}}) - c_{\mathrm{x,r}} + \dot{y}\dot{\psi} \tag{A-21}$$
$$\ddot{y} = -\frac{1}{m}C_{\alpha\mathrm{f}}(\frac{\dot{y} + L_{\mathrm{f}}\dot{\psi}}{\dot{x}})\cos(\delta_{\mathrm{f}}) + \frac{1}{m}C_{\alpha\mathrm{f}}\delta_{\mathrm{f}}\cos(\delta_{\mathrm{f}}) - c_{\mathrm{x,f}}\sin(\delta_{\mathrm{f}}) - \frac{1}{m}C_{\alpha\mathrm{r}}(\frac{\dot{y} - L_{\mathrm{r}}\dot{\psi}}{\dot{x}}) - \dot{x}\dot{\psi} \tag{A-22}$$
$$\ddot{\psi} = -\frac{1}{I_{\mathrm{z}}}L_{\mathrm{f}}C_{\alpha\mathrm{f}}(\frac{\dot{y} + L_{\mathrm{f}}\dot{\psi}}{\dot{x}})\cos(\delta_{\mathrm{f}}) + \frac{1}{I_{\mathrm{z}}}L_{\mathrm{f}}C_{\alpha\mathrm{f}}\delta_{\mathrm{f}}\cos(\delta_{\mathrm{f}}) - \frac{1}{I_{\mathrm{z}}}L_{\mathrm{f}}c_{\mathrm{x,f}}m\sin(\delta_{\mathrm{f}}) + \frac{1}{I_{\mathrm{z}}}L_{\mathrm{r}}C_{\alpha\mathrm{r}}(\frac{\dot{y} - L_{\mathrm{r}}\dot{\psi}}{\dot{x}}) \tag{A-23}$$

which leads to:

$$\ddot{x} = -c_{\mathrm{x,f}}\cos(\delta_{\mathrm{f}}) + \frac{C_{\alpha\mathrm{f}}}{m}(\frac{\dot{y} + L_{\mathrm{f}}\dot{\psi}}{\dot{x}})\sin(\delta_{\mathrm{f}}) - \frac{C_{\alpha\mathrm{f}}}{m}\delta_{\mathrm{f}}\sin(\delta_{\mathrm{f}}) - c_{\mathrm{x,r}} + \dot{y}\dot{\psi} \tag{A-24}$$
$$\ddot{y} = -\frac{C_{\alpha\mathrm{f}}}{m}(\frac{\dot{y} + L_{\mathrm{f}}\dot{\psi}}{\dot{x}})\cos(\delta_{\mathrm{f}}) + \frac{C_{\alpha\mathrm{f}}}{m}\delta_{\mathrm{f}}\cos(\delta_{\mathrm{f}}) - c_{\mathrm{x,f}}\sin(\delta_{\mathrm{f}}) - \frac{C_{\alpha\mathrm{r}}}{m}(\frac{\dot{y} - L_{\mathrm{r}}\dot{\psi}}{\dot{x}}) - \dot{x}\dot{\psi} \tag{A-25}$$
$$\ddot{\psi} = -\frac{L_{\mathrm{f}}C_{\alpha\mathrm{f}}}{I_{\mathrm{z}}}(\frac{\dot{y} + L_{\mathrm{f}}\dot{\psi}}{\dot{x}})\cos(\delta_{\mathrm{f}}) + \frac{L_{\mathrm{f}}C_{\alpha\mathrm{f}}}{I_{\mathrm{z}}}\delta_{\mathrm{f}}\cos(\delta_{\mathrm{f}}) - \frac{L_{\mathrm{f}}}{I_{\mathrm{z}}}c_{\mathrm{x,f}}m\sin(\delta_{\mathrm{f}}) + \frac{L_{\mathrm{r}}C_{\alpha\mathrm{r}}}{I_{\mathrm{z}}}(\frac{\dot{y} - L_{\mathrm{r}}\dot{\psi}}{\dot{x}}) \tag{A-26}$$

With:

$$\delta_{\mathrm{f}} = \delta_{\mathrm{f}} + \triangle\delta_{\mathrm{f}} \tag{A-27}$$
$$c_{\mathrm{x,f}} = c_{\mathrm{x,f}} + \triangle c_{\mathrm{x,f}} \tag{A-28}$$
$$c_{\mathrm{x,r}} = c_{\mathrm{x,r}} + \triangle c_{\mathrm{x,r}} \tag{A-29}$$

$$\ddot{x} = -(c_{\mathrm{x,f}} + \triangle c_{\mathrm{x,f}})\cos(\delta_{\mathrm{f}} + \triangle\delta_{\mathrm{f}}) + \frac{C_{\alpha\mathrm{f}}}{m}(\frac{\dot{y} + L_{\mathrm{f}}\dot{\psi}}{\dot{x}})\sin(\delta_{\mathrm{f}} + \triangle\delta_{\mathrm{f}})\ldots$$
$$- \frac{C_{\alpha\mathrm{f}}}{m}(\delta_{\mathrm{f}} + \triangle\delta_{\mathrm{f}})\sin(\delta_{\mathrm{f}} + \triangle\delta_{\mathrm{f}}) - (c_{\mathrm{x,r}} + \triangle c_{\mathrm{x,r}}) + \dot{y}\dot{\psi} \tag{A-30}$$

$$\ddot{y} = -\frac{C_{\alpha\mathrm{f}}}{m}(\frac{\dot{y} + L_{\mathrm{f}}\dot{\psi}}{\dot{x}})\cos(\delta_{\mathrm{f}} + \triangle\delta_{\mathrm{f}}) + \frac{C_{\alpha\mathrm{f}}}{m}(\delta_{\mathrm{f}} + \triangle\delta_{\mathrm{f}})\cos(\delta_{\mathrm{f}} + \triangle\delta_{\mathrm{f}})\ldots$$
$$- (c_{\mathrm{x,f}} + \triangle c_{\mathrm{x,f}})\sin(\delta_{\mathrm{f}} + \triangle\delta_{\mathrm{f}}) - \frac{C_{\alpha\mathrm{r}}}{m}(\frac{\dot{y} - L_{\mathrm{r}}\dot{\psi}}{\dot{x}}) - \dot{x}\dot{\psi} \tag{A-31}$$

$$\ddot{\psi} = -\frac{L_{\mathrm{f}}C_{\alpha\mathrm{f}}}{I_{\mathrm{z}}}(\frac{\dot{y} + L_{\mathrm{f}}\dot{\psi}}{\dot{x}})\cos(\delta_{\mathrm{f}} + \triangle\delta_{\mathrm{f}}) + \frac{L_{\mathrm{f}}C_{\alpha\mathrm{f}}}{I_{\mathrm{z}}}(\delta_{\mathrm{f}} + \triangle\delta_{\mathrm{f}})\cos(\delta_{\mathrm{f}} + \triangle\delta_{\mathrm{f}})\ldots$$
$$- \frac{L_{\mathrm{f}}}{I_{\mathrm{z}}}(c_{\mathrm{x,f}} + \triangle c_{\mathrm{x,f}})m\sin(\delta_{\mathrm{f}} + \triangle\delta_{\mathrm{f}}) + \frac{L_{\mathrm{r}}C_{\alpha\mathrm{r}}}{I_{\mathrm{z}}}(\frac{\dot{y} - L_{\mathrm{r}}\dot{\psi}}{\dot{x}}) \tag{A-32}$$

Appendix B

Results

The full results are given in this chapter of the appendix. When the term is not implemented in the cost function, the cost of that weight is set to zero.

B-1 Result influence lateral control

B-1-1 Double lane change 80 km/hour

Table B-1: Double lane change 80 km/hour

Controller	J_1	J_2	J_3	J_4	J_5	J_6
Time horizon [s]	1	1	1	1	1	1
RMS ms $[m/s^2]$	0.738	0.66	0.636	0.67	0.644	0.761
Improvement [%]	–	**10.6**	**13.9**	**9.2**	**12.8**	-3.1
RMS gd $[m/s^2]$	0.701	0.654	0.687	0.65	0.677	1.29
Improvement [%]	–	**6.7**	**2**	**7.3**	**3.4**	-84.5
MTVV ms $[m/s^2]$	1.49	1.35	1.3	1.37	1.32	1.51
Improvement [%]	–	**9.3**	**12.3**	**7.9**	**11.5**	-1.4
MTVV gd $[m/s^2]$	1.25	1.15	1.22	1.13	1.21	2.1
Improvement [%]	–	**7.5**	**2.2**	**9.3**	**3.3**	-68.1
mean comfort $[m/s^2]$	1.04	0.954	0.962	0.955	0.961	1.42
Improvement [%]	–	**8.6**	**7.8**	**8.5**	**7.9**	-35.6
y error max $[m]$	0.3	0.299	0.3	0.3	0.3	0.292
v error max $[km/hour]$	0.0529	0.0497	0.0509	0.0505	0.0507	0.0921
Weight cost y	5.44e4	3.33e4	2.86e4	3.59e4	3.01e4	7.04e4
Weight cost psi	2611	6255	4777	7700	3033	3300
Weight cost v	1.08e5	1.07e5	1.07e5	1.07e5	1.07e5	1.01e5
Weight cost $\triangle\delta$	1411	2100	2388	2444	1244	0
Weight cost $\triangle$a	2.66e4	2.65e4	2.65e4	2.64e4	2.65e4	2.44e4
Weight cost ms	0	0	2.79e4	0	1.44e4	0
Weight cost gd	0	0	0	9055	925	0
Weight cost ay	0	3055	0	0	0	0

Improvement compared to the baseline controller J_1 (–)
Bold is a positive effect

B-1-2 Increase time horizon motion sickness

Table B-2: Double lane change 80 km/hour

Controller	J_3	J_3	J_3	J_3
Time horizon $[s]$	1	2	2	5
Sample time $[s]$	0.04	0.04	0.10	0.10
RMS ms $[m/s^2]$	0.667	0.673	0.678	0.667
Improvement [%]	–	-0.9	-1.7	0
RMS gd $[m/s^2]$	0.721	0.56	0.568	0.545
Improvement [%]	–	**22.2**	**21.1**	**24.3**
MTVV ms $[m/s^2]$	1.3	1.32	1.33	1.3
Improvement [%]	–	-1	-1.6	**0.1**
MTVV gd $[m/s^2]$	1.22	0.971	0.993	0.959
Improvement [%]	–	**20.4**	**18.6**	**21.4**
mean comfort $[m/s^2]$	0.978	0.88	0.891	0.869
Improvement [%]	–	**10**	**8.9**	**11.2**
y error max $[m]$	0.3	0.298	0.297	0.298
v error max $[km/hour]$	0.0509	0.048	0.0906	0.0911
Weight cost y	2.86e4	6.51e5	9.91e4	2.76e6
Weight cost psi	4777	7400	9511	15900
Weight cost v	1.07e5	1.07e5	5.20e4	5.19e4
Weight cost $\triangle\delta$	2388	3011	3222	4400
Weight cost $\triangle$a	2.65e4	2.64e4	9644	9777
Weight cost ms	2.78e4	7944	9577	1.15e4
Weight cost gd	0	0	0	0
Weight cost ay	0	0	0	0

The improvements are compared to the first result column (–)
Bold is a positive effect

B-1-3 Sine wave motion sickness

Table B-3: One period of the sine wave at 80 km/hour

Controller	J_1	J_2	J_3	J_4	J_5	J_6
Time horizon [s]	1	1	1	1	1	1
RMS ms $[m/s^2]$	0.93	0.83	0.767	0.847	0.793	0.931
Improvement [%]	–	**10.7**	**17.6**	**8.9**	**14.7**	0
RMS gd $[m/s^2]$	0.413	0.366	0.339	0.374	0.35	0.459
Improvement [%]	–	**11.3**	**18**	**9.5**	**15.3**	-11.1
MTVV ms $[m/s^2]$	1.22	1.1	1.01	1.12	1.05	1.23
Improvement [%]	–	**10.4**	**17.2**	**8.6**	**14.4**	-0.1
MTVV gd $[m/s^2]$	0.528	0.482	0.442	0.495	0.459	0.609
Improvement [%]	–	**8.7**	**16.2**	**6.2**	**13**	-15.4
mean comfort $[m/s^2]$	0.774	0.694	0.64	0.709	0.663	0.806
Improvement [%]	–	**10.3**	**17.2**	**8.4**	**14.4**	-4.1
y error max $[m]$	0.174	0.178	0.25	0.162	0.216	0.386
v error max $[km/hour]$	0.0462	0.0448	0.0441	0.0451	0.0443	0.0403
Weight cost y	3.01e4	1.85e4	1.11e4	2.05e4	1.37e4	4.07e4
Weight cost psi	377	1366	1733	1566	924	1300
Weight cost v	7044	6799	6688	6822	6700	4022
Weight cost $\triangle\delta$	351	529	539	698	311	0
Weight cost $\triangle$a	1777	1699	1699	1699	1699	866
Weight cost ms	0	0	1.88e4	0	1.01e4	0
Weight cost gd	0	0	0	3944	361	0
Weight cost ay	0	1533	0	0	0	0

The improvements are compared to the first result column (–)
Bold is a positive effect

Table B-4: Double lane change with same tuning and different velocities

Controller	J_3	J_3	J_3
Time horizon [s]	1	1	1
Velocity double lane change [km/hour]	80	60	40
RMS ms $[m/s^2]$	0.636	0.378	0.168
Improvement [%]	–	**40.6**	**73.6**
RMS gd $[m/s^2]$	0.687	0.387	0.0914
Improvement [%]	–	**43.6**	**86.7**
MTVV ms $[m/s^2]$	1.3	0.704	0.317
Improvement [%]	–	**46**	**75.7**
MTVV gd $[m/s^2]$	1.22	0.758	0.209
Improvement [%]	–	**37.8**	**82.8**
mean comfort $[m/s^2]$	0.962	0.557	0.197
Improvement [%]	–	**42.1**	**79.6**
y error max $[m]$	0.3	0.484	0.972
v error max $[km/hour]$	0.0509	0.046	0.0428
Weight cost y	28600	28600	100000
Weight cost psi	4777	9744	39900
Weight cost v	107000	125000	192000
Weight cost $\triangle\delta$	2388	2666	1711
Weight cost $\triangle$a	26500	30200	41200
Weight cost ms	27800	113000	265000
Weight cost gd	0	0	0
Weight cost ay	0	0	0

Increase in lateral error when the controller is not re-tuned for different velocities
The improvement is compared to the first result column (–)
Bold is a positive effect

Table B-5: Sine wave at 60 km/hour

Controller	J_1	J_3
Time horizon [s]	1	1
RMS ms $[m/s^2]$	0.931	0.737
Improvement [%]	–	**20.9**
RMS gd $[m/s^2]$	0.443	0.324
Improvement [%]	–	**26.9**
MTVV ms $[m/s^2]$	1.22	0.971
Improvement [%]	–	**20.4**
MTVV gd $[m/s^2]$	0.493	0.423
Improvement [%]	–	**14.1**
mean comfort $[m/s^2]$	0.772	0.614
Improvement [%]	–	**20.5**
y error max $[m]$	0.255	0.324
v error max $[km/hour]$	0.05	0.0471
Weight cost y	5.20e4	1.30e4
Weight cost psi	2844	7522
Weight cost v	7833	7155
Weight cost $\triangle\delta$	815	2277
Weight cost $\triangle$a	1833	1733
Weight cost ms	0	1.43e5
Weight cost gd	0	0
Weight cost ay	0	0

The improvement is compared to the first result column (–)
Bold is a positive effect

B-1-4 Friction change

Table B-6: Double lane change 80 km/hour with $\mu = 0.5$

Controller	J_1	J_2	J_3	J_4	J_5	J_6
Time horizon [s]	1	1	1	1	1	1
RMS ms $[m/s^2]$	0.735	0.674	0.664	0.682	0.662	0.751
Improvement [%]	–	**8.3**	**9.7**	**7.2**	**10**	-2.2
RMS gd $[m/s^2]$	0.691	0.669	0.686	0.672	0.678	1.22
Improvement [%]	–	**3.2**	**0.8**	**2.8**	**1.9**	-77.2
MTVV ms $[m/s^2]$	1.48	1.37	1.36	1.39	1.35	1.5
Improvement [%]	–	**7.2**	**8.2**	**6.1**	**8.8**	-1.2
MTVV gd $[m/s^2]$	1.22	1.18	1.22	1.18	1.21	2.01
Improvement [%]	–	**2.6**	-0.2	**3.2**	**0.8**	-65.5
mean comfort $[m/s^2]$	1.03	0.975	0.982	0.98	0.974	1.37
Improvement [%]	–	**5.4**	**4.7**	**4.9**	**5.5**	-33.1
y error max $[m]$	0.387	0.273	0.29	0.273	0.292	0.371
v error max $[km/hour]$	0.0511	0.0495	0.0503	0.0499	0.0499	0.0605
Weight cost y	5.76e4	3.56e4	3.17e4	3.77e4	3.29e4	7.38e4
Weight cost psi	2811	6077	4099	7300	2833	3722
Weight cost v	1.08e5	1.07e5	1.07e5	1.07e5	1.07e5	9.95e4
Weight cost $\triangle\delta$	1455	2299	2433	2633	1277	0
Weight cost $\triangle$a	2.66e4	2.65e4	2.65e4	2.65e4	2.65e4	2.42e4
Weight cost ms	0	0	1.76e4	0	9077	0
Weight cost gd	0	0	0	6944	709	0
Weight cost ay	0	2266	0	0	0	0

The improvements are compared to the first result column (–)
Bold is a positive effect

B-1-5 Wind disturbance

Table B-7: Double lane change 80 km/hour with wind disturbance

Controller	J_1	J_2	J_3	J_4	J_5	J_6
Time horizon [s]	1	1	1	1	1	1
RMS ms $[m/s^2]$	0.739	0.661	0.634	0.671	0.644	0.782
Improvement [%]	–	**10.6**	**14.2**	**9.2**	**12.9**	-5.8
RMS gd $[m/s^2]$	0.715	0.651	0.689	0.647	0.673	1.86
Improvement [%]	–	**9**	**3.6**	**9.5**	**5.9**	-160
MTVV ms $[m/s^2]$	1.5	1.35	1.29	1.37	1.31	1.52
Improvement [%]	–	**10**	**13.7**	**8.6**	**12.4**	-1.6
MTVV gd $[m/s^2]$	1.3	1.14	1.2	1.12	1.18	3.33
Improvement [%]	–	**12.5**	**7.3**	**13.9**	**9.5**	-156
mean comfort $[m/s^2]$	1.06	0.949	0.955	0.951	0.951	1.87
Improvement [%]	–	**10.7**	**10.1**	**10.5**	**10.5**	-76.3
y error max $[m]$	0.504	0.609	0.688	0.553	0.499	0.473
v error max $[km/hour]$	0.0523	0.0509	0.052	0.0518	0.0506	0.124
Weight cost y	7.86e4	1.12e5	1.24e5	9.86e4	9.40e4	1.24e5
Weight cost psi	2677	6533	5400	8055	3388	7277
Weight cost v	1.08e5	1.07e5	1.07e5	1.07e5	1.07e5	1.04e5
Weight cost $\triangle\delta$	1466	2200	2788	2644	1433	0
Weight cost $\triangle$a	2.66e4	2.65e4	2.65e4	2.65e4	2.65e4	2.57e4
Weight cost ms	0	0	3.66e4	0	1.89e4	0
Weight cost gd	0	0	0	1.16e4	1155	0
Weight cost ay	0	4744	0	0	0	0

The improvements are compared to the first result column (–)
Bold is a positive effect

B-1-6 Sensor noise

Table B-8: Double lane change 80 km/hour with sensor noise

Controller	J_1	J_2	J_3	J_4	J_5	J_6
Time horizon [s]	1	1	1	1	1	1
RMS ms $[m/s^2]$	0.728	0.651	0.625	0.661	0.634	0.704
Improvement [%]	–	**10.6**	**14.1**	**9.3**	**12.9**	**3.4**
RMS gd $[m/s^2]$	0.684	0.659	0.669	0.662	0.671	2.11
Improvement [%]	–	**3.7**	**2.2**	**3.3**	**1.9**	-209
MTVV ms $[m/s^2]$	1.46	1.33	1.28	1.35	1.3	1.41
Improvement [%]	–	**9.2**	**12.5**	**7.8**	**11.4**	**3.8**
MTVV gd $[m/s^2]$	1.22	1.19	1.25	1.19	1.23	3.83
Improvement [%]	–	**2.4**	-2.6	**2.4**	-0.6	-214
mean comfort $[m/s^2]$	1.02	0.958	0.957	0.966	0.957	2.01
Improvement [%]	–	**6.5**	**6.6**	**5.7**	**6.5**	-96.5
y error max $[m]$	0.258	0.262	0.309	0.263	0.265	0.32
v error max $[km/hour]$	0.0528	0.0514	0.052	0.0512	0.0519	0.143
Weight cost y	5.35e4	3.39e4	2.74e4	3.66e4	2.95e4	8.10e4
Weight cost psi	5322	1.47e4	1.02e4	1.80e4	6888	2.16e4
Weight cost v	1.08e5	1.07e5	1.07e5	1.07e5	1.07e5	1.07e5
Weight cost $\triangle\delta$	2288	4522	3800	5322	2266	0
Weight cost $\triangle$a	2.65e4	2.64e4	2.64e4	2.64e4	2.64e4	2.79e4
Weight cost ms	0	0	2.81e4	0	1.48e4	0
Weight cost gd	0	0	0	1.19e4	1099	0
Weight cost ay	0	4122	0	0	0	0

The improvements are compared to the first result column (–)
Bold is a positive effect

B-1-7 Influences of the time horizon

Table B-9: Double lane change 80 km/hour with different time horizons

Controller	J_1	J_1	J_2	J_2	J_4	J_4
Time horizon [s]	1	2	1	2	1	2
Sample time [s]	0.04	0.04	0.04	0.04	0.04	0.04
RMS ms $[m/s^2]$	0.738	0.704	0.66	0.657	0.67	0.674
Improvement [%]	–	**4.7**	–	**0.5**	–	-0.6
RMS gd $[m/s^2]$	0.701	0.557	0.654	0.532	0.65	0.537
Improvement [%]	–	**20.5**	–	**18.7**	–	**17.3**
MTVV ms $[m/s^2]$	1.49	1.43	1.35	1.35	1.37	1.38
Improvement [%]	–	**4.1**	–	-0.1	–	-0.9
MTVV gd $[m/s^2]$	1.25	0.997	1.15	0.951	1.13	0.952
Improvement [%]	–	**20.1**	–	**17.6**	–	**15.8**
mean comfort $[m/s^2]$	1.04	0.921	0.954	0.873	0.955	0.886
Improvement [%]	–	**11.7**	–	**8.6**	–	**7.2**
y error max $[m]$	0.3	0.299	0.299	0.3	0.3	0.3
v error max $[km/hour]$	0.0529	0.0501	0.0497	0.0487	0.0505	0.0497
Weight cost y	5.44e4	8.28e5	3.33e4	7.05e5	3.59e4	7.55e5
Weight cost psi	2611	9277	6255	2.74e4	7700	2.79e4
Weight cost v	1.08e5	1.07e5	1.07e5	1.07e5	1.07e5	1.07e5
Weight cost $\triangle\delta$	1411	5877	2100	1.80e4	2444	2.08e4
Weight cost $\triangle$a	2.66e4	2.65e4	2.65e4	2.65e4	2.64e4	2.65e4
Weight cost ms	0	0	0	0	0	0
Weight cost gd	0	0	0	0	9033	1.08e4
Weight cost ay	0	0	3055	5577	0	0

The improvements are compared to the same controller with time horizon of 1 second (–)
Bold is a positive effect

B-2 Results influence longitudinal control

B-2-1 Velocity profile

Table B-10: Velocity profile

Controller	J_1	J_2	J_3	J_4	J_5	J_6
Time horizon [s]	1	1	1	1	1	1
RMS ms $[m/s^2]$	0.67	0.593	0.616	0.64	0.608	0.709
Improvement [%]	–	**11.5**	**8**	**4.5**	**9.2**	-5.8
RMS gd $[m/s^2]$	0.357	0.354	0.345	0.338	0.335	0.676
Improvement [%]	–	**1**	**3.4**	**5.3**	**6.3**	-89.3
MTVV ms $[m/s^2]$	1.37	1.26	1.3	1.31	1.27	1.63
Improvement [%]	–	**7.8**	**4.5**	**4.1**	**6.8**	-19.7
MTVV gd $[m/s^2]$	0.937	0.958	0.909	0.866	0.902	1.74
Improvement [%]	–	-2.2	**3**	**7.6**	**3.7**	-86.3
mean comfort $[m/s^2]$	0.832	0.791	0.794	0.789	0.779	1.19
Improvement [%]	–	**5**	**4.7**	**5.3**	**6.4**	-43.1
v error max acc. $[km/hour]$	8.58	7.36	8.04	7.06	7.2	7.56
v error max brak. $[km/hour]$	5	4.99	5	5	5	2.32
y error max $[m]$	0	0	0	0	0	0
Weight cost y	0	0	0	0	0	0
Weight cost psi	0	0	0	0	0	0
Weight cost v	4.52e4	5.13e4	3.10e4	2.78e4	2.57e4	1.03e4
Weight cost $\triangle\delta$	0	0	0	0	0	0
Weight cost $\triangle$a	2.01e4	208	1.10e4	1.09	1.11	0
Weight cost ms y	0	0	0	0	0	0
Weight cost gd y	0	0	0	0	0	0
Weight cost ay	0	0	0	0	0	0
Weight cost ms x	0	0	51800	0	708000	0
Weight cost gd x	0	0	0	179	116	0
Weight cost ax	0	7.52e4	0	0	0	0

The improvements are compared to the first result column (–)
Bold is a positive effect

B-2-2 Friction change

Table B-11: Velocity profile with $\mu = 0.5$

Controller	J_1	J_2	J_3	J_4	J_5	J_6
Time horizon [s]	1	1	1	1	1	1
RMS ms $[m/s^2]$	0.633	0.554	0.58	0.611	0.58	0.65
Improvement [%]	–	**12.5**	**8.4**	**3.4**	**8.4**	-2.6
RMS gd $[m/s^2]$	0.367	0.302	0.333	0.342	0.331	0.663
Improvement [%]	–	**17.9**	**9.3**	**6.9**	**10**	-80.5
MTVV ms $[m/s^2]$	1.48	1.26	1.3	1.43	1.29	1.6
Improvement [%]	–	**14.9**	**11.8**	**3.4**	**12.8**	-8.5
MTVV gd $[m/s^2]$	1.23	0.917	0.995	1.2	1.13	1.9
Improvement [%]	–	**25.5**	**19.1**	**2.4**	**8**	-54.5
mean comfort $[m/s^2]$	0.928	0.758	0.803	0.896	0.833	1.2
Improvement [%]	–	**18.3**	**13.4**	**3.4**	**10.2**	-29.9
v error max acc. $[km/hour]$	12.2	11.7	11.8	11.6	11.4	12.4
v error max brak. $[km/hour]$	5	4.99	5	5	5	3.75
y error max $[m]$	0	0	0	0	0	0
Weight cost y	0	0	0	0	0	0
Weight cost psi	0	0	0	0	0	0
Weight cost v	6.02e4	6.47e4	4.64e4	4.75e4	4.31e4	3.25e4
Weight cost $\triangle\delta$	0	0	0	0	0	0
Weight cost $\triangle$a	1.84e4	234	1.09e4	1.21	1.22	0
Weight cost ms y	0	0	0	0	0	0
Weight cost gd y	0	0	0	0	0	0
Weight cost ay	0	0	0	0	0	0
Weight cost ms x	0	0	5.74e4	0	7.94e5	0
Weight cost gd x	0	0	0	200	137	0
Weight cost ax	0	7.98e4	0	0	0	0

The improvements are compared to the first result column (–)
Bold is a positive effect

Table B-12: Velocity profile with $\mu = 0.5$, Longitudinal control value constraint by maximum of 3.0

Controller	J_1	J_2	J_3	J_4	J_5	J_6
Time horizon [s]	1	1	1	1	1	1
RMS ms $[m/s^2]$	0.622	0.567	0.582	0.603	0.577	0.656
Improvement [%]	–	**8.9**	**6.4**	**3.2**	**7.2**	-5.3
RMS gd $[m/s^2]$	0.312	0.305	0.302	0.291	0.288	0.554
Improvement [%]	–	**2.2**	**3.2**	**6.6**	**7.7**	-77.5
MTVV ms $[m/s^2]$	1.37	1.26	1.3	1.31	1.27	1.6
Improvement [%]	–	**7.9**	**4.5**	**4.1**	**6.9**	-17.4
MTVV gd $[m/s^2]$	0.939	0.917	0.911	0.821	0.826	1.36
Improvement [%]	–	**2.3**	**2.9**	**12.5**	**12**	-45.2
mean comfort $[m/s^2]$	0.81	0.762	0.775	0.757	0.741	1.04
Improvement [%]	–	**5.9**	**4.3**	**6.6**	**8.5**	-28.9
v error max acc. $[km/hour]$	11.3	10.5	10.8	10.2	10.2	11.2
v error max brak. $[km/hour]$	5	4.99	5	5	5	3.75
y error max $[m]$	0	0	0	0	0	0
Weight cost y	0	0	0	0	0	0
Weight cost psi	0	0	0	0	0	0
Weight cost v	71600	74900	59100	51900	49700	51000
Weight cost $\triangle\delta$	0	0	0	0	0	0
Weight cost $\triangle$a	14400	196	8066	0.976	1	0
Weight cost ms y	0	0	0	0	0	0
Weight cost gd y	0	0	0	0	0	0
Weight cost ay	0	0	0	0	0	0
Weight cost ms x	0	0	46700	0	45200	0
Weight cost gd x	0	0	0	20800	13500	0
Weight cost ax	0	75500	0	0	0	0

The improvements are compared to the first result column (–)
Bold is a positive effect

B-2-3 Sensor noise

Table B-13: Velocity profile with sensor noise

Controller	J_1	J_2	J_3	J_4	J_5	J_6
Time horizon [s]	1	1	1	1	1	1
RMS ms $[m/s^2]$	0.663	0.62	0.613	0.678	0.645	0.808
Improvement [%]	–	**6.4**	**7.6**	-2.2	**2.8**	-21.9
RMS gd $[m/s^2]$	0.353	0.423	0.344	0.368	0.378	0.842
Improvement [%]	–	-20	**2.3**	-4.3	-7.3	-139
MTVV ms $[m/s^2]$	1.31	1.27	1.26	1.31	1.28	1.62
Improvement [%]	–	**3.3**	**4.3**	**0.4**	**2.6**	-23.4
MTVV gd $[m/s^2]$	0.942	0.951	0.916	0.819	0.892	1.54
Improvement [%]	–	-1	**2.7**	**13.1**	**5.3**	-64
mean comfort $[m/s^2]$	0.817	0.816	0.782	0.793	0.798	1.2
Improvement [%]	–	**0.2**	**4.3**	**3**	**2.3**	-47.3
v error max acc. $[km/hour]$	8.38	8.17	8	7.66	7.58	8.79
v error max brak. $[km/hour]$	4.92	5.37	4.98	6.02	5.89	4.54
y error max $[m]$	0	0	0	0	0	0
Weight cost y	0	0	0	0	0	0
Weight cost psi	0	0	0	0	0	0
Weight cost v	7.61e4	8.11e4	5.88e4	7.01e4	6.07e4	7.13e4
Weight cost $\triangle\delta$	0	0	0	0	0	0
Weight cost $\triangle$a	2.94e4	550	1.95e4	2.05	2.1	0
Weight cost ms y	0	0	0	0	0	0
Weight cost gd y	0	0	0	0	0	0
Weight cost ay	0	0	0	0	0	0
Weight cost ms x	0	0	52000	0	718000	0
Weight cost gd x	0	0	0	317	218	0
Weight cost ax	0	92400	0	0	0	0

The improvements are compared to the first result column (–)
Bold is a positive effect

B-2-4 Influences of the time horizon

Table B-14: Double lane change 80 km/hour with different time horizons

Controller	J_2	J_2	J_3	J_3	J_4	J_4
Time horizon [s]	1	2	1	2	1	2
Sample time [s]	0.04	0.04	0.04	0.04	0.04	0.04
RMS ms $[m/s^2]$	0.593	0.553	0.616	0.543	0.64	0.599
Improvement [%]	–	**6.7**	–	**11.8**	–	**6.4**
RMS gd $[m/s^2]$	0.354	0.262	0.345	0.267	0.338	0.288
Improvement [%]	–	**25.9**	–	**22.6**	–	**14.9**
MTVV ms $[m/s^2]$	1.26	1.14	1.3	1.15	1.31	1.23
Improvement [%]	–	**9.6**	–	**12**	–	**6.3**
MTVV gd $[m/s^2]$	0.958	0.696	0.909	0.704	0.866	0.728
Improvement [%]	–	**27.3**	–	**22.5**	–	**15.9**
mean comfort $[m/s^2]$	0.791	0.662	0.794	0.666	0.789	0.711
Improvement [%]	–	**16.2**	–	**16.1**	–	**9.8**
v error max acc. $[km/hour]$	7.36	7.33	8.04	7.78	7.06	7.5
v error max brak. $[km/hour]$	4.99	5	5	5	5	5
y error max $[m]$	0	0	0	0	0	0
Weight cost y	0	0	0	0	0	0
Weight cost psi	0	0	0	0	0	0
Weight cost v	5.13e4	7.68e4	3.10e4	7.51e4	2.78e4	4.89e4
Weight cost $\triangle\delta$	0	0	0	0	0	0
Weight cost $\triangle$a	208	1.12e4	1.10e4	1.77e4	1.09	6811
Weight cost ms y	0	0	0	0	0	0
Weight cost gd y	0	0	0	0	0	0
Weight cost ay	0	0	0	0	0	0
Weight cost ms x	0	0	5.18e4	2.09e5	0	0
Weight cost gd x	0	0	0	0	2.70e4	4.75e4
Weight cost ax	7.52e4	1.59e5	0	0	0	0

The improvements are compared to the same controller with time horizon of 1 second (–)
Bold is a positive effect

B-3 Results combined control

B-3-1 Double lane change with velocity change

Table B-15: Double lane change with velocity change

Controller	J_1	J_2	J_3	J_4	J_5
Time horizon [s]	1	1	1	1	1
RMS ms $[m/s^2]$	0.881	0.748	0.747	0.757	0.748
Improvement [%]	–	**15.1**	**15.2**	**14.1**	**15.1**
RMS gd $[m/s^2]$	0.703	0.641	0.698	0.628	0.674
Improvement [%]	–	**8.7**	**0.7**	**10.7**	**4.1**
MTVV ms $[m/s^2]$	1.75	1.51	1.55	1.53	1.53
Improvement [%]	–	**13.8**	**11.6**	**12.8**	**13.1**
MTVV gd $[m/s^2]$	1.38	1.34	1.36	1.33	1.39
Improvement [%]	–	**3.3**	**1.4**	**3.7**	-0.1
mean comfort $[m/s^2]$	1.18	1.06	1.09	1.06	1.08
Improvement [%]	–	**10.2**	**7.7**	**10.1**	**8.3**
v error max $[km/hour]$	0.75	0.78	0.779	0.779	0.79
y error max $[m]$	0.325	0.325	0.325	0.324	0.324
Weight cost y	7.06e4	3.00e4	3.97e4	3.28e4	2.95e4
Weight cost psi	4866	7100	7444	8744	3777
Weight cost v	568	1166	1533	1166	801
Weight cost $\triangle\delta$	2322	1666	3466	2177	1199
Weight cost $\triangle$a	356	750	988	754	508
Weight cost ms y	0	0	5.09e4	0	2.08e4
Weight cost gd y	0	0	0	1.25e4	2400
Weight cost ay	0	4688	0	0	0
Weight cost ms x	0	0	0	0	0
Weight cost gd x	0	0	0	0	0
Weight cost ax	0	0	0	0	0

The improvements are compared to the first result column (–)
Bold is a positive effect

B-3-2 Motion sickness

Table B-16: Sine wave for lateral and longitudinal control

Controller	J_1	J_2	J_3	J_4	J_5
Time horizon [s]	1	1	1	1	1
RMS ms $[m/s^2]$	1.28	0.988	0.887	1.01	0.961
Improvement [%]	–	**22.9**	**30.7**	**21.2**	**24.9**
RMS gd $[m/s^2]$	0.673	0.53	0.513	0.534	0.532
Improvement [%]	–	**21.4**	**23.8**	**20.7**	**21**
MTVV ms $[m/s^2]$	1.91	1.48	1.33	1.52	1.43
Improvement [%]	–	**22.6**	**30.4**	**20.7**	**25**
MTVV gd $[m/s^2]$	1.25	1.08	1.12	1.04	1.12
Improvement [%]	–	**13.5**	**10.2**	**16.8**	**9.9**
mean comfort $[m/s^2]$	1.28	1.02	0.963	1.02	1.01
Improvement [%]	–	**20.3**	**24.7**	**19.9**	**20.8**
v error max $[km/hour]$	0.53	0.495	0.513	0.493	0.5
y error max $[m]$	0.836	0.312	0.273	0.359	0.294
Weight cost y	7.02e5	2.53e5	1.36e5	2.85e5	2.07e5
Weight cost psi	1.11e4	1.88e4	2.79e4	2.23e4	1.09e4
Weight cost v	618	1033	1677	1000	715
Weight cost $\triangle\delta$	6200	3977	6822	5666	2800
Weight cost $\triangle$a	155	316	447	317	219
Weight cost ms y	0	0	1.92e5	0	8.72e4
Weight cost gd y	0	0	0	3.99e4	7055
Weight cost ay	0	1.60e4	0	0	0
Weight cost ms x	0	0	0	0	0
Weight cost gd x	0	0	0	0	0
Weight cost ax	0	0	0	0	0

The improvements are compared to the first result column (–)
Bold is a positive effect

Table B-17: Sine wave with different longitudinal terms

Controller	J_3	$J_{3,\text{ms,x}}$	$J_{3,\text{ax}}$
Time horizon [s]	1	1	1
RMS ms $[m/s^2]$	0.887	0.876	0.869
Improvement [%]	–	**1.3**	**2.1**
RMS gd $[m/s^2]$	0.513	0.506	0.5
Improvement [%]	–	**1.4**	**2.6**
MTVV ms $[m/s^2]$	1.33	1.28	1.28
Improvement [%]	–	**3.6**	**4**
MTVV gd $[m/s^2]$	1.12	1.11	1.11
Improvement [%]	–	**1.3**	**1.2**
mean comfort $[m/s^2]$	0.963	0.943	0.938
Improvement [%]	–	**2.1**	**2.6**
v error max $[km/hour]$	0.513	1.82	1.97
y error max $[m]$	0.273	0.271	0.269
Weight cost y	1.36e5	1.32e5	1.30e5
Weight cost psi	2.79e4	2.81e4	2.88e4
Weight cost v	1677	6.09e4	7.36e4
Weight cost $\triangle\delta$	6822	6800	6766
Weight cost $\triangle$a	447	313	1133
Weight cost ms y	1.92e5	1.94e5	1.99e5
Weight cost gd y	0	0	0
Weight cost ay	0	0	0
Weight cost ms x	0	6.39e4	0
Weight cost gd x	0	0	0
Weight cost ax	0	0	2.97e4

The improvements are compared to the first result column (–)
Bold is a positive effect

B-3-3 General discomfort

Table B-18: Double lane change with velocity shift

Controller	J_4	$J_{4,\mathrm{gd,x}}$	$J_{4,\mathrm{ax}}$
Time horizon [s]	1	1	1
RMS ms $[m/s^2]$	0.757	0.773	0.727
Improvement [%]	–	-2.2	**3.9**
RMS gd $[m/s^2]$	0.628	0.607	0.643
Improvement [%]	–	**3.3**	-2.5
MTVV ms $[m/s^2]$	1.53	1.58	1.53
Improvement [%]	–	-3	-0.2
MTVV gd $[m/s^2]$	1.33	1.3	1.3
Improvement [%]	–	**2.8**	**2.8**
mean comfort $[m/s^2]$	1.06	1.06	1.05
Improvement [%]	–	-0.1	**1.1**
v error max $[km/hour]$	0.779	1.76	4.67
y error max $[m]$	0.324	0.325	0.324
Weight cost y	3.28e4	3.34e4	3.44e4
Weight cost psi	8744	9311	8922
Weight cost v	1166	1.59e4	1.28e5
Weight cost $\triangle\delta$	2177	2100	2077
Weight cost $\triangle$a	754	255	1655
Weight cost ms y	0	0	0
Weight cost gd y	1.25e4	1.31e4	1.19e4
Weight cost ay	0	0	0
Weight cost ms x	0	0	0
Weight cost gd x	0	62.4	0
Weight cost ax	0	0	6.32e+04

The improvements are compared to the first result column (–)
Bold is a positive effect

B-3-4 Friction change

Table B-19: Double lane change with velocity change, friction change to $\mu = 0.5$

Controller	J_1	J_2	J_3	J_4	J_5
Time horizon [s]	1	1	1	1	1
RMS ms $[m/s^2]$	0.883	0.774	0.813	0.78	0.788
Improvement [%]	–	**12.4**	**8**	**11.7**	**10.8**
RMS gd $[m/s^2]$	0.699	0.659	0.743	0.655	0.687
Improvement [%]	–	**5.7**	-6.3	**6.3**	**1.7**
MTVV ms $[m/s^2]$	1.76	1.59	1.7	1.6	1.64
Improvement [%]	–	**9.9**	**3.2**	**9.3**	**7.1**
MTVV gd $[m/s^2]$	1.36	1.4	1.36	1.42	1.41
Improvement [%]	–	-2.3	**0.5**	-3.9	-3.3
mean comfort $[m/s^2]$	1.18	1.1	1.15	1.11	1.13
Improvement [%]	–	**6.2**	**1.9**	**5.5**	**4**
v error max $[km/hour]$	0.749	0.779	0.777	0.778	0.789
y error max $[m]$	0.321	0.224	0.423	0.227	0.215
Weight cost y	7.42e4	3.50e4	6.28e4	3.68e4	3.84e4
Weight cost psi	5122	6544	5944	7999	3233
Weight cost v	566	1155	1522	1166	801
Weight cost $\triangle\delta$	2411	1733	3999	2222	1244
Weight cost $\triangle$a	355	747	981	750	505
Weight cost ms y	0	0	3.32e4	0	1.30e4
Weight cost gd y	0	0	0	9699	1866
Weight cost ay	0	3766	0	0	0
Weight cost ms x	0	0	0	0	0
Weight cost gd x	0	0	0	0	0
Weight cost ax	0	0	0	0	0

The improvements are compared to the first result column (–)
Bold is a positive effect

B-3-5 Wind disturbance

Table B-20: Double lane change with velocity change under wind disturbance

Controller	J_1	J_2	J_3	J_4	J_5
Time horizon [s]	1	1	1	1	1
RMS ms $[m/s^2]$	0.88	0.744	0.732	0.753	0.741
Improvement [%]	–	**15.5**	**16.9**	**14.4**	**15.8**
RMS gd $[m/s^2]$	0.701	0.643	0.695	0.633	0.668
Improvement [%]	–	**8.3**	**0.9**	**9.7**	**4.8**
MTVV ms $[m/s^2]$	1.76	1.5	1.51	1.52	1.5
Improvement [%]	–	**14.8**	**14.5**	**13.8**	**14.8**
MTVV gd $[m/s^2]$	1.37	1.35	1.34	1.34	1.38
Improvement [%]	–	**1.9**	**2.6**	**2.3**	-0.2
mean comfort $[m/s^2]$	1.18	1.06	1.07	1.06	1.07
Improvement [%]	–	**10.2**	**9.4**	**10**	**9.1**
v error max $[km/hour]$	0.748	0.768	0.774	0.762	0.782
y error max $[m]$	0.385	0.814	1.05	0.768	0.736
Weight cost y	7.64e4	1.60e5	2.42e5	1.45e5	1.27e5
Weight cost psi	4733	7733	8577	9688	4099
Weight cost v	561	1155	1544	1155	800
Weight cost $\triangle\delta$	2355	1855	3899	2544	1366
Weight cost $\triangle$a	354	744	989	749	506
Weight cost ms y	0	0	6.41e4	0	2.59e4
Weight cost gd y	0	0	0	1.59e4	2977
Weight cost ay	0	6944	0	0	0
Weight cost ms x	0	0	0	0	0
Weight cost gd x	0	0	0	0	0
Weight cost ax	0	0	0	0	0

The improvements are compared to the first result column (–)
Bold is a positive effect

B-3-6 Sensor noise

Table B-21: Double lane change with velocity change with sensor noise

Controller	J_1	J_2	J_3	J_4	J_5
Time horizon [s]	1	1	1	1	1
RMS ms $[m/s^2]$	0.893	0.757	0.759	0.765	0.758
Improvement [%]	–	**15.3**	**15**	**14.4**	**15.2**
RMS gd $[m/s^2]$	0.751	0.712	0.761	0.709	0.74
Improvement [%]	–	**5.1**	-1.3	**5.6**	**1.5**
MTVV ms $[m/s^2]$	1.79	1.53	1.58	1.55	1.55
Improvement [%]	–	**14.4**	**11.7**	**13.5**	**13.6**
MTVV gd $[m/s^2]$	1.51	1.51	1.5	1.51	1.54
Improvement [%]	–	**0.3**	**1**	**0.4**	-1.8
mean comfort $[m/s^2]$	1.24	1.13	1.15	1.13	1.15
Improvement [%]	–	**8.8**	**7**	**8.4**	**7.3**
v error max $[km/hour]$	1.17	1.2	1.21	1.2	1.2
y error max $[m]$	0.367	0.307	0.36	0.31	0.301
Weight cost y	7.70e4	3.46e4	4.76e4	3.73e4	3.39e4
Weight cost psi	8044	1.45e4	1.31e4	1.77e4	7433
Weight cost v	1.31e4	2.65e4	3.58e4	2.66e4	1.75e4
Weight cost $\triangle\delta$	3444	3855	5199	5055	2244
Weight cost $\triangle$a	4333	8922	11900	8955	6022
Weight cost ms y	0	0	5.29e4	0	2.16e4
Weight cost gd y	0	0	0	1.96e4	2999
Weight cost ay	0	6455	0	0	0
Weight cost ms x	0	0	0	0	0
Weight cost gd x	0	0	0	0	0
Weight cost ax	0	0	0	0	0

The improvements are compared to the first result column (–)
Bold is a positive effect

B-3-7 Combination acceleration terms filtered and unfiltered

Table B-22: Double lane change, different controllers

Controller	J_2	J_3	J_4	J_7	J_8
Time horizon [s]	1	1	1	1	1
RMS ms $[m/s^2]$	0.748	0.747	0.757	0.746	0.75
Improvement [%]	–	**0.2**	-1.1	**0.3**	-0.2
RMS gd $[m/s^2]$	0.641	0.698	0.628	0.648	0.632
Improvement [%]	–	-8.8	**2.1**	-1.1	**1.5**
MTVV ms $[m/s^2]$	1.51	1.55	1.53	1.52	1.52
Improvement [%]	–	-2.6	-1.1	-0.8	-0.4
MTVV gd $[m/s^2]$	1.34	1.36	1.33	1.33	1.32
Improvement [%]	–	-1.9	**0.5**	**1.1**	**1.5**
mean comfort $[m/s^2]$	1.06	1.09	1.06	1.06	1.05
Improvement [%]	–	-2.8	-0.1	-0.1	**0.5**
v error max $[km/hour]$	0.78	0.779	0.779	0.788	0.799
y error max $[m]$	0.325	0.325	0.324	0.325	0.325
Weight cost y	3.00e4	3.97e4	3.28e4	3.36e4	3.11e4
Weight cost psi	7100	7444	8744	7822	9133
Weight cost v	1166	1533	1166	1466	1333
Weight cost $\triangle\delta$	1666	3466	2177	2677	2266
Weight cost $\triangle$a	750	988	754	932	845
Weight cost ms y	0	5.09e4	0	3.25e4	0
Weight cost gd y	0	0	1.25e4	0	1199
Weight cost ay	4688	0	0	0	0
Weight cost ms x	0	0	0	0	0
Weight cost gd x	0	0	0	0	0
Weight cost ax	0	0	0	0	0

The improvements are compared to the first result column (–)
Bold is a positive effect

Bibliography

[1] M. Doumiati, A. Victorino, A. Charara, and D. Lechner, "A method to estimate the lateral tire force and the sideslip angle of a vehicle: Experimental validation," in *Proceedings of the 2010 American Control Conference*, pp. 6936–6942, IEEE, 2010.

[2] D. Karimi and D. D. Mann, "A study of tractor yaw dynamics for application in a tractor driving simulator," in *ASABE/CSBE North Central Intersectional Meeting*, p. 1, American Society of Agricultural and Biological Engineers, 2006.

[3] MATLAB, *version 9.5 (R2018b)*. Natick, Massachusetts: The MathWorks Inc., 2018.

[4] M. Kyriakidis, J. C. de Winter, N. Stanton, T. Bellet, B. van Arem, K. Brookhuis, M. H. Martens, K. Bengler, J. Andersson, N. Merat, *et al.*, "A human factors perspective on automated driving," *Theoretical Issues in Ergonomics Science*, vol. 20, no. 3, pp. 223–249, 2019.

[5] A. H. Eichelberger and A. T. McCartt, "Toyota drivers' experiences with dynamic radar cruise control, pre-collision system, and lane-keeping assist," *Journal of safety research*, vol. 56, pp. 67–73, 2016.

[6] M. Dikmen and C. M. Burns, "Autonomous driving in the real world: Experiences with tesla autopilot and summon," in *Proceedings of the 8th international conference on automotive user interfaces and interactive vehicular applications*, pp. 225–228, 2016.

[7] V. A. Banks, A. Eriksson, J. O'Donoghue, and N. A. Stanton, "Is partially automated driving a bad idea? Observations from an on-road study," *Applied ergonomics*, vol. 68, pp. 138–145, 2018.

[8] C. Diels and J. E. Bos, "Self-driving carsickness," *Applied ergonomics*, vol. 53, pp. 374–382, 2016.

[9] T. Wada, "Motion sickness in automated vehicles," in *Advanced Vehicle Control: Proceedings of the 13th International Symposium on Advanced Vehicle Control, September 13-16, 2016, Munich, Germany*, p. 169, 2016.

[10] M. Turner, "Motion sickness in public road transport: passenger behaviour and susceptibility," *Ergonomics*, vol. 42, no. 3, pp. 444–461, 1999.

[11] Y. Marjanen and N. J. Mansfield, "Relative contribution of translational and rotational vibration to discomfort," *Industrial health*, vol. 48, no. 5, pp. 519–529, 2010.

[12] M. G. Da Silva, "Measurements of comfort in vehicles," *Measurement Science and Technology*, vol. 13, no. 6, p. R41, 2002.

[13] A. F. Van der Merwe, *An air suspension cushion to reduce human exposure to vibration*. PhD thesis, Stellenbosch: University of Stellenbosch, 2007.

[14] B. E. Donohew and M. J. Griffin, "Motion sickness: effect of the frequency of lateral oscillation," *Aviation, Space, and Environmental Medicine*, vol. 75, no. 8, pp. 649–656, 2004.

[15] R. Solea and U. Nunes, "Trajectory planning with velocity planner for fully-automated passenger vehicles," in *2006 IEEE Intelligent Transportation Systems Conference*, pp. 474–480, IEEE, 2006.

[16] L. Labakhua, U. Nunes, R. Rodrigues, and F. S. Leite, "Smooth trajectory planning for fully automated passengers vehicles," in *Third Int. Conf. on Informatics in Control, Automation and Robotics*, 2006.

[17] K. Macek, R. Philippsen, and R. Siegwart, "Path following for autonomous vehicle navigation with inherent safety and dynamics margin," in *2008 IEEE Intelligent Vehicles Symposium*, pp. 108–113, IEEE, 2008.

[18] X. Li, Z. Sun, Z. He, Q. Zhu, and D. Liu, "A practical trajectory planning framework for autonomous ground vehicles driving in urban environments," in *2015 IEEE Intelligent Vehicles Symposium (IV)*, pp. 1160–1166, IEEE, 2015.

[19] P. Polack, F. Altché, B. d'Andréa Novel, and A. de La Fortelle, "Guaranteeing consistency in a motion planning and control architecture using a kinematic bicycle model," in *2018 Annual American Control Conference (ACC)*, pp. 3981–3987, IEEE, 2018.

[20] J. Ziegler, P. Bender, T. Dang, and C. Stiller, "Trajectory planning for berthaâĂŤa local, continuous method," in *2014 IEEE intelligent vehicles symposium proceedings*, pp. 450–457, IEEE, 2014.

[21] P. Belvén, "Implementation of model predictivecontrol for path following with the kth research concept vehicle," 2015.

[22] L.-h. Luo, H. Liu, P. Li, and H. Wang, "Model predictive control for adaptive cruise control with multi-objectives: comfort, fuel-economy, safety and car-following," *Journal of Zhejiang University SCIENCE A*, vol. 11, no. 3, pp. 191–201, 2010.

[23] A. Jezierski, J. Mozaryn, and D. Suski, "A comparison of LQR and MPC control algorithms of an inverted pendulum," in *Polish Control Conference*, pp. 65–76, Springer, 2017.

[24] J. Cartró Benavides, "Desenvolupament del control d'un vehicle autònom en un entorn de simulació," Master's thesis, Universitat Politècnica de Catalunya, 2019.

[25] P.-E. Danielsson, "Euclidean distance mapping," *Computer Graphics and image processing*, vol. 14, no. 3, pp. 227–248, 1980.

[26] G. G. Slabaugh, "Computing euler angles from a rotation matrix," *Retrieved on August*, vol. 6, no. 2000, pp. 39–63, 1999.

[27] M. A. Sotelo, "Lateral control strategy for autonomous steering of ackerman-like vehicles," *Robotics and Autonomous Systems*, vol. 45, no. 3-4, pp. 223–233, 2003.

[28] L. M. Laudański, *Between Certainty and Uncertainty: Statistics and Probability in Five Units with Notes on Historical Origins and Illustrative Numerical Examples*, vol. 31. Springer Science & Business Media, 2012.

[29] Simulink, *version 9.2 (R2018b)*. Natick, Massachusetts: The MathWorks Inc., 2018.

[30] Z. Lu, B. Shyrokau, B. Boulkroune, S. Van Aalst, and R. Happee, "Performance benchmark of state-of-the-art lateral path-following controllers," in *2018 IEEE 15th International Workshop on Advanced Motion Control (AMC)*, pp. 541–546, IEEE, 2018.

[31] Delft Tyre, *version 6.2*. http://www.delft-tyre.nl: TNO, 2017.

[32] Simscape Multibody, *version 6.0*. Natick, Massachusetts: The MathWorks Inc., 2018.

[33] E. H. Lim and J. K. Hedrick, "Lateral and longitudinal vehicle control coupling for automated vehicle operation," in *Proceedings of the 1999 American Control Conference (Cat. No. 99CH36251)*, vol. 5, pp. 3676–3680, IEEE, 1999.

[34] C. E. Beal and J. C. Gerdes, "Model predictive control for vehicle stabilization at the limits of handling," *IEEE Transactions on Control Systems Technology*, vol. 21, no. 4, pp. 1258–1269, 2012.

[35] J. Kong, M. Pfeiffer, G. Schildbach, and F. Borrelli, "Kinematic and dynamic vehicle models for autonomous driving control design," in *2015 IEEE Intelligent Vehicles Symposium (IV)*, pp. 1094–1099, IEEE, 2015.

[36] R. Pepy, A. Lambert, and H. Mounier, "Path planning using a dynamic vehicle model," in *2006 2nd International Conference on Information & Communication Technologies*, vol. 1, pp. 781–786, IEEE, 2006.

[37] N. Singh, A. Sharma, S. Shah, and B. Gardampaali, "Mechatronics based accident alarming system with automatic roadblock prevention system," tech. rep., SAE Technical Paper, 2017.

[38] C. C. Smith, D. Y. McGehee, and A. J. Healey, "The prediction of passenger riding comfort from acceleration data," *Journal of Dynamic Systems, Measurement, and Control*, vol. 100, no. 1, pp. 34–41, 1978.

[39] Y. Marjanen, *Validation and improvement of the ISO 2631-1 (1997) standard method for evaluating discomfort from whole-body vibration in a multi-axis environment*. PhD thesis, © Yka Marjanen, 2010.

[40] T. Keviczky, P. Falcone, F. Borrelli, J. Asgari, and D. Hrovat, "Predictive control approach to autonomous vehicle steering," in *2006 American control conference*, pp. 6–pp, IEEE, 2006.

[41] T. Besselmann and M. Morari, "Hybrid parameter-varying model predictive control for autonomous vehicle steering," *European Journal of Control*, vol. 14, no. 5, pp. 418–431, 2008.

[42] A. Norouzi, R. Kazemi, and S. Azadi, "Vehicle lateral control in the presence of uncertainty for lane change maneuver using adaptive sliding mode control with fuzzy boundary layer," *Proceedings of the Institution of Mechanical Engineers, Part I: Journal of Systems and Control Engineering*, vol. 232, no. 1, pp. 12–28, 2018.

[43] K. Jalali, T. Uchida, J. McPhee, and S. Lambert, "Development of an advanced fuzzy active steering controller and a novel method to tune the fuzzy controller," *SAE International Journal of Passenger Cars - Electronic and Electrical Systems*, vol. 6, pp. 241–254, 04 2013.

[44] I. Chiha, N. Liouane, and P. Borne, "Tuning pid controller using multiobjective ant colony optimization," *Applied Computational Intelligence and Soft Computing*, vol. 2012, p. 11, 2012.

[45] M. Francisco and P. Vega, "Automatic tuning of model predictive controllers based on multiobjective optimization," *Latin American applied research*, vol. 40, no. 3, pp. 255–265, 2010.

[46] A. Domahidi and J. Jerez, "Forces professional." Embotech AG, https://embotech.com/FORCES-Pro, 2014–2019.

[47] A. Zanelli, A. Domahidi, J. Jerez, and M. Morari, "Forces nlp: an efficient implementation of interior-point... methods for multistage nonlinear nonconvex programs," *International Journal of Control*, pp. 1–17, 2017.

[48] L. R. Ray, "Nonlinear tire force estimation and road friction identification: Simulation and experiments," *Automatica*, vol. 33, no. 10, pp. 1819–1833, 1997.

[49] F. Gustafsson, "Slip-based tire-road friction estimation," *Automatica*, vol. 33, no. 6, pp. 1087–1099, 1997.